Tutorial Topic: Emerging Solid-State-Transformer based Electric-Vehicle Ultra-fast Charging Station

Introduction - Changing Distribution Grid Paradigm and the Emerging Importance of EVs

Tutorial Presentation, IEEE SPEC, 2024, Brisbane

Prof. Sanjib Kumar Panda

Director of Power & Energy group

Department of Electrical and Computer Engineering

National University of Singapore

IEEE Fellow

SEGMENTS OF THE TUTORIAL

- Introduction and comprehensive overview [Prof. Sanjib Kumar Panda, NUS]
- Universal electric-vehicle ultra-fast charging concept [Dr. Jaydeep, ST Engineering/Ex-NUS]

- ML-aided design optimization of grid-interface [Dr. Jaydeep, ST Engineering/Ex-NUS]
- Coordinated control of renewable integrated ultra-fast charging stations [Dr. Jaydeep, ST Engineering]
- Conclusion [Prof. Sanjib Kumar Panda, NUS]

INTRODUCTION: SMART GRID

- Energy grid 2.0:
  - Decentralized/distributed energy generation
  - Diversified nature of loads – both AC and DC
  - Bidirectional power and information flow

- Microgrids - building blocks of future grid

- *Key for economic and efficient operation of microgrids* - architectures that avoids multiple energy conversions

- **Microgrids are interconnected to other microgrids or grid at higher voltages through energy control centers (ECC)**

- Objectives of ECC:
  - Active power-flow control & compensation
  - VAR & harmonic compensation

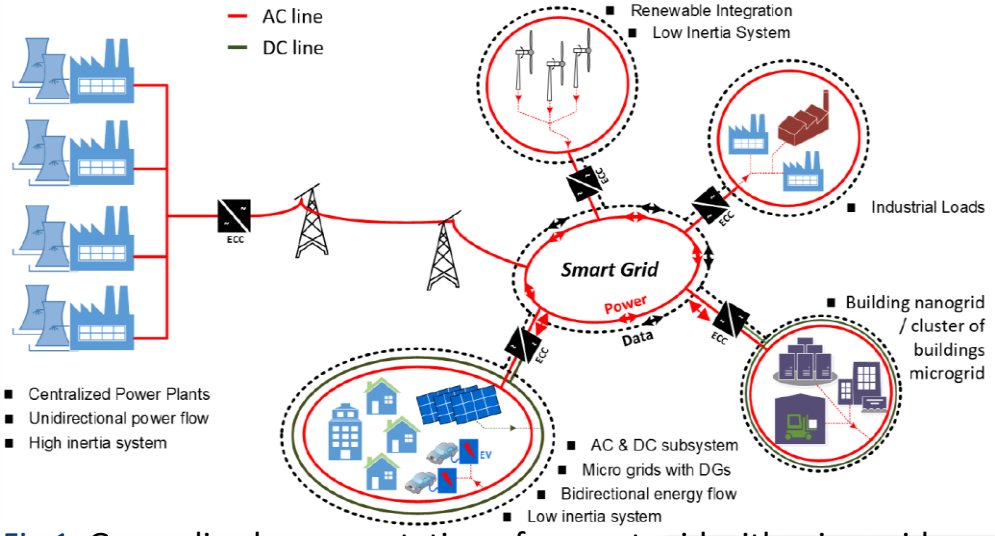

Fig 1. Generalized representation of a smart grid with microgrids as building blocks

- Control of DC bus to integrate renewables & storage
- Microgrid control during islanding/grid connection
- Information sharing between microgrid and rest of the n/w

INTRODUCTION: GRID-CONNECTED MICROGRID

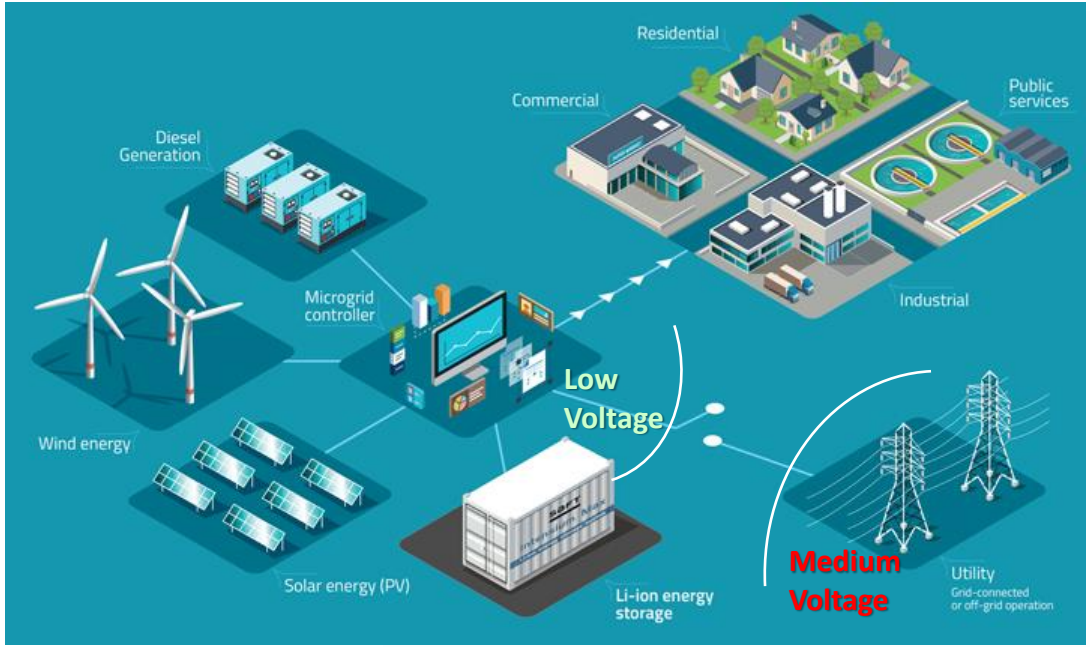

- Utility distribution-grid is a medium-voltage (MV) network – few kVs to few 10s of kVs depending on the country.
- Microgrids are usually low-voltage (LV) networks.
- Thus, interfacing microgrids with utility distribution-grids require a bidirectional MV-LV conversion.
- EV fast charging stations are fundamentally grid-connected microgrids (as they often have energy storage and renewable generation within)

MEDIUM-VOLTAGE (MV) GRID INTERFACE

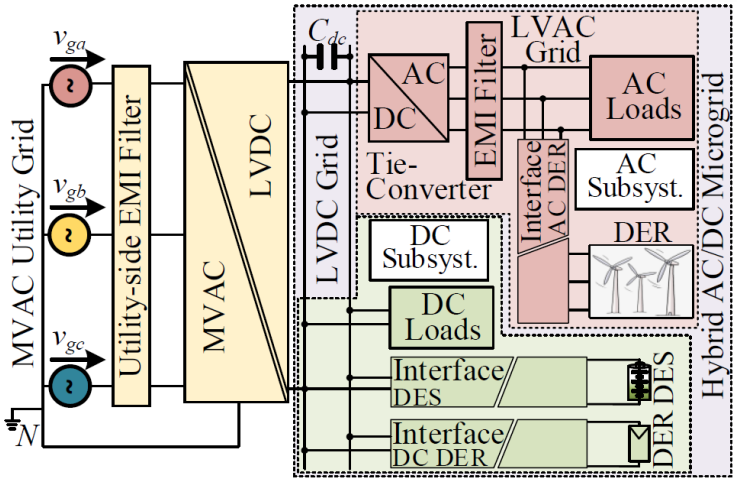

Fig 2. Generalized schematic of a Hybrid AC/DC Micro-grid (few 100s kW to few MW) interfaced with the MVAC utility grid (few kV to few 10s kV)

- Modern and futuristic microgrids are expected to be increasingly hybrid AC/DC.

Examples of hybrid AC/DC microgrids:

(i) A cluster of buildings having renewables
(ii) Green Data-centers
(iii) Off-grid villages

- MVAC grid-connected DC microgrid systems are also becoming common-place like:

(i) EV fast-charging stations
(ii) DC green data-centers

- Necessity to have MVAC-LVDC Interface solutions to facilitate grid integration has increased.

- **How should MVAC-LVDC interface be realized?**

[1] X. Liu, P.Wang and P. C. Loh, "A Hybrid AC/DC Microgrid and Its Coordination Control," in IEEE Transactions on Smart Grid, vol. 2, no. 2, pp. 278-286, June 2011.
[2] M. Shahidehpour, Z. Li, W. Gong, S. Bahramirad and M. Lopata, "A Hybrid ac/dc Nanogrid: The Keating Hall Installation at the Illinois Institute of Technology," in IEEE Electrification Magazine, vol. 5, no. 2, pp. 36-46, June 2017.

HISTORY OF TRANSFORMERS & ELECTRONIC-TRANSFORMERS

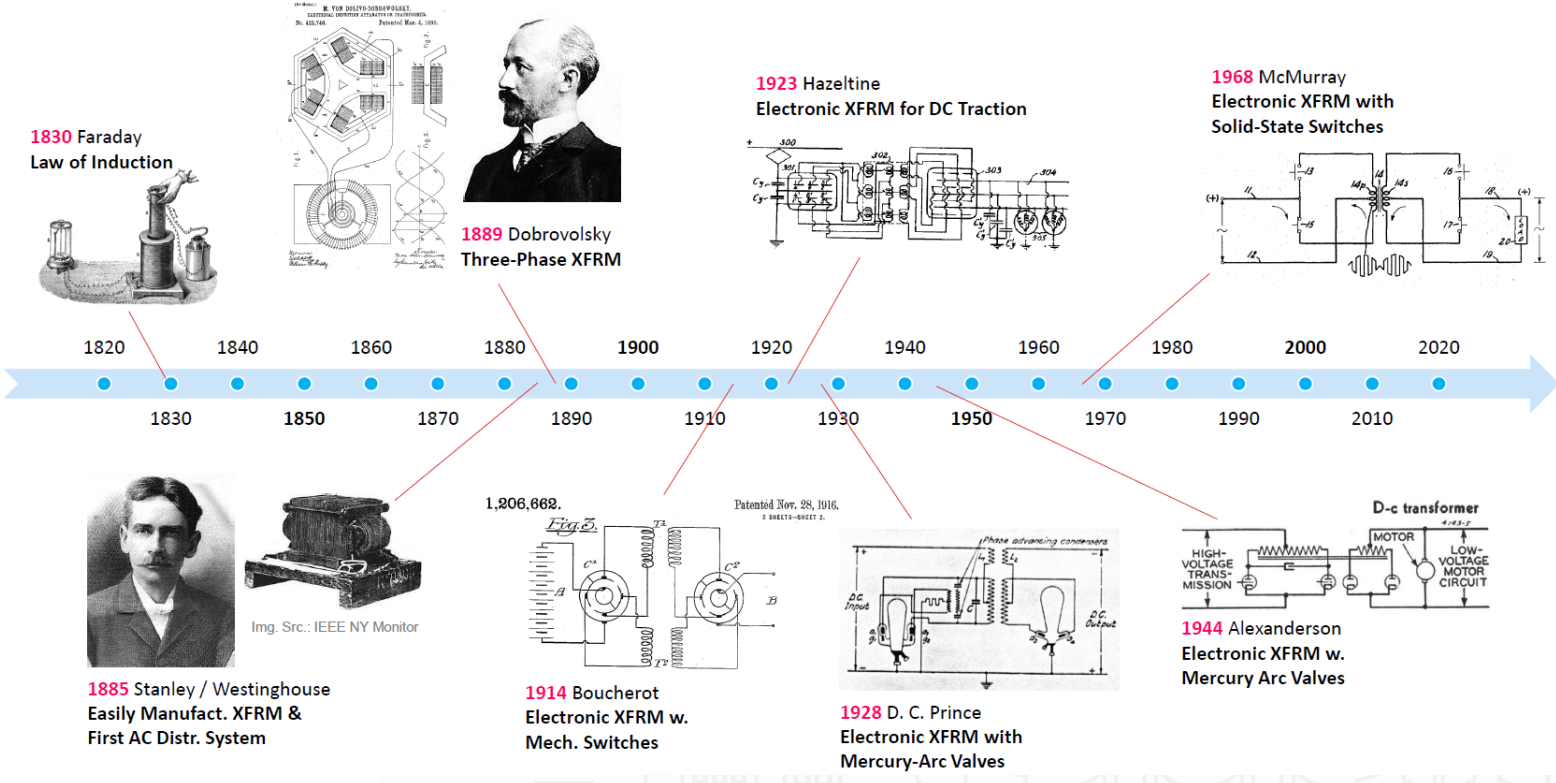

[3] J. W. Kolar and J. Huber, "Solid-State Transformers: Fundamentals, Industrial Applications, Challenges," Tutorial at Energy Conversion Congress and Expo, Detroit, Michigan, USA, Oct, 2022.

HISTORY OF ELECTRONIC/SOLID-STATE-TRANSFORMERS

1968 McMurray
Electronic XFRM with Solid-State Switches

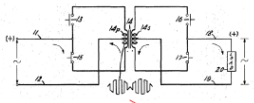

1978 Mennicken / BBC
Medium-Freq. Isol. for Traction

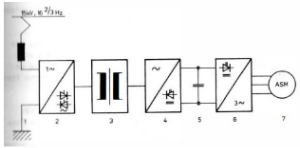

1984 Weiss & Rentmeister
Isolated Front-End for Traction

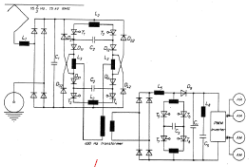

2011 GE
1 MW AC-AC SST w. 10 kV SiC

2021 Delta
13.2 kV / 400 kW EV Fast Charger

1950 — 1960 — 1970 — 1980 — 1990 — 2000 — 2010 — 2020 — 2030

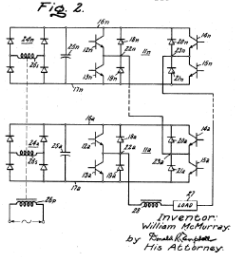

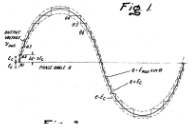

1969 McMurray
Cascaded H-Bridge (CHB)

1996 Steiner & Reinold
Multi-Cell CHB SST for Traction

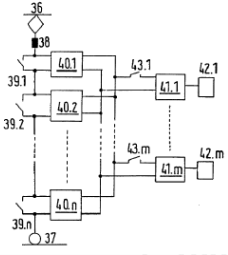

2004 Marquardt & Glinka
Modular Multilevel Conv. (MMC)

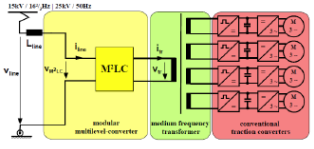

2012 ABB
1.2 MW Traction SST
Field Test

2021 Wen et al.
2 MW HFAC-Bus SST

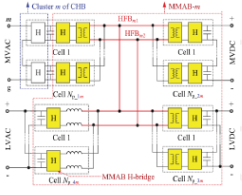

[3] J. W. Kolar and J. Huber, "Solid-State Transformers: Fundamentals, Industrial Applications, Challenges," Tutorial at Energy Conversion Congress and Expo, Detroit, Michigan, USA, Oct, 2022.

FUNDAMENTALS OF TRANSFORMER

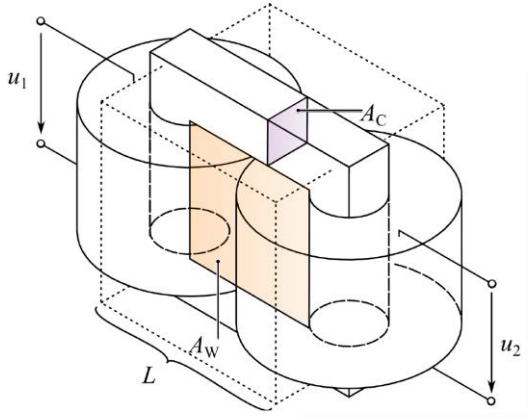

Area Product $A_C A_W \propto \dfrac{S}{k_W J_{rms} B_{max} f}$

S	Rated Power ($S = U_1 I_1$)
k_W	Window Utilization Factor
B_{max}	Flux Density Amplitude
J_{rms}	Winding Current Density
f	Frequency

Construction Volume $A_C A_W \propto L^4 \propto \dfrac{S}{f} \rightarrow V \propto L^3 \propto \dfrac{S}{f^{3/4}}$

for given B_{max}, J_{rms}, k_W

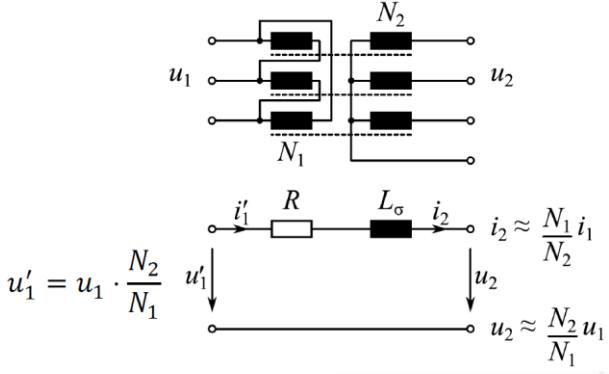

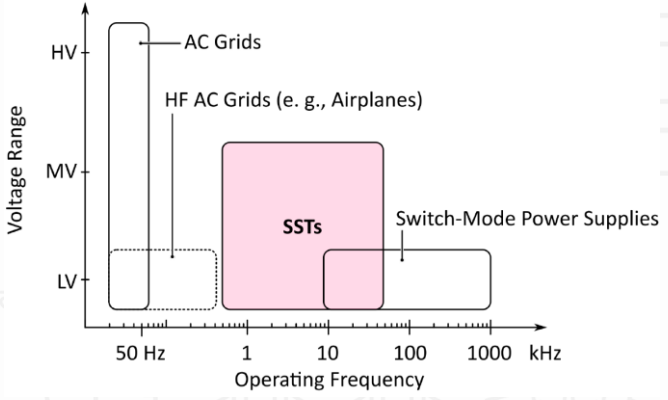

[3] J. W. Kolar and J. Huber, "Solid-State Transformers: Fundamentals, Industrial Applications, Challenges," Tutorial at Energy Conversion Congress and Expo, Detroit, Michigan, USA, Oct, 2022.

CONVENTIONAL AND EMERGING MV INTERFACE

Conventional On-Load Tap Changer (OLTC) Transformers [4]

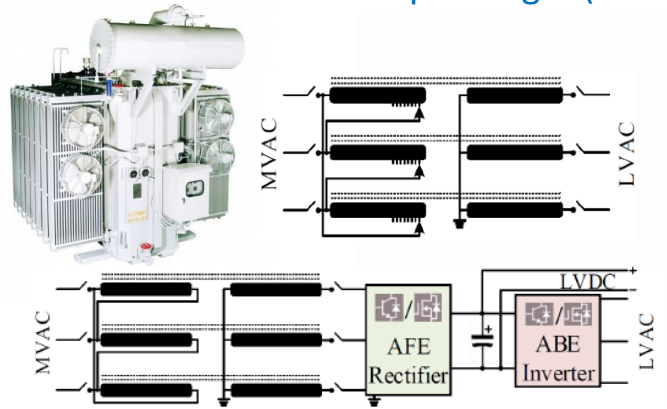

Fig 3. OLTC Transformer based solutions

- Robust and reliable
- Power flow control: Discrete & Unidirectional
- DC sub-system for renewables: Needs power electronics
- Low frequency isolation: Bulky

Vs

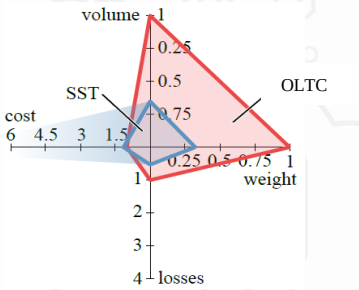

Emerging Solid State Transformer [5]

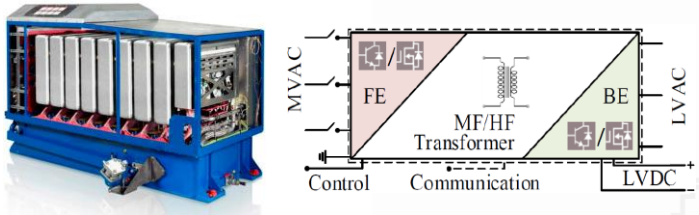

Fig 4. Solid-state transformer-based solutions

- Reliability and robustness: Design-based
- Power flow control: Continuous and Bidirectional
- DC sub-systems for renewables: Easily Possible
- Medium frequency isolation: Less bulky

[4] E. I. Amoiralis, M. A. Tsili and A. G. Kladas, "Transformer Design and Optimization: A Literature Survey," in IEEE Trans. on Power Delivery, vol. 24, no. 4, pp. 1999-2024, Oct. 2009.
[5] M. Shahidehpour, Z. Li, W. Gong, S. Bahramirad and M. Lopata, "A Hybrid ac/dc Nanogrid: The Keating Hall Installation at the Illinois Institute of Technology," in IEEE Electrification Magazine, vol. 5, no. 2, pp. 36-46, June 2017.

APPLICABILITY OF SOLID-STATE-TRANSFORMERS

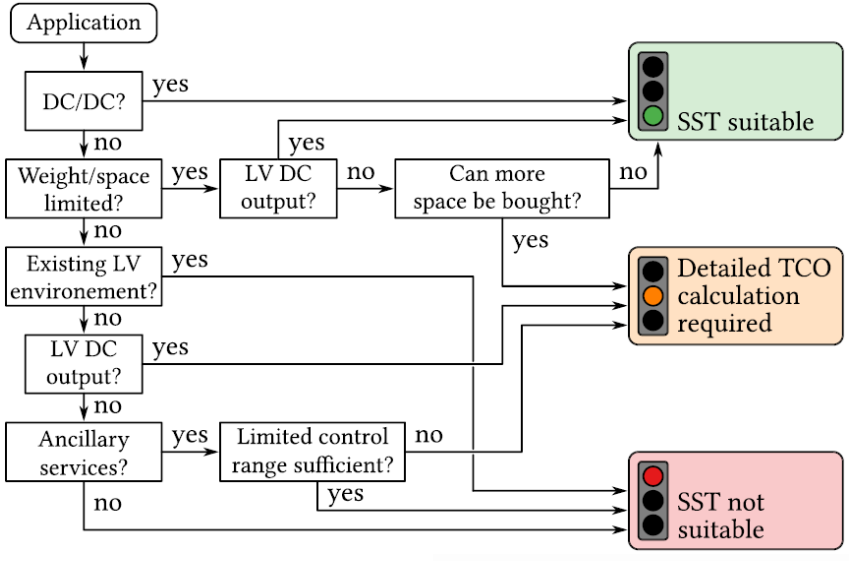

Fig 5. Applicability guideline for SST Technology [6]

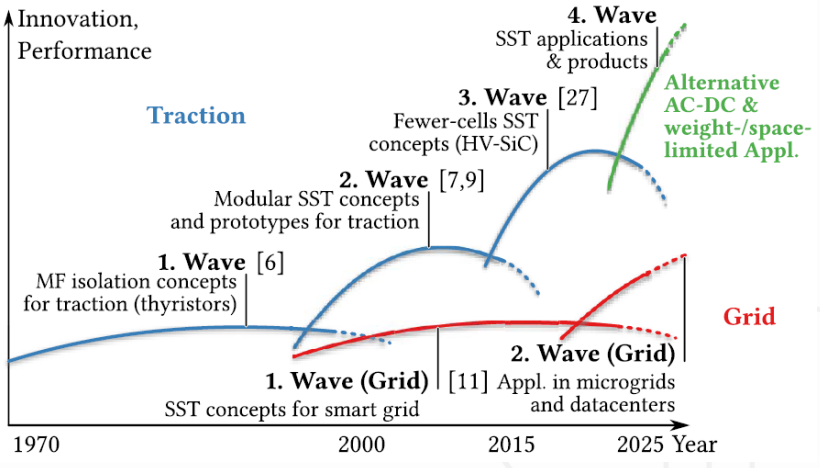

Fig 6. Waves of SST innovation [6]

- Having an LVDC interface in the grid-connected SST infrastructure makes it economically justifiable, as AC-DC. conversion requires power electronics even for LFT + inverter-based solution.
- The trend of SST technology innovation has shifted to AC-DC type SSTs both for traction and grid applications.

[6] J. E. Huber and J. W. Kolar, "Applicability of Solid-State Transformers in Today's and Future Distribution Grids," in IEEE Trans. Smart Grid, vol. 10, no. 1, pp. 317-326, Jan. 2019.

GRID-CONNECTED SOLID-STATE-TRANSFORMERS

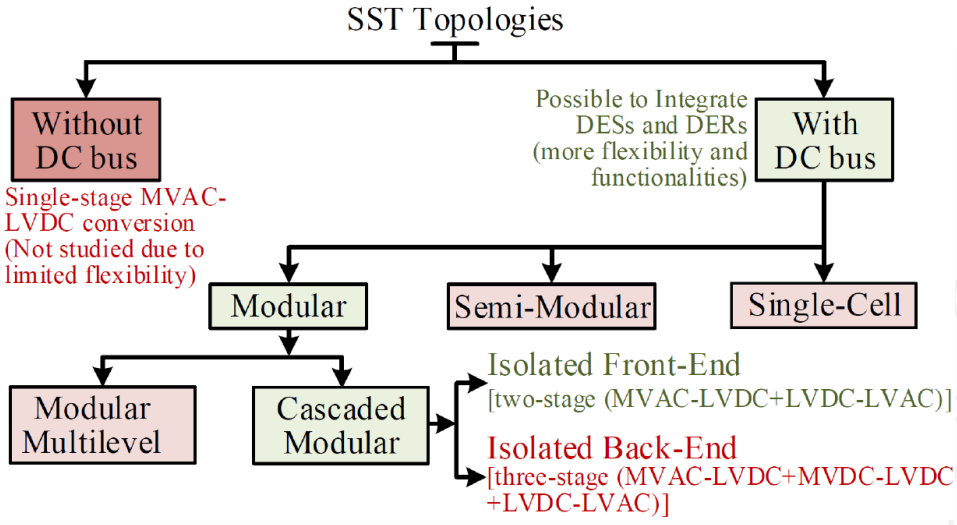

Fig 7. A broad classification of relevant SST topologies

- Major focus of the SST technology is regarding the development of MVAC-LVDC conversion strategy, as the LVDC-LVAC conversion constitutes a well-developed bidirectional inverter.

GRID-CONNECTED SST (CASCADED-MODULAR)

- This fully modular SST type is preferred due to the following reasons:
  - Use of standardized medium-voltage lower-power (kW range) WBG semiconductor devices and MFTs.
  - Effective PFC and harmonic filtering, smaller grid-side filter required, convenient soft-switching.
  - Star (Y) - delta (Δ) flexibility, complete flexibility for scalability and maintenance.
- The broad categorization of cascaded-modular SSTs are given as:

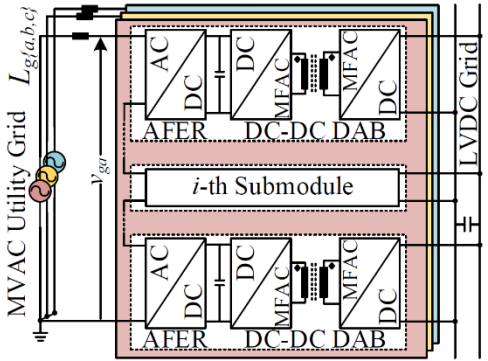

Fig 8a. Isolated Back-end (IBE) MVAC-LVDC Converter

- **Lower efficiency** due to two stages
- **Lower power density** due to bulky DC-link electrolytic capacitors filtering second harmonic component [|AC|]
- **Low reliability**

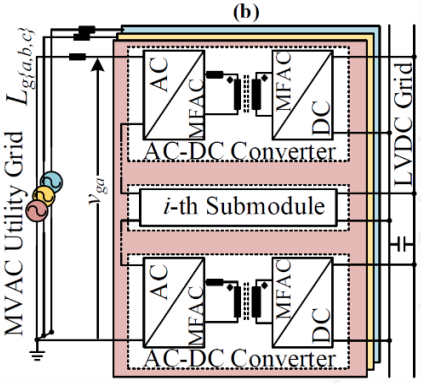

Fig 8b. Isolated front-end (IFE) MVAC-LVDC Converter

- **Higher efficiency** due to single stage
- **Higher power density** mainly due to elimination of bulky electrolytic capacitors (second harmonic components from 3-phases get cancelled at LVDC bus)
- **Higher reliability**

EMERGING IMPORTANCE OF ELECTRIC-VEHICLES

Global electric car sales are on track to grow strongly again this year, reaching about 17 million

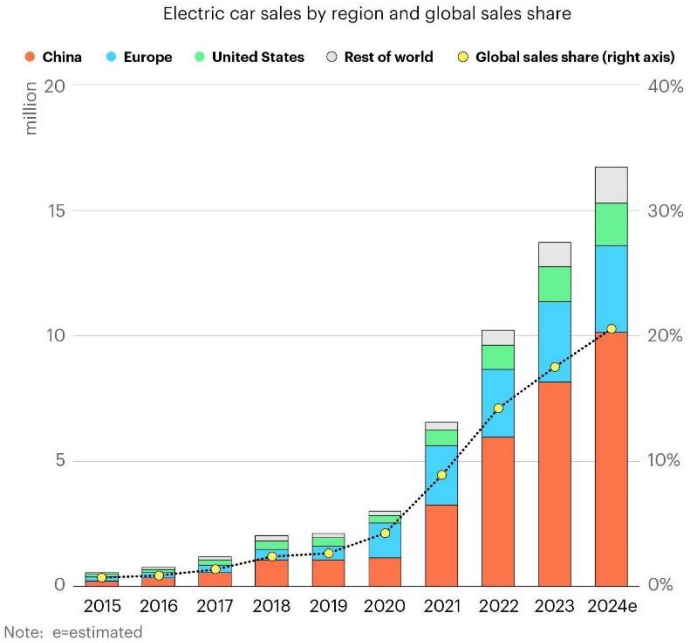

International Energy Agency

- ~20% of all cars sold worldwide in 2024 is estimated to be electric (higher market share in China); with the present energy, climate and industrial policy settings, the projected EV share in 2035 will be ~50%.
- Electric cars are getting cheaper as the competition intensifies, particularly in China.
- In developing economies outside China, cheaper electric car models are arriving, and the future of electric two- and three-wheelers already looks bright.
- The global number of installed public charging points was up 40% in 2023 relative to 2022, and growth for fast chargers outpaced that of slower ones.
- As more electric vehicles of various types hit the road, dedicated, universal and flexible public fast-charging is the need of the hour.

[7] "Global EV Outlook 2024", International Energy Agency (IEA), Apr. 2024.

POWER CONVERSION FOR EV CHARGING

- Power conversion (unidirectional or bidirectional) is critical for EV charging at different power levels ('slow' and 'fast' charging terms are subjective)

- Power conversion strategies at a functional block level are similar for charging at various power levels (various possibilities shown below) – the topologies and implementation changes for different power levels

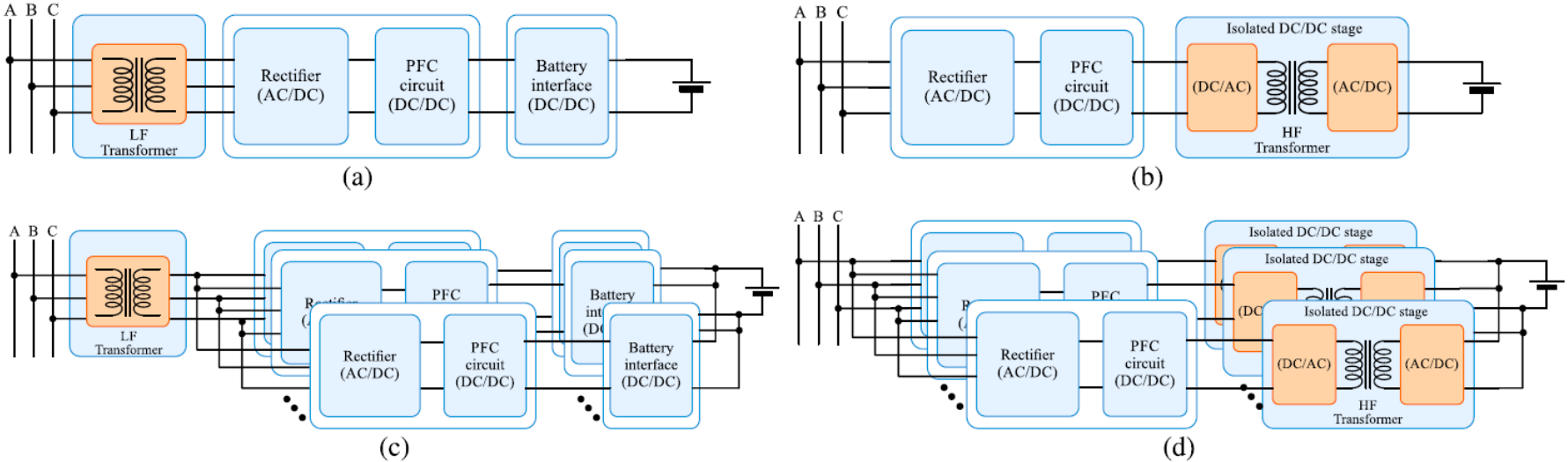

Fig 10. Conventional DC slow/fast EV charging power conversion systems.

ULTRA-FAST EV CHARGING STATION

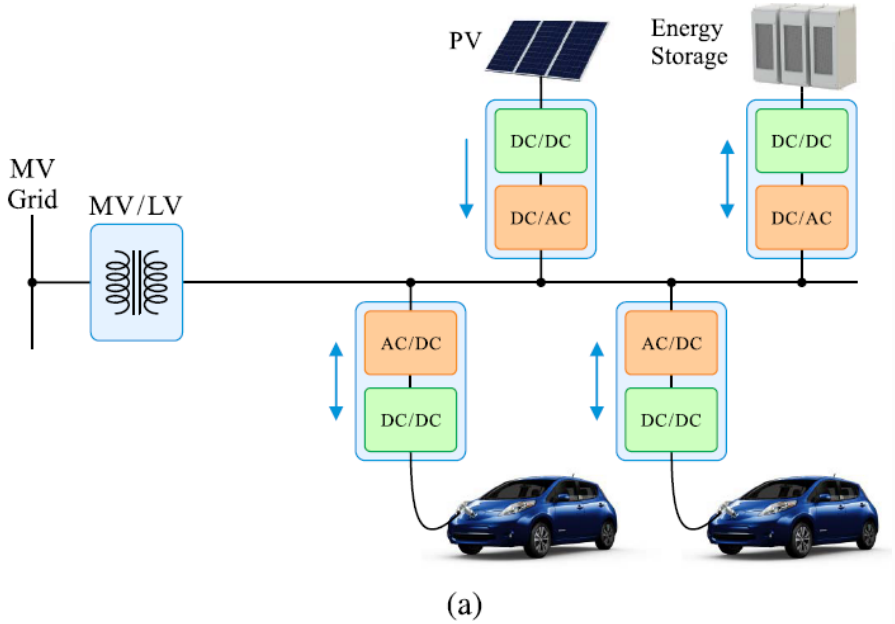

- Lesser conversion stages
- Higher efficiency
- Simpler control
- Complex protection

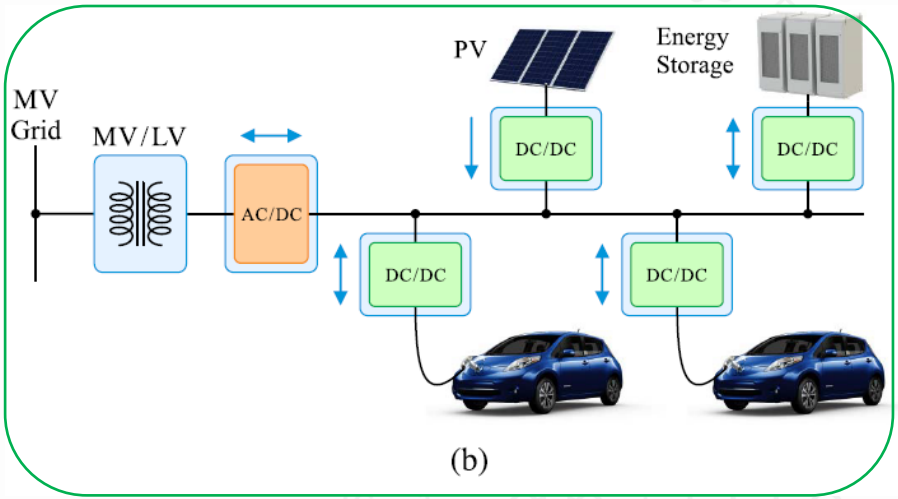

Fig 11. Configurations for ultra-fast EV charging stations: (a) AC connected; (b) DC connected [8], [9].

[8] H. Tu, H. Feng, S. Srdic and S. Lukic, "Extreme Fast Charging of Electric Vehicles: A Technology Overview," IEEE Trans. Transport. Electrific., vol. 5, no. 4, pp. 861-878, Dec. 2019.
[9] S. Srdic and S. Lukic, "Toward Extreme Fast Charging: Challenges and Opportunities in Directly Connecting to Medium-Voltage Line," IEEE Electrific. Mag., vol. 7, no. 1, pp. 22-31, Mar. 2019.

ULTRA-FAST EV CHARGING STATION

- As explained earlier, SST provides a cost-competitive alternative for isolated MVAC-LVDC conversion (indispensable need for ultra-fast EV charging stations) with better efficiency and power-density (critical for urban-centers).

- Various MW-scale SST-grid-interface based ultra-fast EV charging concepts has been implemented with some of them getting commercialized recently! (provided in details in the tutorial referenced as [10] below)

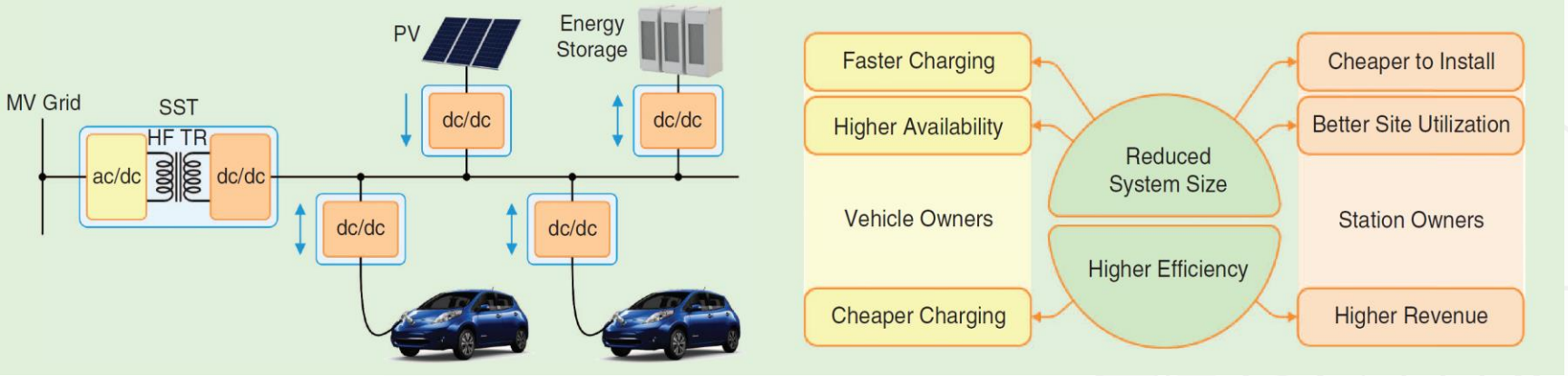

Fig 12. Ultra-fast EV charging station concept based on SST technology [9].

[9] S. Srdic and S. Lukic, "Toward Extreme Fast Charging: Challenges and Opportunities in Directly Connecting to Medium-Voltage Line," IEEE Electrific. Mag., vol. 7, no. 1, pp. 22-31, Mar. 2019.
[10] J. W. Kolar and J. Huber, "The Essence of Solid-State Transformers: Fundamentals, Design Challenges, R&D Overview, Comparative Evaluation, Outlook," IEEE APEC 2023, Florida, USA, Mar. 2023.

RELEVANT PUBLICATIONS FOR THIS SEGMENT (BY EMDL, NUS)

NUS National University of Singapore | College of Design and Engineering

Books/Thesis

1. ***Jaydeep Saha**, "Analysis, Optimization and Control of grid-Interfaced Matrix-Based Isolated AC-DC Converters", Springer Nature, Nov. 2022.*
2. ***Naga Brahmendra Yadav Gorla**, "Analysis, Design and Control of cascaded Modular Solid-State Transformer," Ph.D. Dissertation, NUS, Singapore, 2019.*
3. ***Sandeep Kolluri**, "Analysis and Control of Circulating Current in modular Multilevel Converter," Ph.D. Dissertation, NUS, Singapore, 2019.*

Journals

1. ***Jaydeep Saha** and **Sanjib Kumar Panda**, "Overview and Comparative Analysis of Bidirectional Cascaded Modular Isolated Medium-Voltage AC - Low-Voltage DC (MVAC-LVDC) Power Conversion for Renewable Energy Rich Microgrids," in Renewable and Sustainable Energy Reviews, 2023.*

Conferences

1. ***Jaydeep Saha**, Marif Daula Siddique, Prasanth Sundararajan and **Sanjib Kumar Panda**, "An Overview of Power Conversion Systems in Contemporary Grid-Interactive Efficient Buildings (GEBs)," in IEEE 14th Energy Conversion Congress and Exposition – Asia (ECCE-Asia), 2023.*
2. ***Jaydeep Saha**, **Naga Brahmendra Yadav Gorla** and **Sanjib Kumar Panda**, "Comparative Overview of Power Balance Control for Two-stage and Single-stage Isolated MVAC-LVDC Cascaded Converters," in IEEE 13th Energy Conversion Congress and Exposition – Asia (ECCE-Asia), 2022.*
3. ***Jaydeep Saha**, **Naga Brahmendra Yadav Gorla** and **Sanjib Kumar Panda**, "A Review on Bidirectional Matrix-Based AC-DC Conversion for Modular Solid-State-Transformers," in IEEE 4th International Future Energy Electronics Conference (IFEEC), Singapore, 2019.*
4. ***Naga Brahmendra Yadav Gorla**, S. Kolluri and **Sanjib Kumar Panda**, "Solid-state-transformer control aspects for various smart grid scenarios," 2017 IEEE Innovative Smart Grid Technologies - Asia (ISGT-Asia), Auckland, 2017, pp. 1-6.*

Thank You

Hope you enjoy the Rest!

See you at the end for conclusion

Tutorial Topic: Emerging Solid-State-Transformer based Electric-Vehicle Ultra-fast Charging Station

Universal EV ultra-fast charging station concept

Tutorial Presentation, IEEE SPEC, 2024, Brisbane

Dr. Jaydeep Saha

Assistant Principal Engineer
ST Engineering Satellite Systems
Ex-Research Fellow
National University of Singapore

IEEE Member

CONTENTS

INTRODUCTION: ULTRA-FAST EV CHARGING STATION

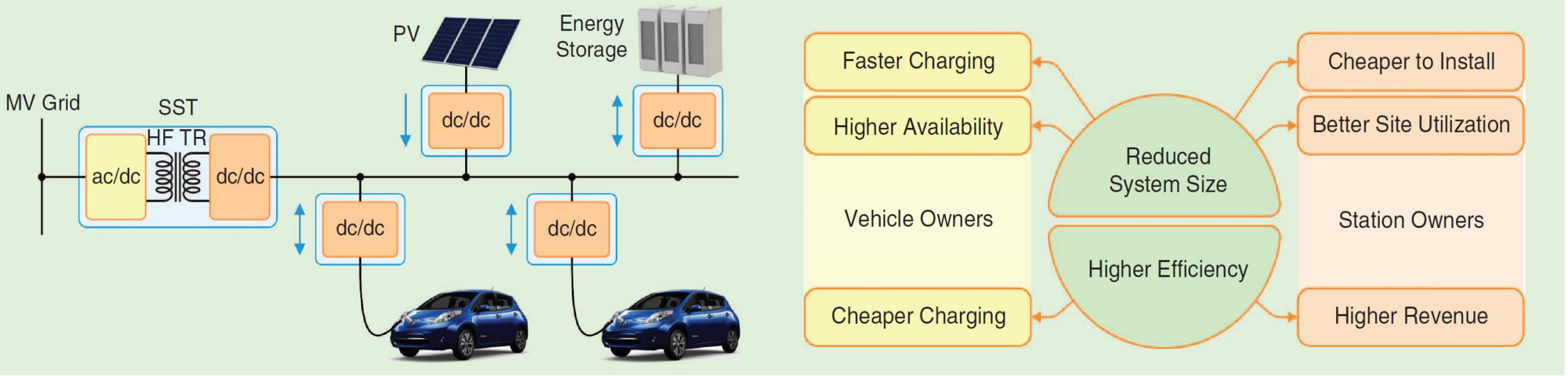

Fig 1. Ultra-fast EV charging station concept based on SST technology [2].

[1] H. Tu, H. Feng, S. Srdic and S. Lukic, "Extreme Fast Charging of Electric Vehicles: A Technology Overview," IEEE Trans. Transport. Electrific., vol. 5, no. 4, pp. 861-878, Dec. 2019.
[2] S. Srdic and S. Lukic, "Toward Extreme Fast Charging: Challenges and Opportunities in Directly Connecting to Medium-Voltage Line," IEEE Electrific. Mag., vol. 7, no. 1, pp. 22-31, Mar. 2019.

SST BASED COMPACT EV FAST-CHARGING STATION CONCEPT

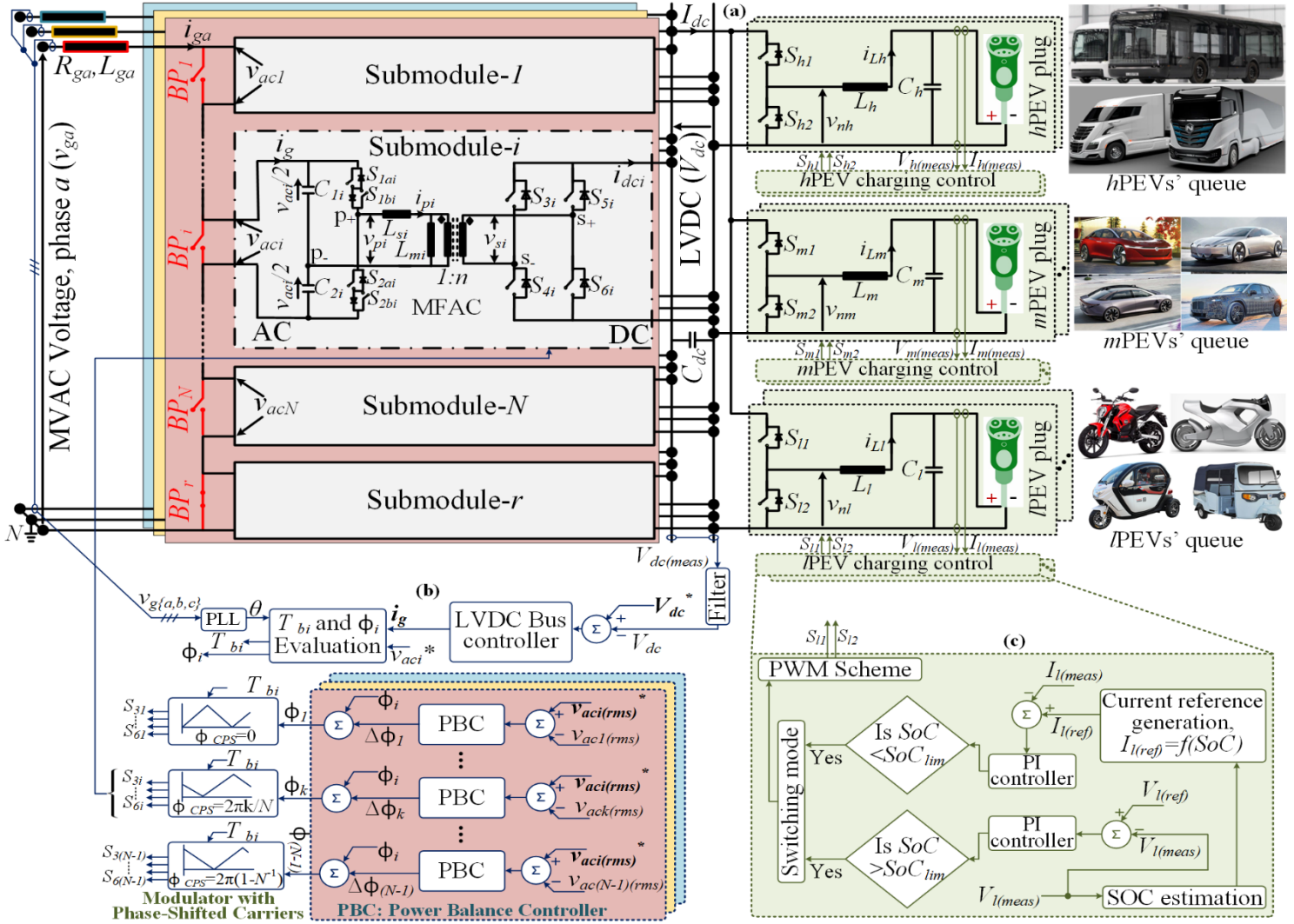

Fig 2. (a) Proposed architecture of universal public Ultra-Fast-charging/discharging station, (b) Front-end medium-voltage (MV) grid-interface MVAC-LVDC stage's control, (c) Control of BE DC-DC converter.

MODULATION AND CLOSED-LOOP CONTROL

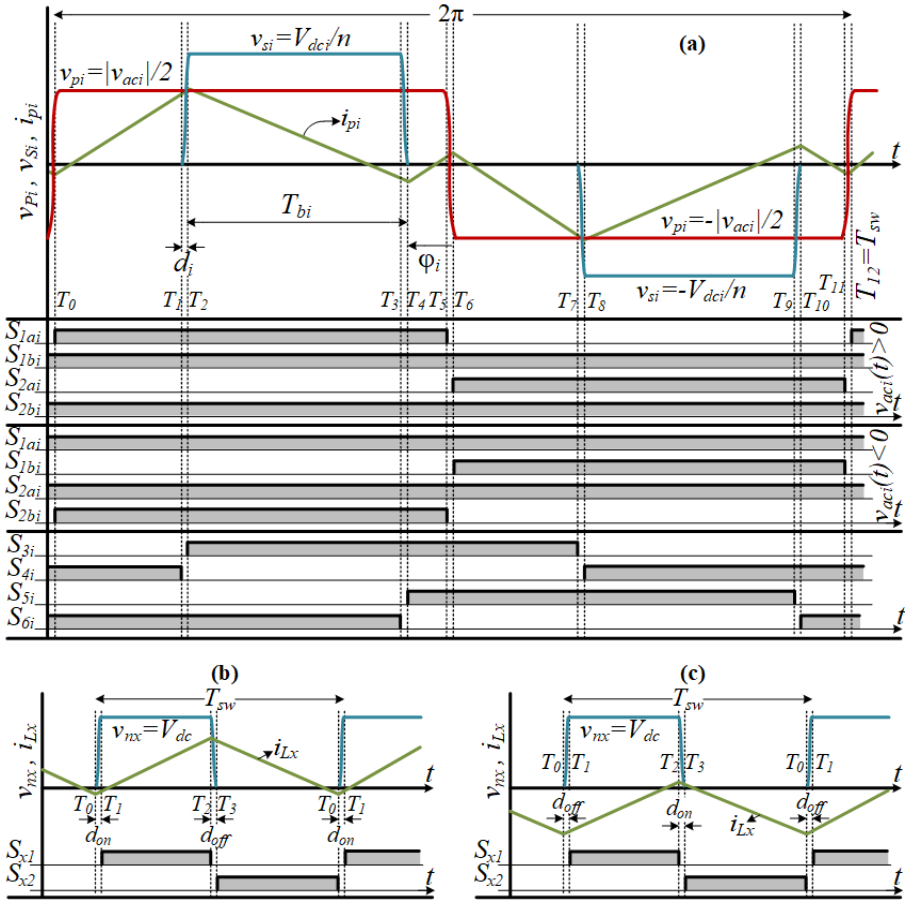

Fig 3. (a) zero-voltage-switching (ZVS) modulation of SiC-based front-end isolated AC-DC submodules of MVAC-LVDC stage; back-end DC-DC converters' ZVS modulation in (b) buck-mode during G2V, (c) boost-mode during V2G.

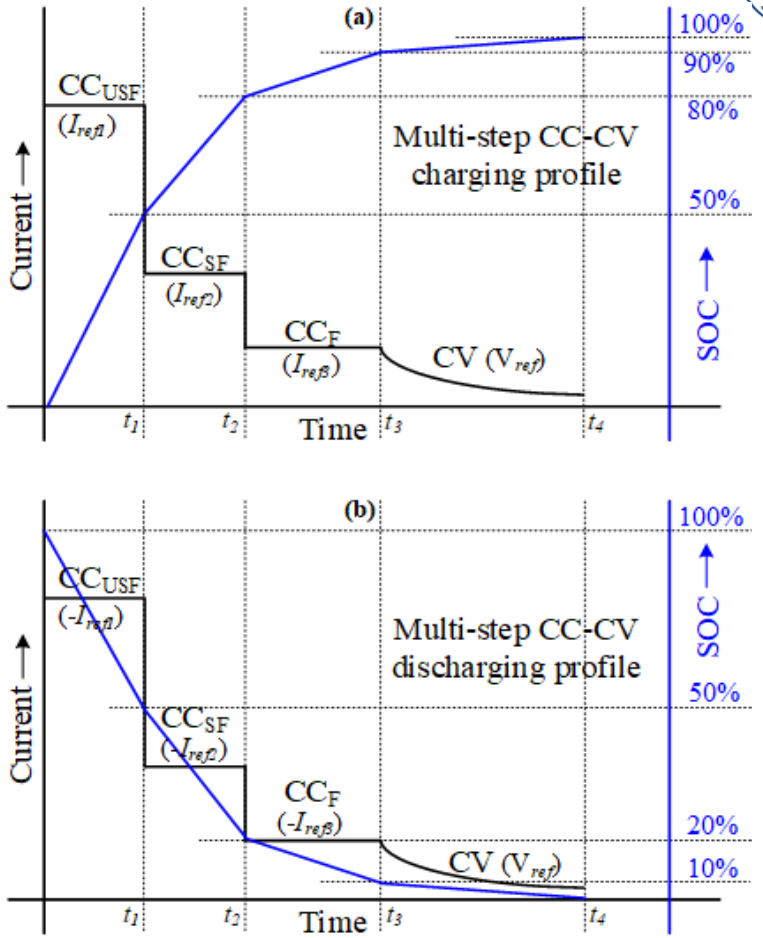

Fig 4. Current and SoC profiles of Plug-in Electric-Vehicle battery during (a) multi-step CC-CV charging (b) multi-step CC-CV discharging.

SCALED-DOWN PROTOTYPING AND PRACTICAL IMPLEMENTATION

Tab 1. Experimental setup parameters.

Parameter name	Value
Grid voltage, v_g	1 kV
Grid/line frequency, f	50 Hz
Specifications of FE MVAC-LVDC stage	
Nominal power rating, P_{FE}	13.2 kVA
Number of submodules, N	3
Grid-side voltage reference, v^*_{aci}	472.5 V(pk)
LVDC voltage, V_{dc}	0.5 kV
Switching frequency, f_{sw}	20 kHz
Leakage inductors, $\{L_{s1}, L_{s2}, L_{s3}\}$	$\{22, 20, 18\}$ μH
Phase-shift between carriers, $\phi_{CPS} = 2\pi/N$	$2\pi/3$
Grid-side filter inductor, L_g	0.5 mH
LVDC filter capacitor, C_{dc}	1.41 mF
Half-bridge capacitors, $C_{1i} = C_{2i}$	10 μF
Specifications of BE DC-DC converters	
Nominal power ratings, $\{P_h, P_m, P_l\}$	$\{5.27, 2.63, 0.66\}$ kW
Nominal bat. volt., $\{V_{h(bat)}, V_{m(bat)}, V_{l(bat)}\}$	$\{400, 200, 100\}$ V
Switching frequency, $f_{s\{h,m,l\}}$	20 kHz
Inductors, $L_{\{h,m,l\}}$	1 mH
Filter capacitors, $C_{\{h,m,l\}}$	1 mF

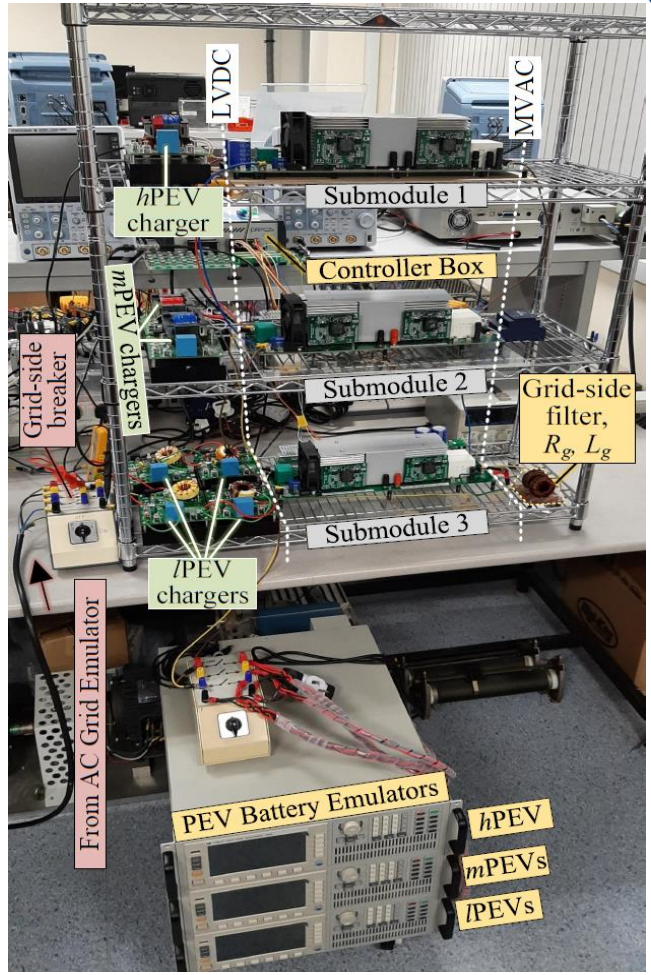

Fig 5. Scaled-down experimental setup of the proposed bidirectional EV ultra-fast charging station.

SCALED-DOWN PROTOTYPING AND PRACTICAL IMPLEMENTATION

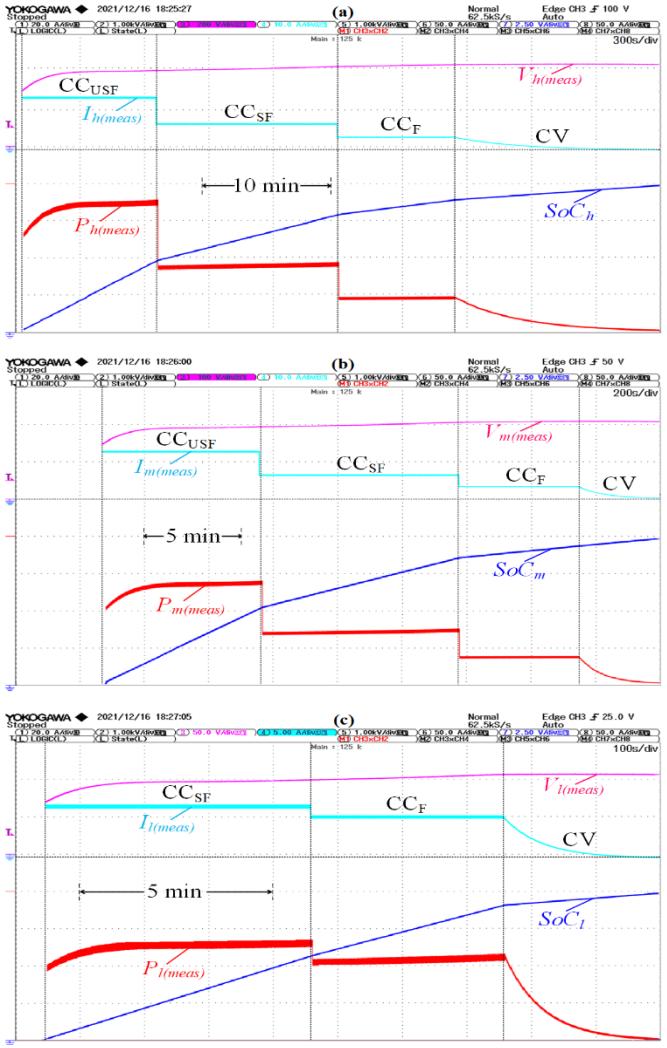

Fig 6. Experimental results of back-end side for multi-step CC-CV G2V charging of 3 types of EVs.

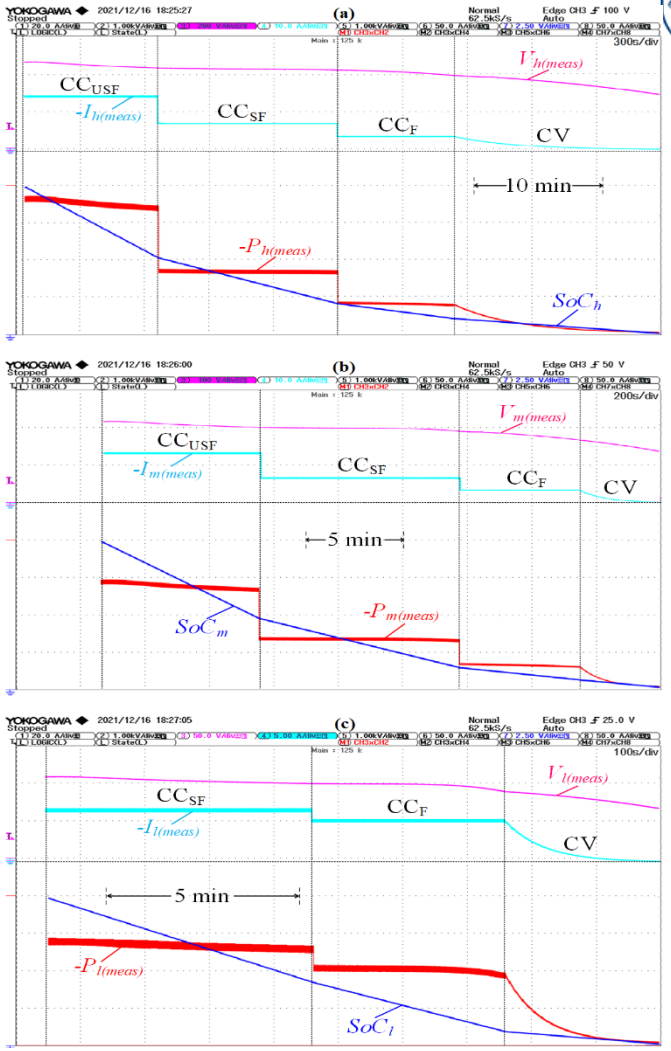

Fig 7. Experimental results of back-end side for multi-step CC-CV V2G discharging of 3 types of EVs.

SCALED-DOWN PROTOTYPING AND PRACTICAL IMPLEMENTATION

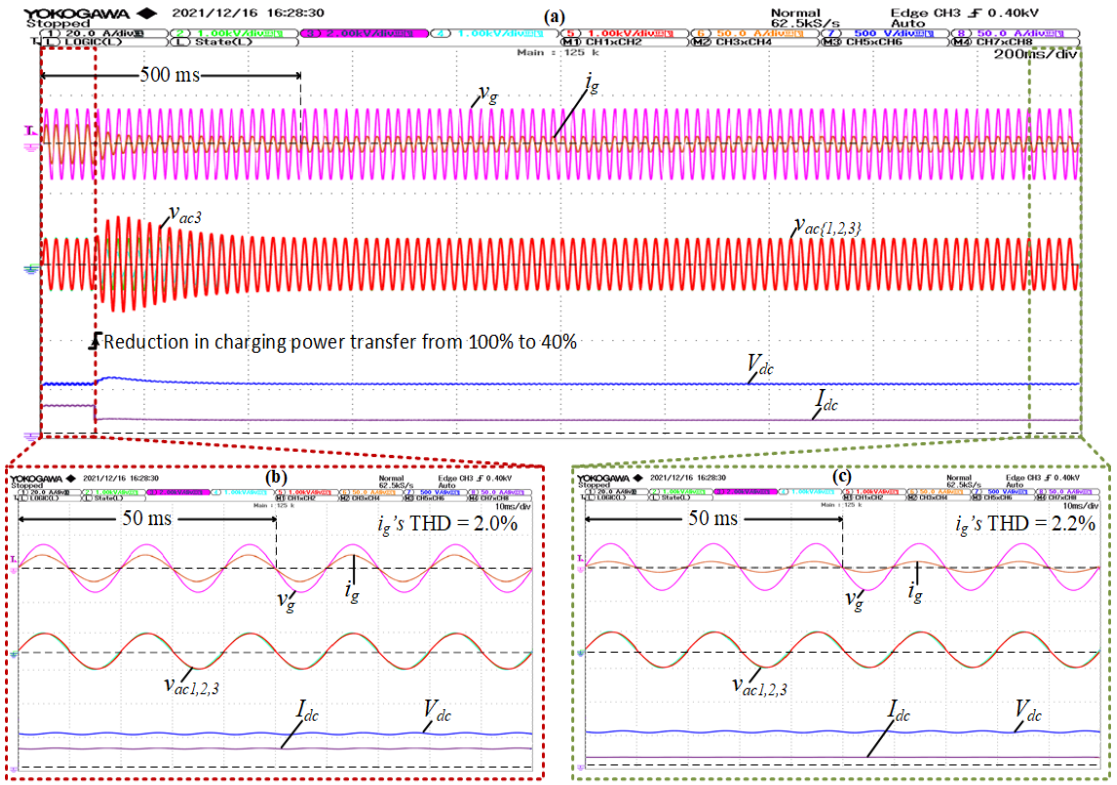

Fig 8. Experimental results of front-end side MVAC-LVDC conversion for (a) Step reduction of charging (G2V) power transfer from 100% to 40% by plugging out mPEVs and lPEVs, (b,c) steady-state conditions before and after drastic charging power transfer reduction event.

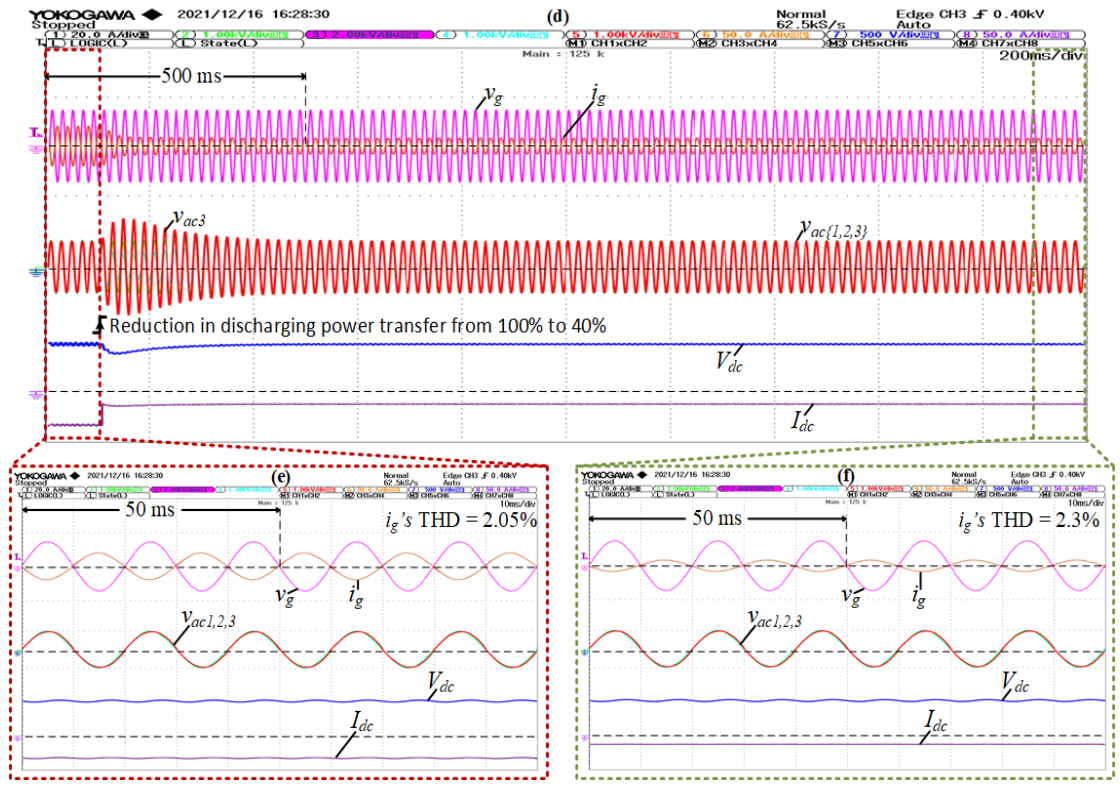

Fig 9. Experimental results of front-end side MVAC-LVDC conversion for (a) Step reduction of discharging (V2G) power transfer from 100% to 40% by plugging out mPEVs and lPEVs, (b,c) steady-state conditions before and after drastic discharging power transfer reduction event.

SCALED-DOWN PROTOTYPING AND PRACTICAL IMPLEMENTATION

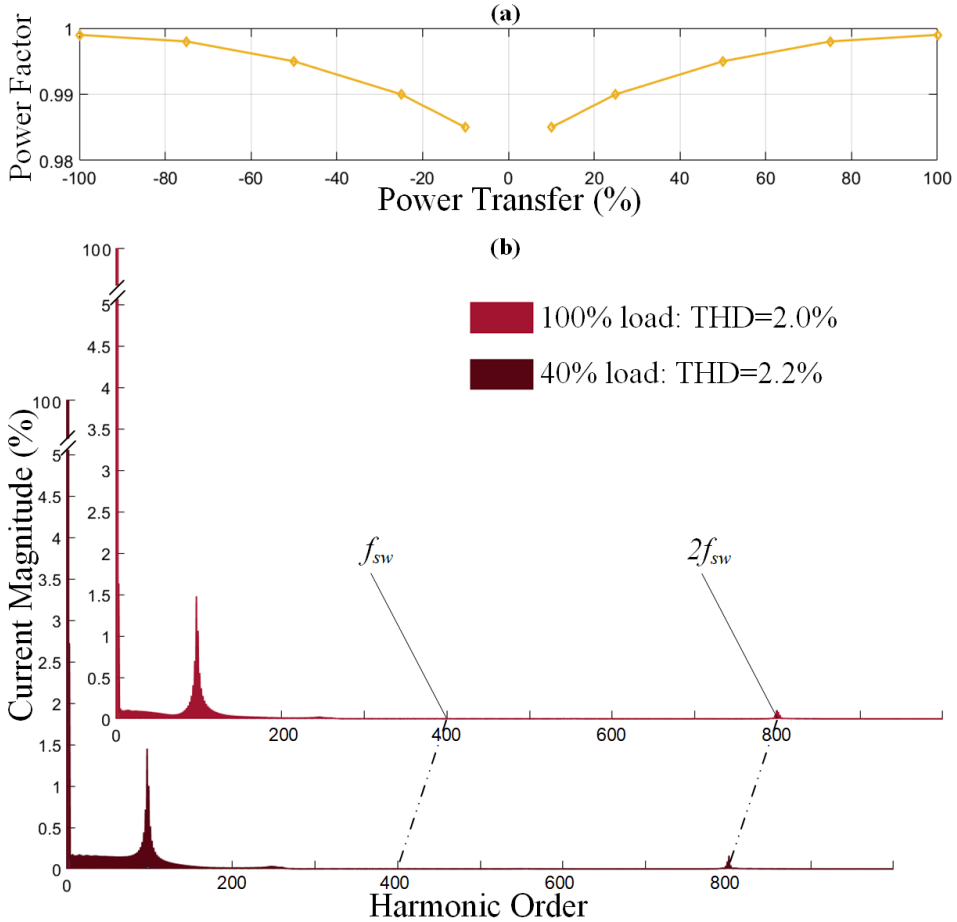

Fig 10. Experimentally measured grid-side power quality parameters using Yokogawa WT3000 precision power analyzer: (a) FE side power factor; (b) grid side current's harmonic spectrum at 100% and 40% power transfers.

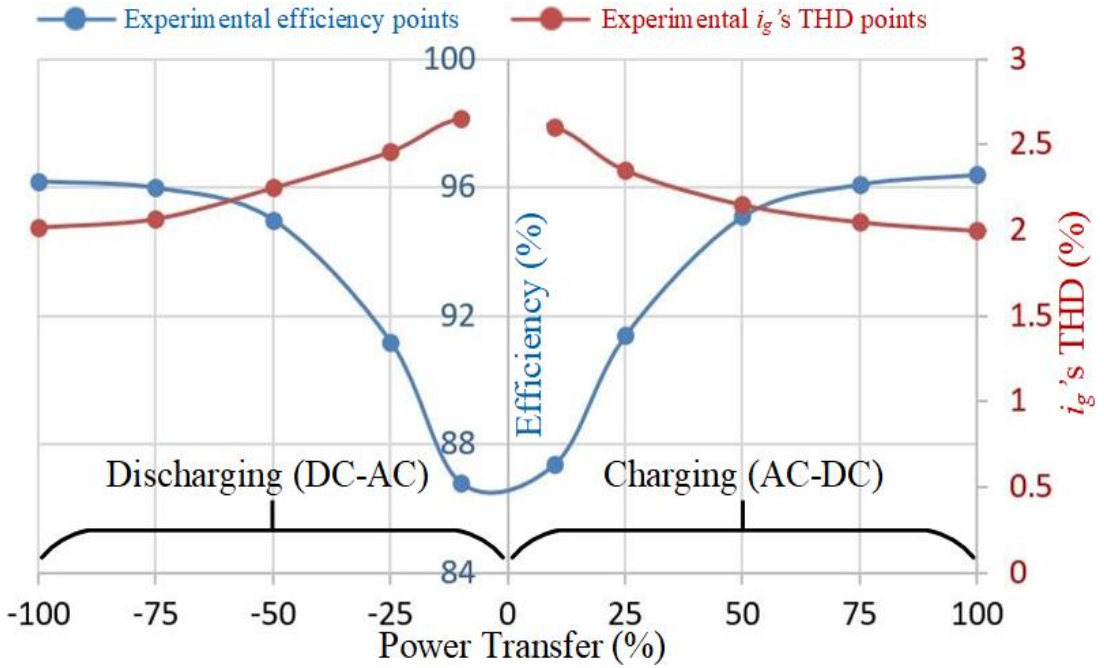

Fig 11. Experimentally obtained efficiency and grid side current's THD profiles of the bidirectional architecture's prototype during charging (G2V) and discharging (V2G).

SST BASED COMPACT EV FAST-CHARGING STATION CONCEPT

Tab 2. Benchmarking of the proposed full-scale (22 kV, 1 MVA) bidirectional EV ultra-fast-charging/discharging station with Commercialized/Certified fast-charging infrastructure products.

Manufacturer Model Status	ABB [4] Terra 53 Commercial	ABB [4] Terra HP Commercial	Tesla [4] Supercharger Commercial	EVTEC [4] espresso&charge Commercial	DELTA [17] SST-based Certified	**Proposed** **FC/dC architecture** -
Peak Power	50 kVA	350 kVA	135 kVA	150 kVA	400 kVA	**1000 kVA**
Supported PEV types	*l*PEVs, *m*PEVs	only *m*PEVs	only *m*PEVs	only *m*PEVs	only *m*PEVs	***l*PEVs, *m*PEVs** **and *h*PEVs**
Functions	only G2V	only G2V	only G2V	only G2V	only G2V	**G2V and V2G**
Grid Voltage	480 Vac	400 Vac	380-480 Vac	400 Vac	1 kVac	**22 kVac**
PEV side FC/dC DC voltage(s)	200-500 V or 50-500 V	150-900 V	50-410 V	170-500 V	200-1000 V	**400-900 V (*h*PEV)** **200-500 V (*m*PEV)** **100-300 V (*l*PEV)**
PEV side peak DC current(s)	120 A	375 A	330 A	300 A	400 A or 500 A	**500 A (*h*PEV)** **500 A (*m*PEV)** **250 A (*l*PEV)**
Peak Efficiency	94%	94.5%	91%	93%	96%	**>96.4%**
Power Density	0.07 kVA/L	0.2 kVA/L	0.14 kVA/L	0.1 kVA/L	~1.2 kVA/L	**~3 kVA/L**
Time required to add range of 200 miles	- 72 min (*m*PEV) 20 min (*l*PEV)	- 16 min (*m*PEV) -	- 28 min (*m*PEV) -	- 24 min (*m*PEV) -	- 16 min (*m*PEV) -	**49.5 min (1 *h*PEV)+** **28 min (2 *m*PEVs)+** **16 min (4 *l*PEVs)**

MULTI-OBJECTIVE OPTIMAL ANALYTICAL BALANCE CONTROL

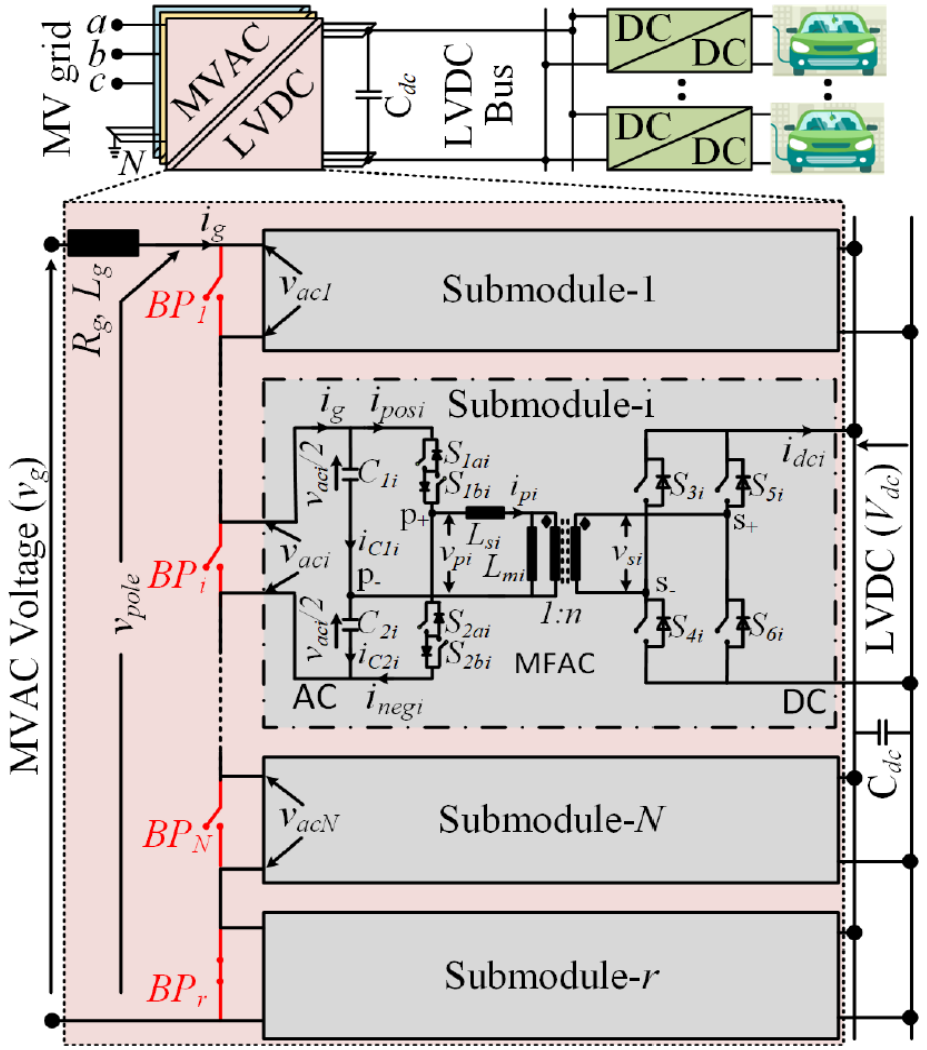

Fig 12. Schematic of the Single-stage MVAC-LVDC SST within a MV utility-grid interfaced EV-UFCS.

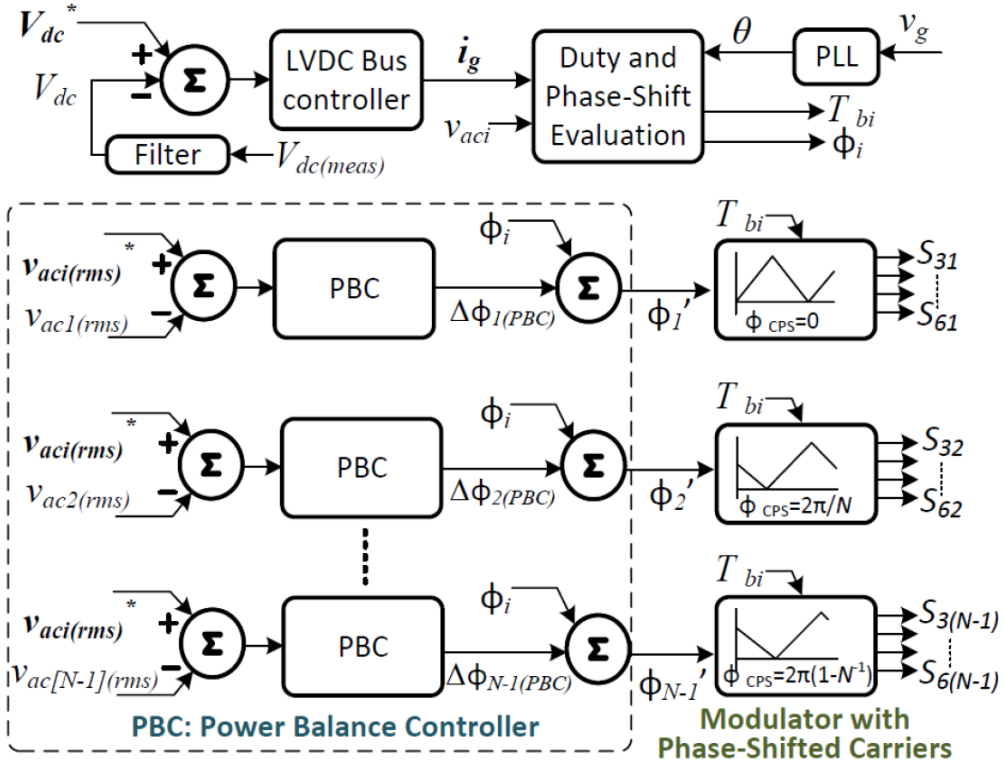

Fig 13. Conventional PBC strategy to remediate power imbalance amongst single-stage submodules in MVAC-LVDC solid-state-transformer.

MULTI-OBJECTIVE OPTIMAL ANALYTICAL BALANCE CONTROL

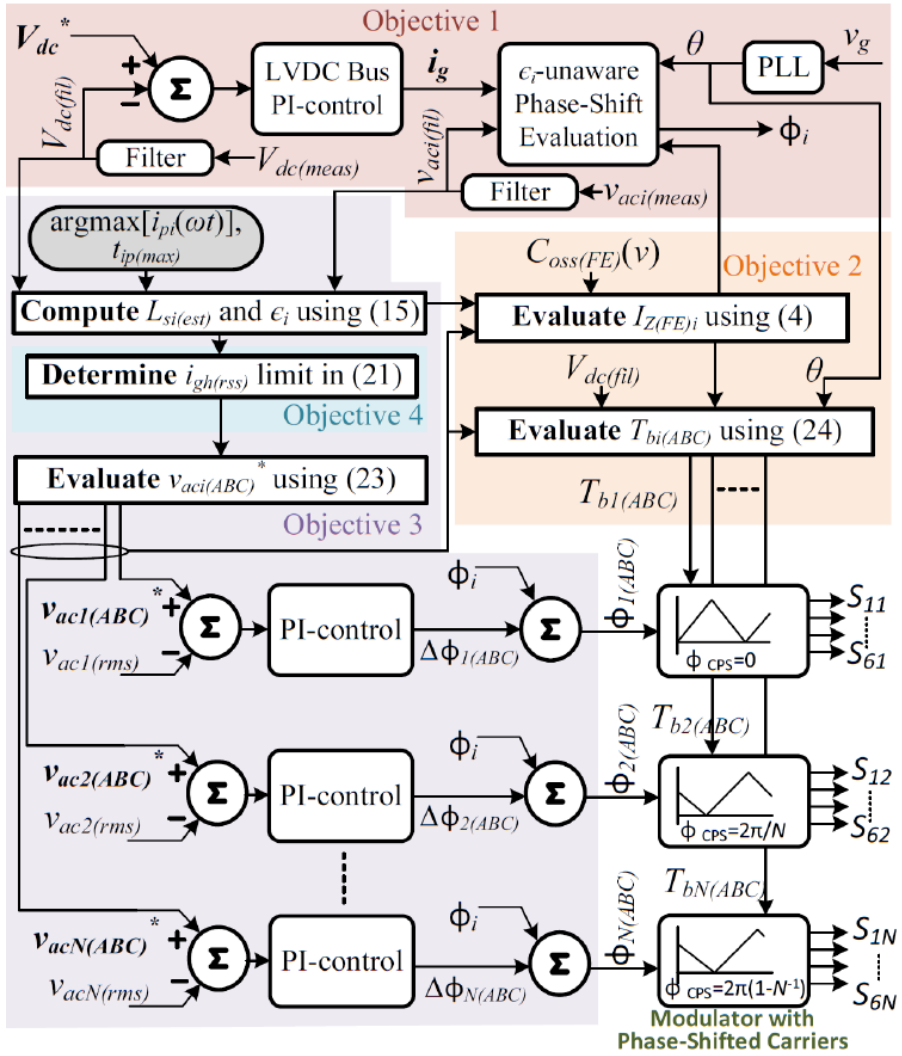

Fig 14. Schematic of the Single-stage MVAC-LVDC SST within a MV utility-grid interfaced EV-UFCS.

- Maintaining LVDC bus voltage at reference V_{dc}*;
- Achieving complete ZVS of all front-end (FE) side MOSFETs;
- Maximizing ZVS range of back-end (BE) side MOSFETs of each submodule and minimizing the difference in the constituting submodules' losses;
- Restricting $i_{gh(rss)}$ within grid-code limits

Condition for restricting current harmonics to grid-code limits:

$$i_{gh(rss)} = \sqrt{\sum_{k=2}^{10f_{sw}} i_{ghk}^2} = 4.9\% \cdot i_{g1}, \qquad (21)$$

Expression for submodules' optimal grid-side reference voltages:

$$v^*_{aci(ABC)} = \frac{v_{g(rms)}}{N} + \left\{ 0.049 \cdot \frac{i_{g1}}{\sqrt{2}} (\omega_h L_g) \cdot \frac{\epsilon_i}{\sum_{i=1}^{N} |\epsilon_i|} \right\}. \qquad (23)$$

Each submodule's optimal pulse-width expression:

$$T_{bi(ABC)} = \frac{n|v^*_{aci(ABC)}|(\pi/2 - d_i) - 2n\omega_s L_{si(est)} I_{Z(FE)i}}{V_{dc(fil)}}. \qquad (24)$$

MULTI-OBJECTIVE OPTIMAL ANALYTICAL BALANCE CONTROL

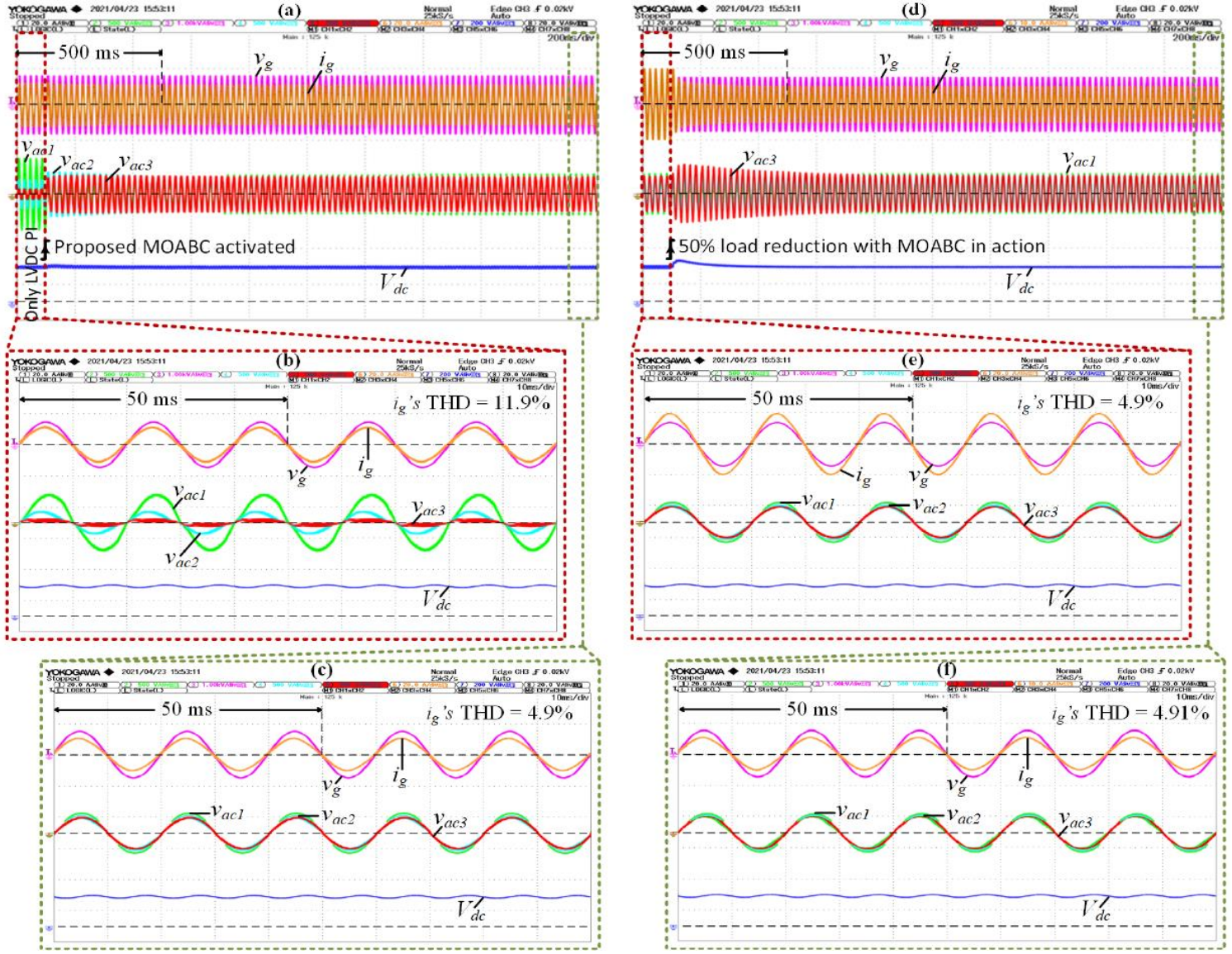

Fig 15. Experimental results: (a) Proposed MOABC's activation replacing LVDC bus voltage PI control at 100% load, (b,c) steady-state conditions before and after MOABC activation.

MULTI-OBJECTIVE OPTIMAL ANALYTICAL BALANCE CONTROL

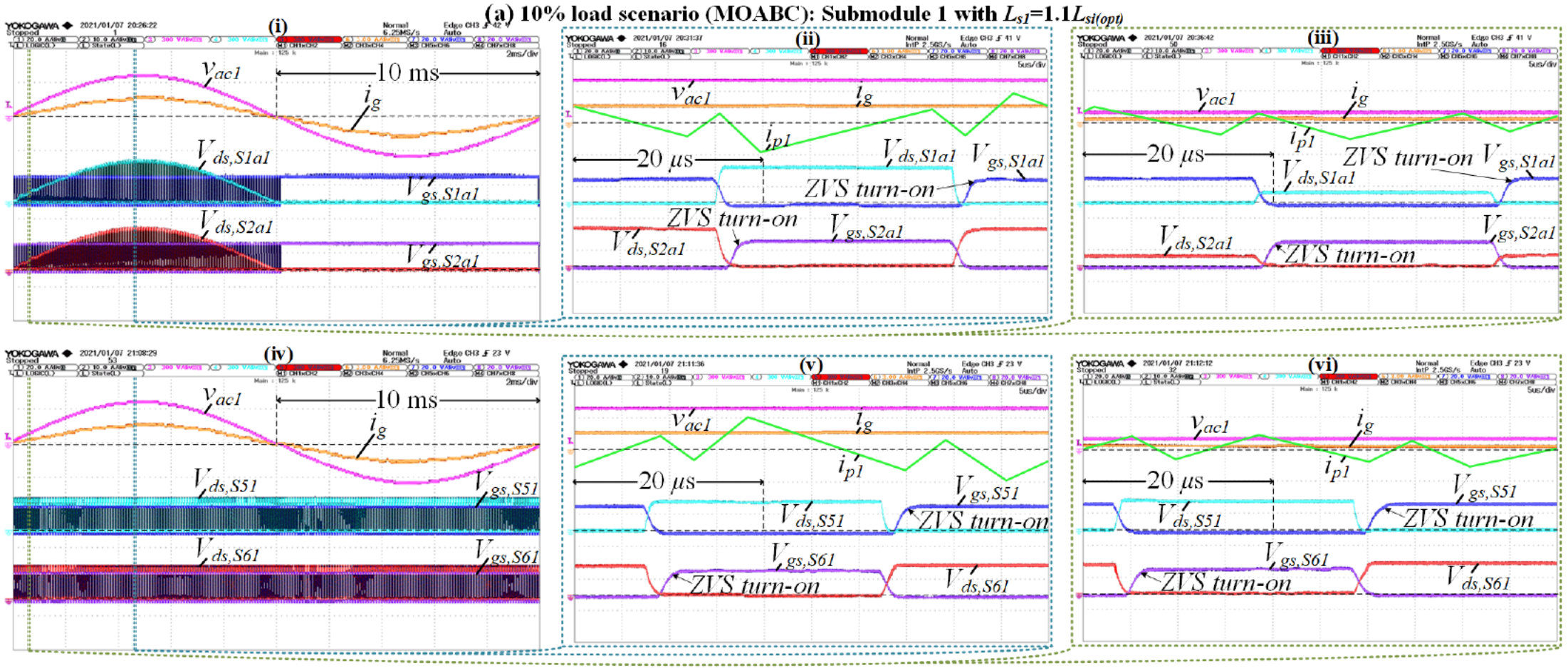

Fig 16. Experimental results of MOABC's action at 10% load in (a) submodule 1 with L_{s1}=1.1$L_{si(opt)}$, where, FE MOSFETs' complete ZVS switching are shown in (i) zoomed-out, and (ii), (iii) zoomed-in at $v_{aci}(t)=V_{aci}$ and $v_{aci}(t)=0.25V_{aci}$ respectively, and BE MOSFETs' near full-cycle ZVS switching are shown in (iv) zoomed-out, and (v), (vi) zoomed-in at $v_{aci}(t)=V_{aci}$ and $v_{aci}(t)=0.25V_{aci}$ respectively.

MULTI-OBJECTIVE OPTIMAL ANALYTICAL BALANCE CONTROL

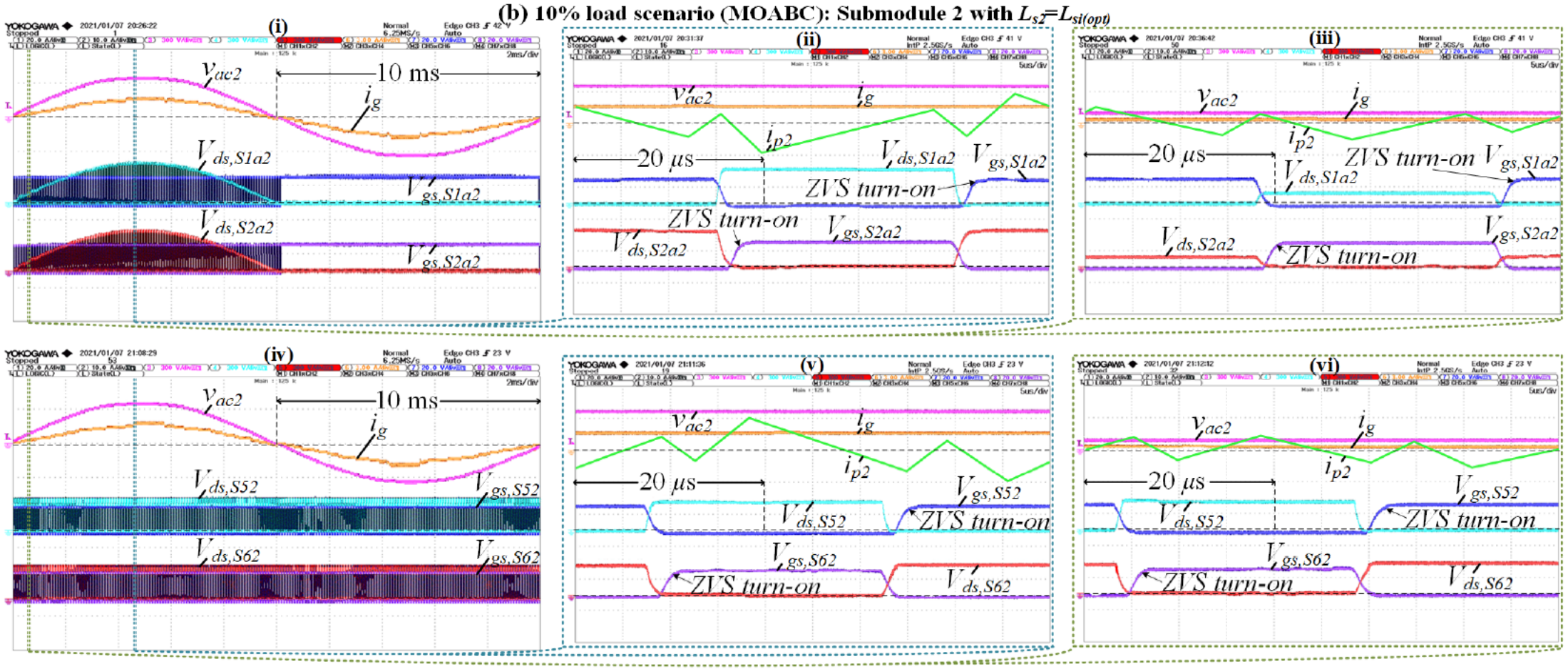

Fig 16. Experimental results of MOABC's action at 10% load in (b) submodule 2 with $L_{s2}=L_{si(opt)}$, where, FE MOSFETs' complete ZVS switching are shown in (i) zoomed-out, and (ii), (iii) zoomed-in at $v_{aci}(t)=V_{aci}$ and $v_{aci}(t)=0.25V_{aci}$ respectively, and BE MOSFETs' near full-cycle ZVS switching are shown in (iv) zoomed-out, and (v), (vi) zoomed-in at $v_{aci}(t)=V_{aci}$ and $v_{aci}(t)=0.25V_{aci}$ respectively.

MULTI-OBJECTIVE OPTIMAL ANALYTICAL BALANCE CONTROL

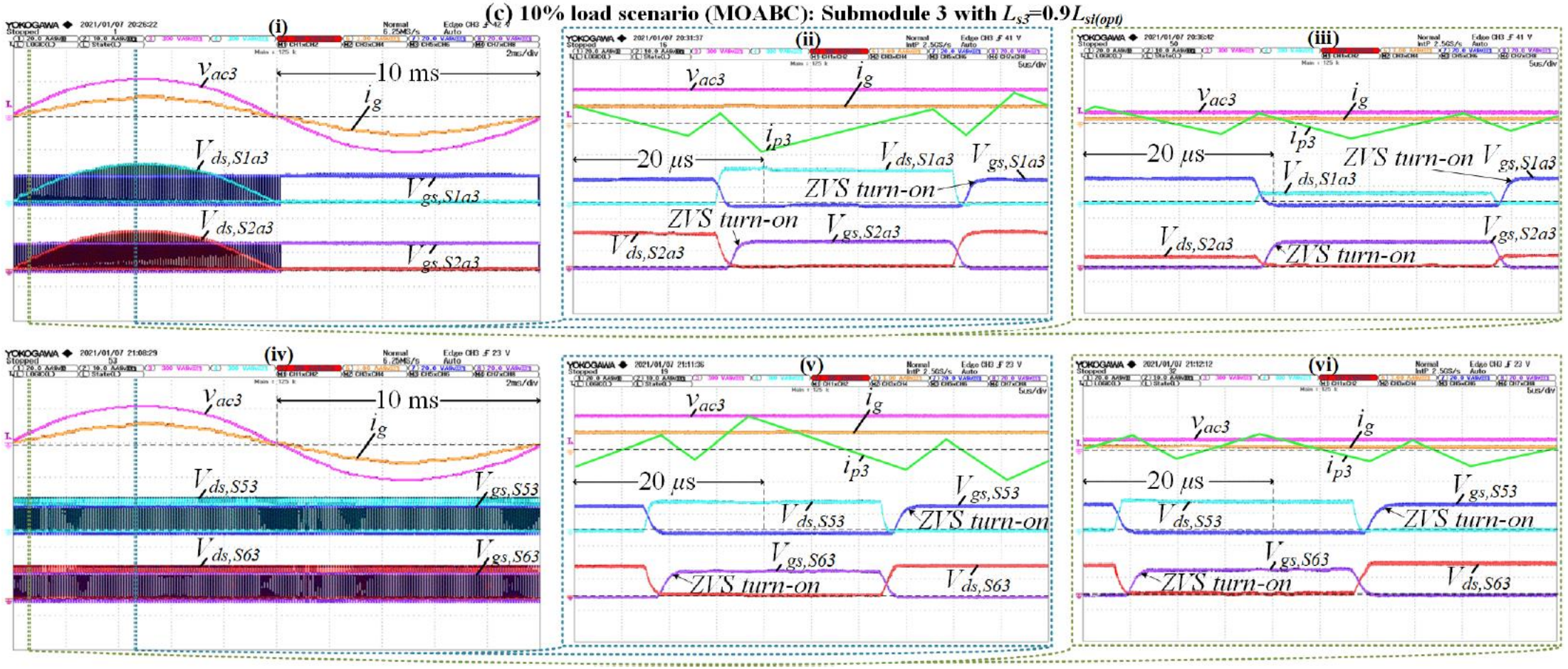

Fig 16. Experimental results of MOABC's action at 10% load in (c) submodule 3 with L_{s3}=0.9$L_{si(opt)}$, where, FE MOSFETs' complete ZVS switching are shown in (i) zoomed-out, and (ii), (iii) zoomed-in at $v_{aci}(t)=V_{aci}$ and $v_{aci}(t)=0.25V_{aci}$ respectively, and BE MOSFETs' near full-cycle ZVS switching are shown in (iv) zoomed-out, and (v), (vi) zoomed-in at $v_{aci}(t)=V_{aci}$ and $v_{aci}(t)=0.25V_{aci}$ respectively.

MULTI-OBJECTIVE OPTIMAL ANALYTICAL BALANCE CONTROL

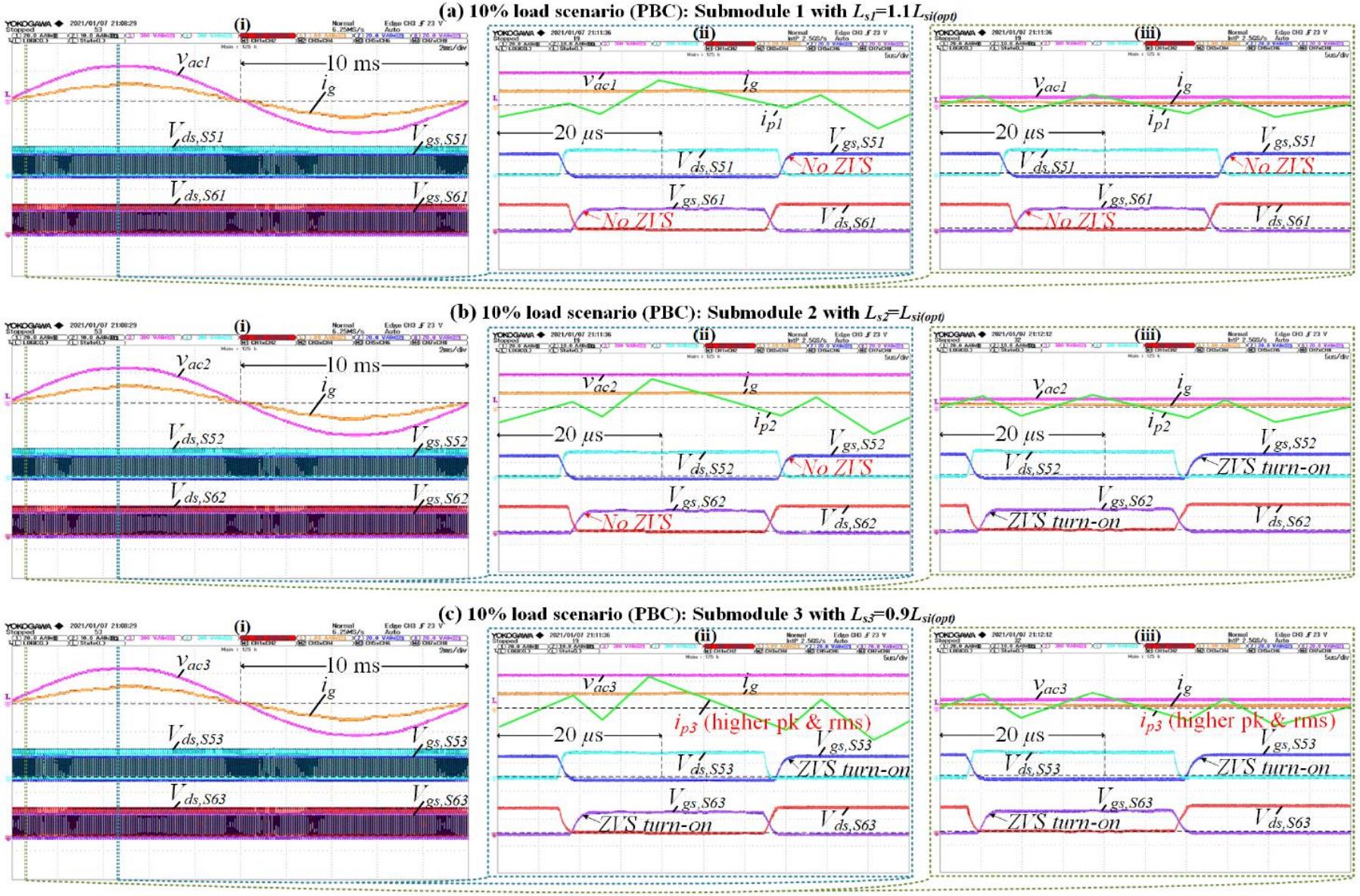

Fig 17. Experimental results of PBC's action (in contrast to MOABC's action) at 10% load in (a) submodule 1 with L_{s1}=1.1$L_{si(opt)}$, (b) submodule 2 with L_{s2}=$L_{si(opt)}$, and (c) submodule 3 with L_{s3}=0.9$L_{si(opt)}$, where, BE MOSFETs' ZVS switching are shown in (i) zoomed-out, and (ii), (iii) zoomed-in at $v_{aci}(t)$=V_{aci} and $v_{aci}(t)$=0.25V_{aci} respectively.

MULTI-OBJECTIVE OPTIMAL ANALYTICAL BALANCE CONTROL

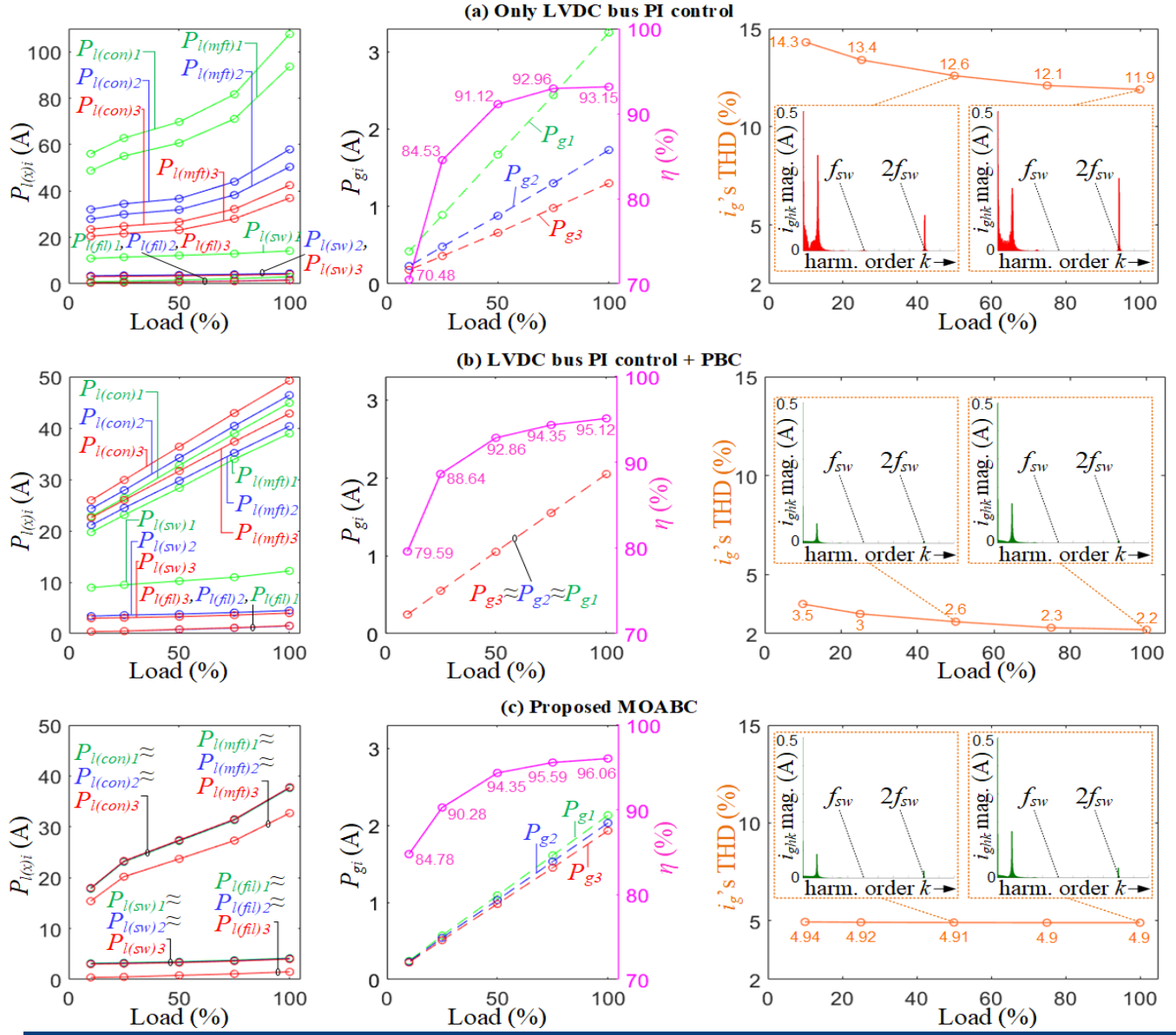

Fig 18. Comparative experimental results: (a) Only LVDC bus PI control in action, (b) LVDC bus PI control with augmented PBC in action, and (c) proposed MOABC in action, with clear presentations of loss breakdowns and grid-side power drawn for constituting submodules, overall efficiency and i_g's THD.

TAKEAWAY-POINTS

- A futuristic MV grid-connected bidirectional FC/dC station architecture is proposed for facilitating bidirectional (G2V and V2G) functionality for all three PEV categories (*h*PEVs, *m*PEVs and *l*PEVs). An explanation for power electronics topology is given, along with the important features of the modulation schemes and control schemes for the front-end MVAC-LVDC conversion stage and back-end DC-DC converters for interfacing with the PEVs.

- Experimental results validate the merits of the proposed modulation, control strategies, SoC estimation technique and adherence to multi-step CC-CV charging schedules; experimental efficiency and grid current's THD profiles are presented that show a peak efficiency of 96.4% and current THD restricted within 2.65%, whereas, the measured power density of the prototype is >3 kVA/L.

- It can be observed from the benchmarking with other FC products that the proposed MV grid-connected fast-charging/discharging architecture is not only expected to provide superior efficiency and power density, but also dual functionality of G2V and V2G as well as low dwell times for all three PEV categories - such distinct advantages are also not available jointly in any proposed architecture in the literature.

- A proposed multi-objective analytical balance control is capable of not only ensuring complete ZVS for front-end and back-end MOSFETs for wide load range, but also capable of restricting the grid-side current harmonics within the standard-prescribed grid-code limits.

RELEVANT PUBLICATIONS

Journals

1. ***Jaydeep Saha**, Nishant Kumar and **Sanjib Kumar Panda**, "A Futuristic Silicon-Carbide (SiC) Based Electric-Vehicle Fast Charging/Discharging (FC/dC) Station," in IEEE Journ. of Emerg. & Selec. Top. in Power Electronics, 2022.*
2. ***Jaydeep Saha**, Nishant Kumar Naga Brahmendra Yadav Gorla and **Sanjib Kumar Panda**, "Closed-form Solution for Multi-Objective Optimal Analytical Balance Control for a Single-Stage Isolated MVAC-LVDC Converter in an Electric-Vehicle Ultra-Fast Charging-Station," in IEEE Transactions on Transport. Electrific., 2024.*
3. ***Jaydeep Saha** and **Sanjib Kumar Panda**, "Overview and comparative analysis of bidirectional cascaded modular isolated medium-voltage ac - low-voltage dc (mvac-lvdc) power conversion for renewable energy rich microgrids," Renew. and Sust. Ener. Rev., Mar. 2023.*
4. ***Jaydeep Saha**, Naga Brahmendra Yadav Gorla, Aravinth Subramaniam and **Sanjib Kumar Panda**, "Analysis of Modulation and Optimal Design Methodology for Half-Bridge Matrix-Based Dual-Active-Bridge (MB-DAB) AC-DC Converter," in IEEE Journ. of Emerg. & Selec. Top. in Power Electronics, vol. 10, no. 1, pp. 881-894, Feb. 2022.*
5. ***Jaydeep Saha**, Naga Brahmendra Yadav Gorla and **Sanjib Kumar Panda**, "Implementation of Power Balance Control Scheme for a Cascaded Matrix-Based Dual-Active-Bridge (CMB-DAB) MVAC-LVDC Converter," in IEEE Transactions on Industry Applications, vol. 58, no. 1, Jan. 2022.*
6. ***Jaydeep Saha**, Naga Brahmendra Yadav Gorla and Sanjib Kumar Panda, "Analytical Expression-Based Modulation for Soft-Switched Matrix-Based Dual-Active-Bridge (S^2MB-DAB) Single-Phase AC-DC Converter," in IEEE Journ. of Emerg. & Selec. Top. in Power Electronics, vol. 10, no. 6, pp. 6511-6522, Dec. 2022.*

Conferences

1. ***Jaydeep Saha,** P. Sundararajan and **Sanjib Kumar Panda**, "Evaluation of Closed-loop Control Techniques for Single-stage MVAC-LVDC Solid-State-Transformers in Compact EV Ultra-Fast Charging Stations," 2024 IEEE 10th International Power Electronics and Motion Control Conference (IPEMC2024-ECCE Asia), Chengdu, China, 2024, pp. 182-187.*
2. ***Jaydeep Saha,** Diptak Pal and **Sanjib Kumar Panda**, "Evolutionary Optimization Algorithm Based Optimal Tuning of Cascaded Control Scheme for Single-Stage AC-DC Solid-State-Transformers," 2024 IEEE 10th International Power Electronics and Motion Control Conference (IPEMC2024-ECCE Asia), Chengdu, China, 2024, pp. 188-193.*
3. ***Jaydeep Saha**, Nishant Kumar and **Sanjib Kumar Panda**, "A Grid-Supportive Current Ramp-Rate Constrained (GS-CR2C) Control Strategy for a SST-Based Bidirectional Multi-Port Fast-Charging Station," 2022 IEEE International Conference on Power Electronics, Drives and Energy Systems (PEDES), Jaipur, India, 2022, pp. 1-6.*
4. ***Jaydeep Saha**, Naga Brahmendra Yadav Gorla and **Sanjib Kumar Panda**, "Comparative Overview of Power Balance Control for Two-stage and Single-stage Isolated MVAC-LVDC Cascaded Converters," in IEEE 13th Energy Conversion Congress and Exposition – Asia (ECCE-Asia), 2022.*
5. ***Jaydeep Saha**, Naga Brahmendra Yadav Gorla and **Sanjib Kumar Panda**, "Modulation of Direct Matrix-Based Dual-Active- Bridge (MB-DAB) AC-DC Converters," in IEEE 12th Energy Conversion Congress and Exposition – Asia (ECCE-Asia), 2021, pp. 74-79 [virtual] **– Best Paper Award.***
6. ***Jaydeep Saha**, Aravinth Subramaniam and Sanjib Kumar Panda, "Design of Integrated Medium Frequency Transformer (iMFT) for Dual-Active-Bridge (DAB) Based Solid-State-Transformers," in IEEE 12th Energy Conversion Congress and Exposition – Asia (ECCE-Asia), 2021, pp. 893-898 [virtual].*
7. ***Jaydeep Saha**, Naga Brahmendra Yadav Gorla and **Sanjib Kumar Panda**, "Power Balance Control of Cascaded Matrix-Based Dual-Active-Bridge Converter," in 2020 IEEE International Conference on Power Electronics, Drives and Energy Systems (PEDES), 2020, pp. 1-6 [virtual].*
8. ***Jaydeep Saha**, Naga Brahmendra Yadav Gorla and **Sanjib Kumar Panda**, "A Bidirectional Matrix-Based AC-DC Dual-Active Bridge for Modular Solid-State-Transformers," in IECON 2020, Singapore, Singapore, 2020, pp. 1136-1141 [virtual]."*

Tutorial Topic: Emerging Solid-State-Transformer based Electric-Vehicle Ultra-fast Charging Station

Machine-Learning Aided Design Optimization of Grid-Interface

Tutorial Presentation, IEEE SPEC, 2024, Brisbane

Dr. Jaydeep Saha

Assistant Principal Engineer
ST Engineering Satellite Systems
Ex-Research Fellow
National University of Singapore

IEEE Member

CONTENTS

- Introduction
- Grid-interface Design Optimization Framework
- Optimization Routine and Results
- Scaled-down Validation of the Proposed Framework
- Conclusion

RECAP: UNIVERSAL EV FAST-CHARGING STATION

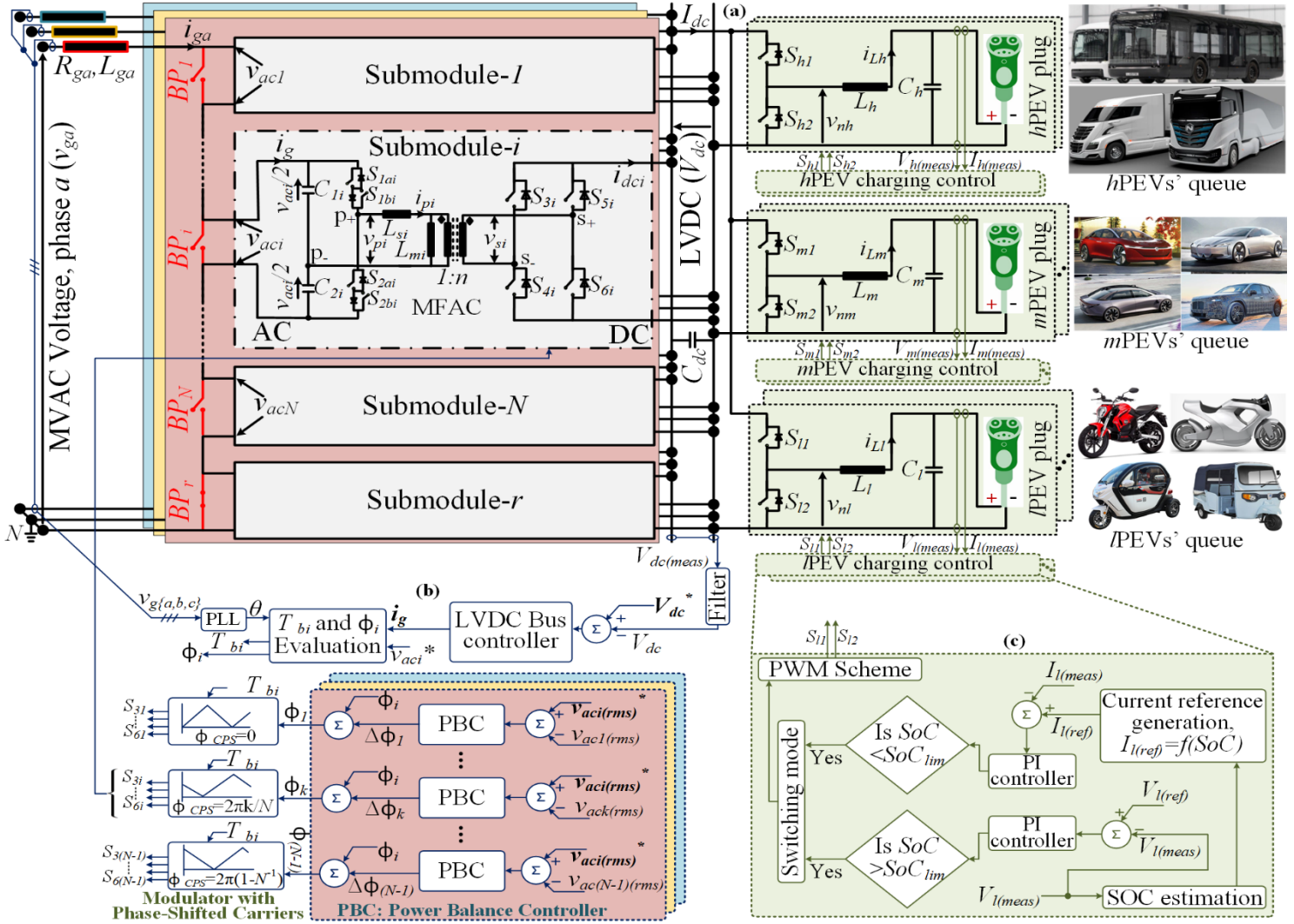

Fig 1. (a) Proposed architecture of universal public Ultra-Fast-charging/discharging station, (b) Front-end medium-voltage (MV) grid-interface MVAC-LVDC stage's control, (c) Control of BE DC-DC converter.

INTRODUCTION: SCOPE OF DESIGN OPTIMIZATION

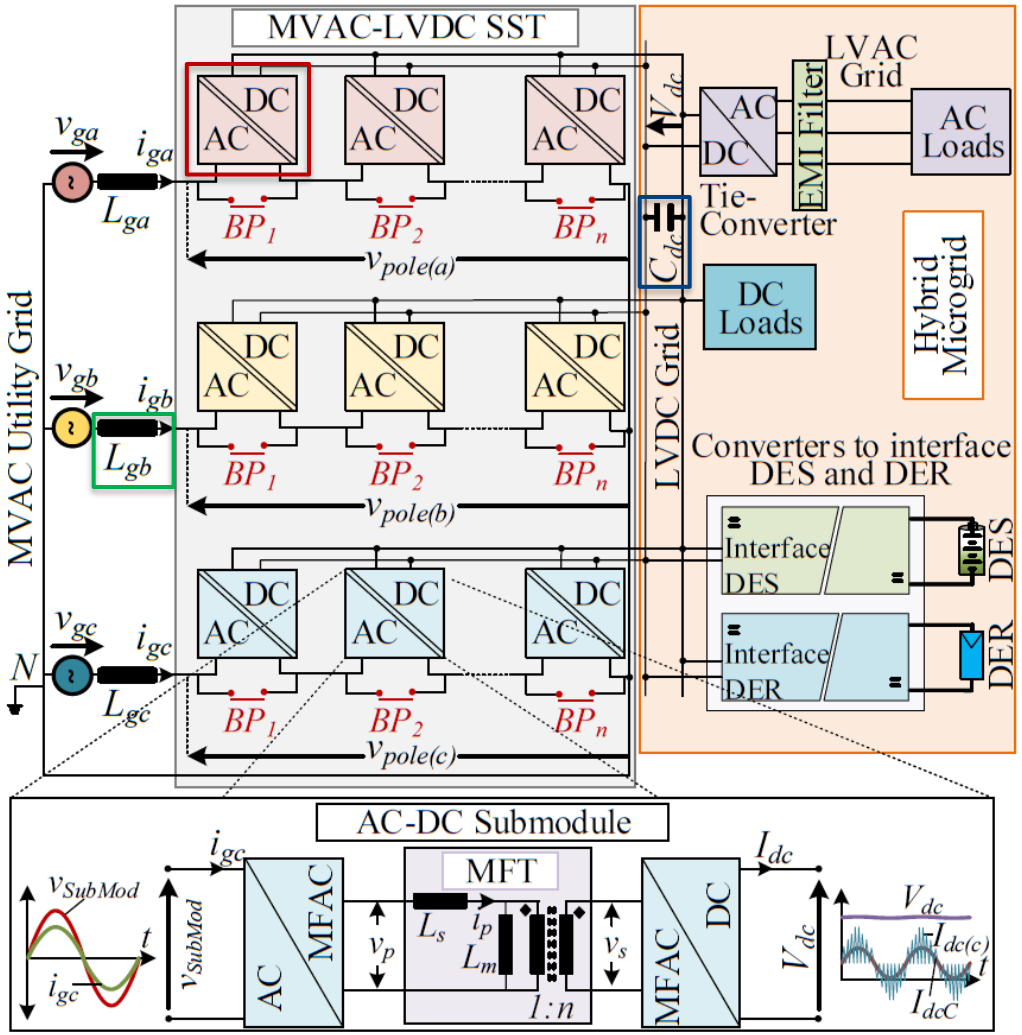

Fig 2. Schematic of a MVAC-LVDC Modular SST

- AC-DC Submodule: Semiconductor devices, MFT, Passive Components
- AC Filter Inductor: Core, winding, turns
- DC Filter Capacitor: Uniform **(negligible scope)**

✓ Efficiency (η)

✓ Power Density (ρ)

✗ Cost (σ)

INTRODUCTION: EFFORTS SO FAR IN THE LITERATURE

- Efforts have been presented to optimise the design of medium-frequency transformer (MFT) for SST applications [1], [2] - developed frameworks are dedicated to Pareto optimize the MFT's design for given specifications, and thus **doesn't consider their effect on the semiconductor's performance**

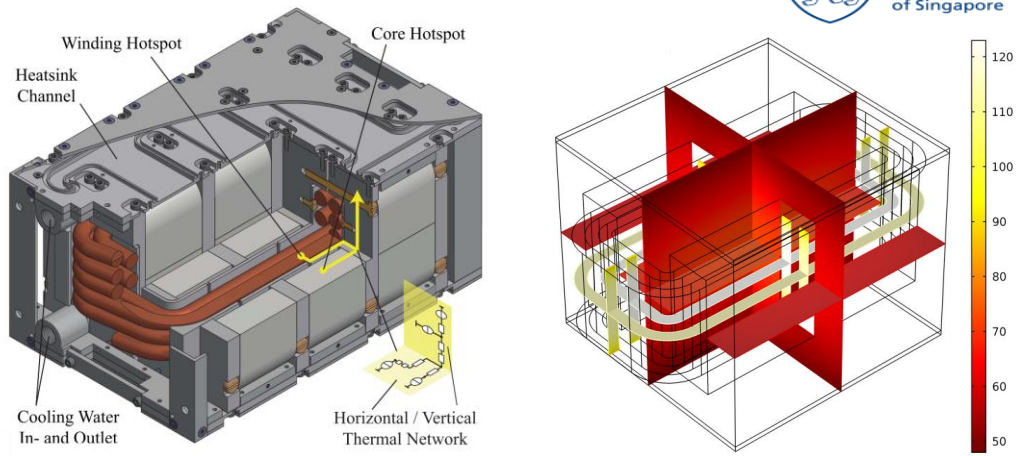

- A workflow has been developed that uses FEM simulation data to train regression artificial neural networks (ANNs) [3] for the magnetic and thermal modeling of a dc–dc converter's inductor during its design selection process – **requires GPUs and just optimizes one passive component's design**

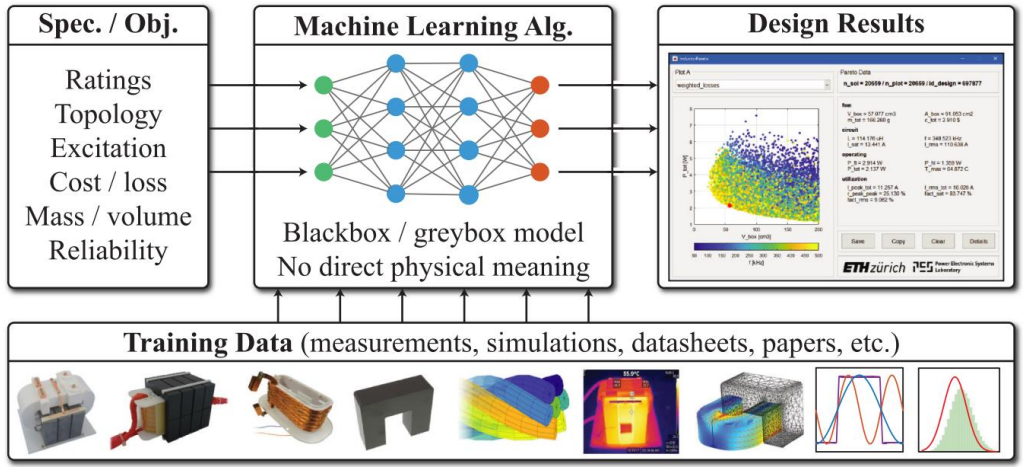

[1] M. Leibl, G. Ortiz, and J. W. Kolar, "Design and experimental analysis of a medium-frequency transformer for solid-state transformer applications," IEEE J. Emerg. Sel. Topics Power Electron., vol. 5, no. 1, pp. 110–123, Mar. 2017.
[2] M. Mogorovic and D. Dujic, "100 kW, 10 kHz medium frequency transformer design optimization and experimental verification," IEEE Trans. Power Electron., vol. 34, no. 2, pp. 1696–1708, Feb. 2019.
[3] T. Guillod, P. Papamanolis and J. W. Kolar, "Artificial Neural Network (ANN) Based Fast and Accurate Inductor Modeling and Design," in IEEE Open Journal of Power Electronics, vol. 1, pp. 284-299, 2020.

INTRODUCTION: EFFORTS SO FAR IN THE LITERATURE

- Pareto optimization of IGBT-based MV non-isolated cascaded H-bridge (CHB) rectifier [4], [5] has been presented, and thus, it **does not include the additional complexities of isolation transformer design**

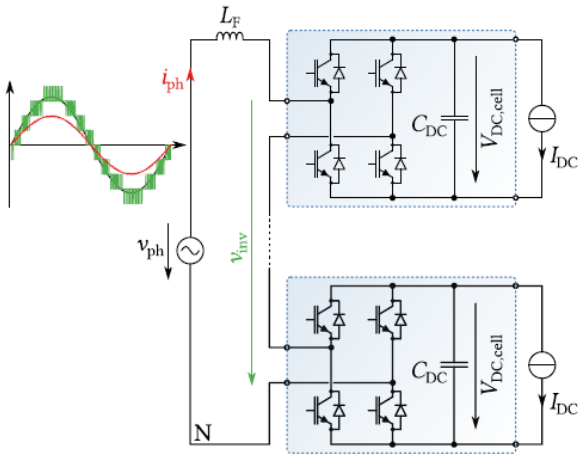

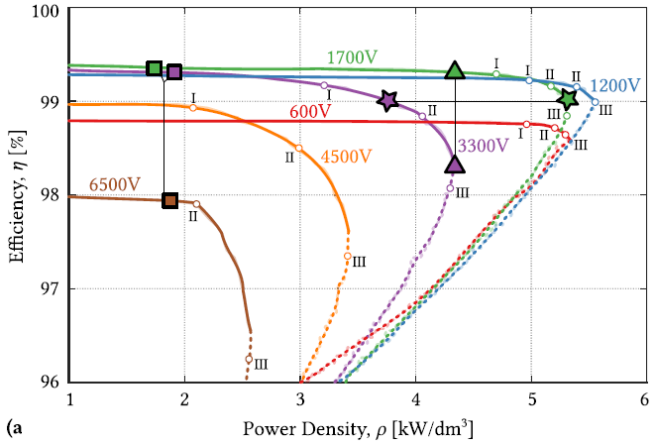

Due to the lack of a comprehensive multi-objective solid-state transformer (SST) design framework, **SST designs are mostly obtained through trial/experience**.

[4] J. E. Huber and J. W. Kolar, "Optimum number of cascaded cells for high-power medium-voltage AC–DC converters," IEEE J. Emerg. Sel. Topics Power Electron., vol. 5, no. 1, pp. 213–232, Mar. 2017.
[5] J. E. Huber, "Conceptualisation and multi-objective analysis of multi-cell solid-state transformers," Ph.D. dissertation, HC-DCM SRC Isolation Stage, ETH Zurich, Zürich, Switzerland, 2016.

MVAC-LVDC SST DESIGN OPTIMIZATION FRAMEWORK

Critical Design Objectives:

✔ Efficiency (η) ✔ Power Density (ρ)

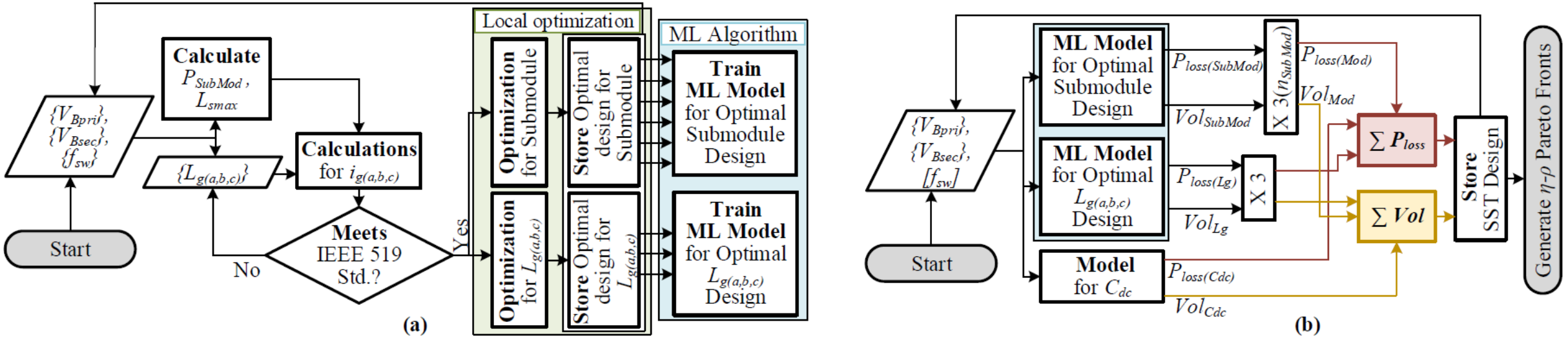

Fig 3. Machine-learning aided optimization framework a. Training η-ρ locally optimal AC-DC submodule and AC filter inductor designs b. η-ρ Pareto front generations for Optimal SST Designs.

OPTIMIZATION ROUTINE FOR A 1-STAGE MVAC-LVDC SST

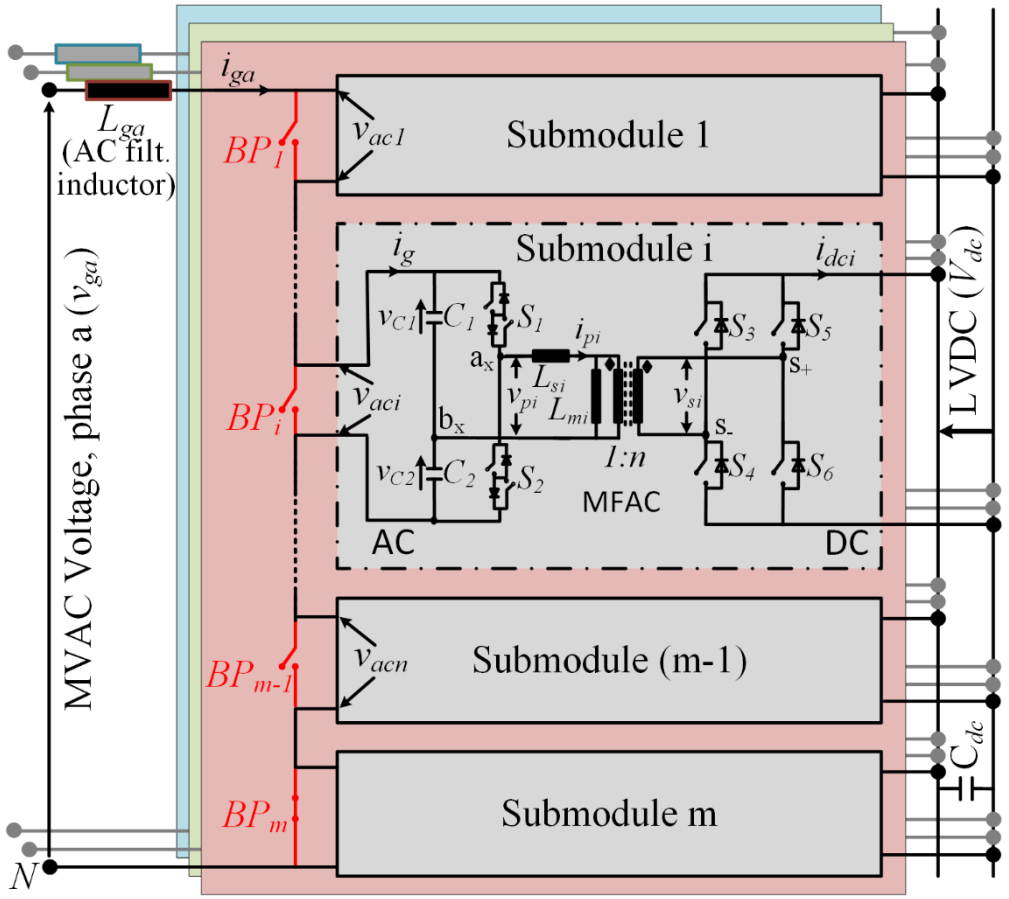

Fig 4. Schematic of a CMB-DAB MVAC-LVDC Modular SST

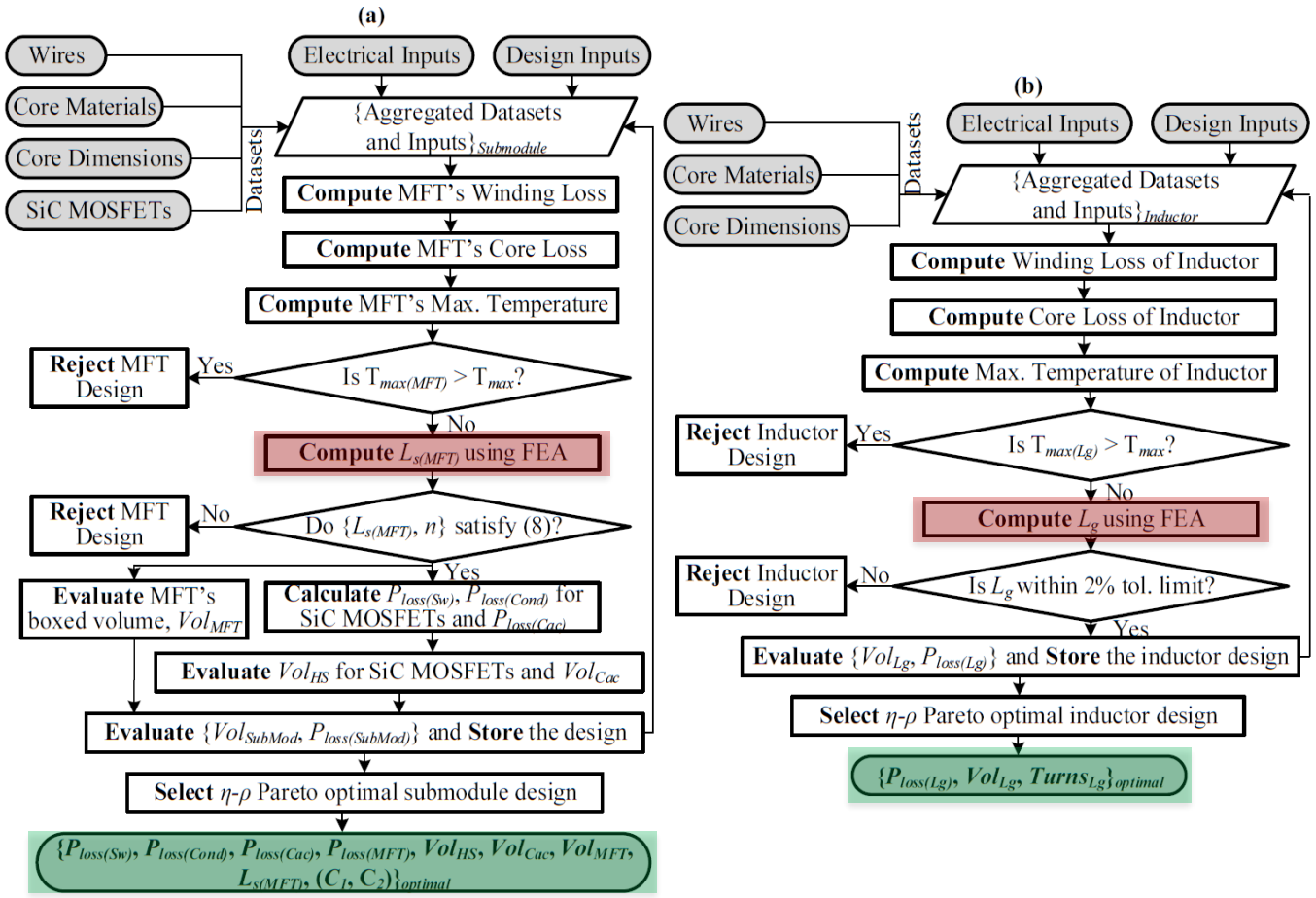

Fig 5. Hybrid local η-ρ optimization algorithms for (a) isolated AC-DC submodule design for CMB-DAB SST (b) AC filter inductor design

OPTIMIZATION RESULTS FOR A 1-STAGE MVAC-LVDC SST

Tab 1. Categories of 22 kV, 1 MVA CMB-DAB SST Structures According to the Front-End Voltage Blocking Capability

Label	Front-end devices (V_{Bpri})	Back-end devices (V_{Bsec})	uf_{FE}	$v_{aci(pk)}$ (V pk)	uf_{BE}	V_{dc} (V)	P_{SubMod} (kW)	N_{SubMod}
Category 1	1700 V modules	1200 V modules	0.56	945.2	0.66	800	17.55	19
Category 2	1700 V discretes	1200 V discretes	0.56	945.2	0.66	800	17.55	19
Category 3	1200 V modules	1200 V modules	0.55	664.8	0.66	800	12.35	27
Category 4	1200 V discretes	1200 V discretes	0.55	664.8	0.66	800	12.35	27
Category 5	900 V discretes	1200 V discretes	0.55	498.6	0.66	800	9.26	36
Category 6	650 V discretes	1200 V discretes	0.55	359.5	0.66	800	6.66	50

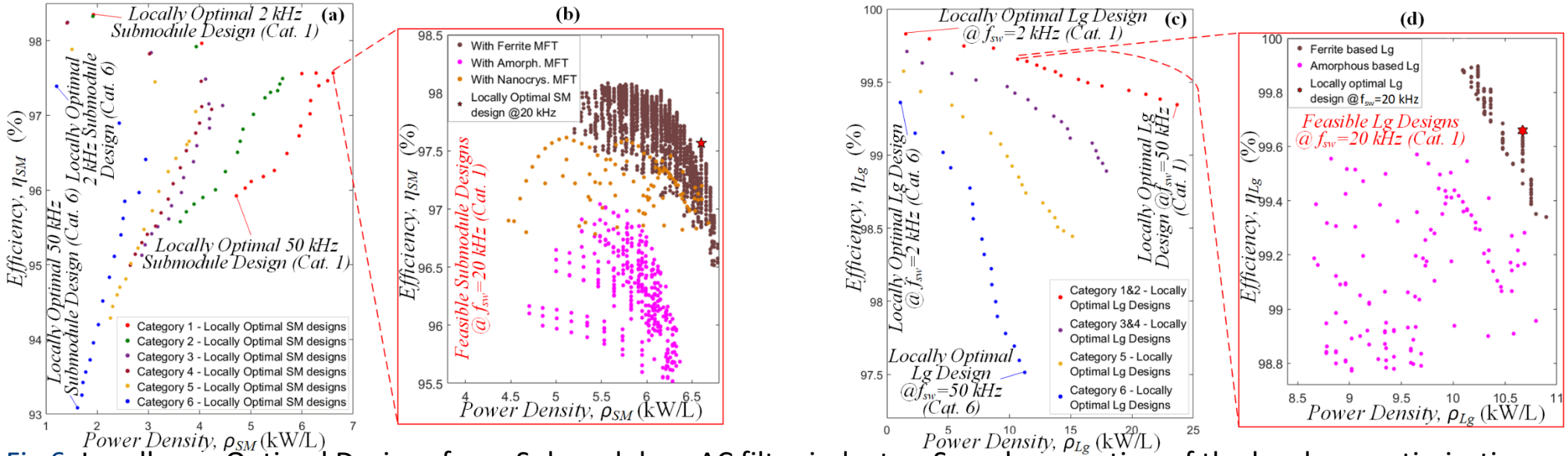

Fig 6. Locally η-ρ Optimal Designs for a. Submodule c. AC filter inductor; Sample execution of the local η-ρ optimization algorithms at f_{sw}=20 kHz in Category 1 for b. MB-DAB Submodule d. AC filter inductor

OPTIMIZATION RESULTS FOR A CMB-DAB SST (CONTD.)

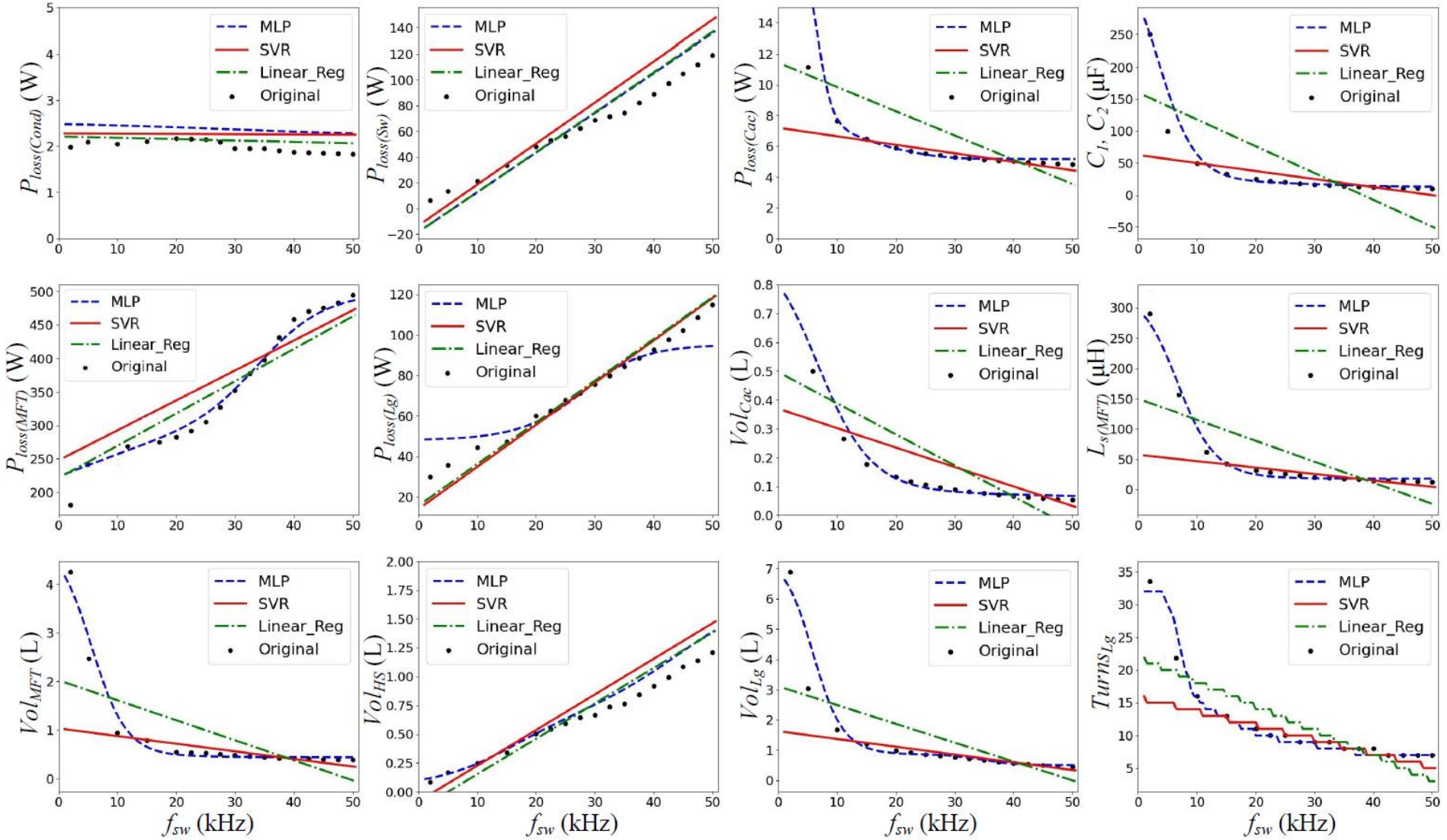

Fig 7. Trained ML models in Category 1, along with the original data-points obtained via iterations of hybrid local η-ρ optimization

OPTIMIZATION RESULTS FOR A 1-STAGE MVAC-LVDC SST (CONTD.)

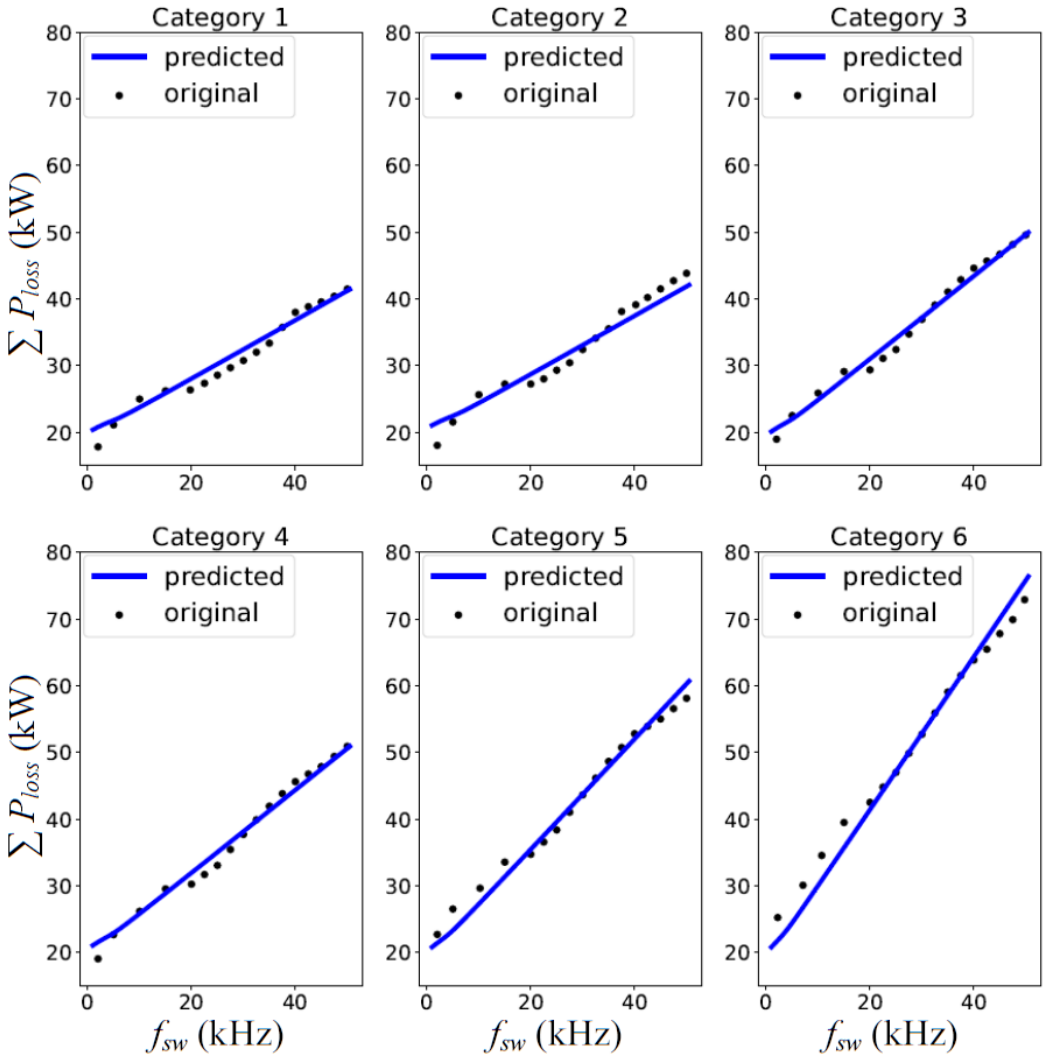

Fig 8. The predicted total loss of optimal SST designs

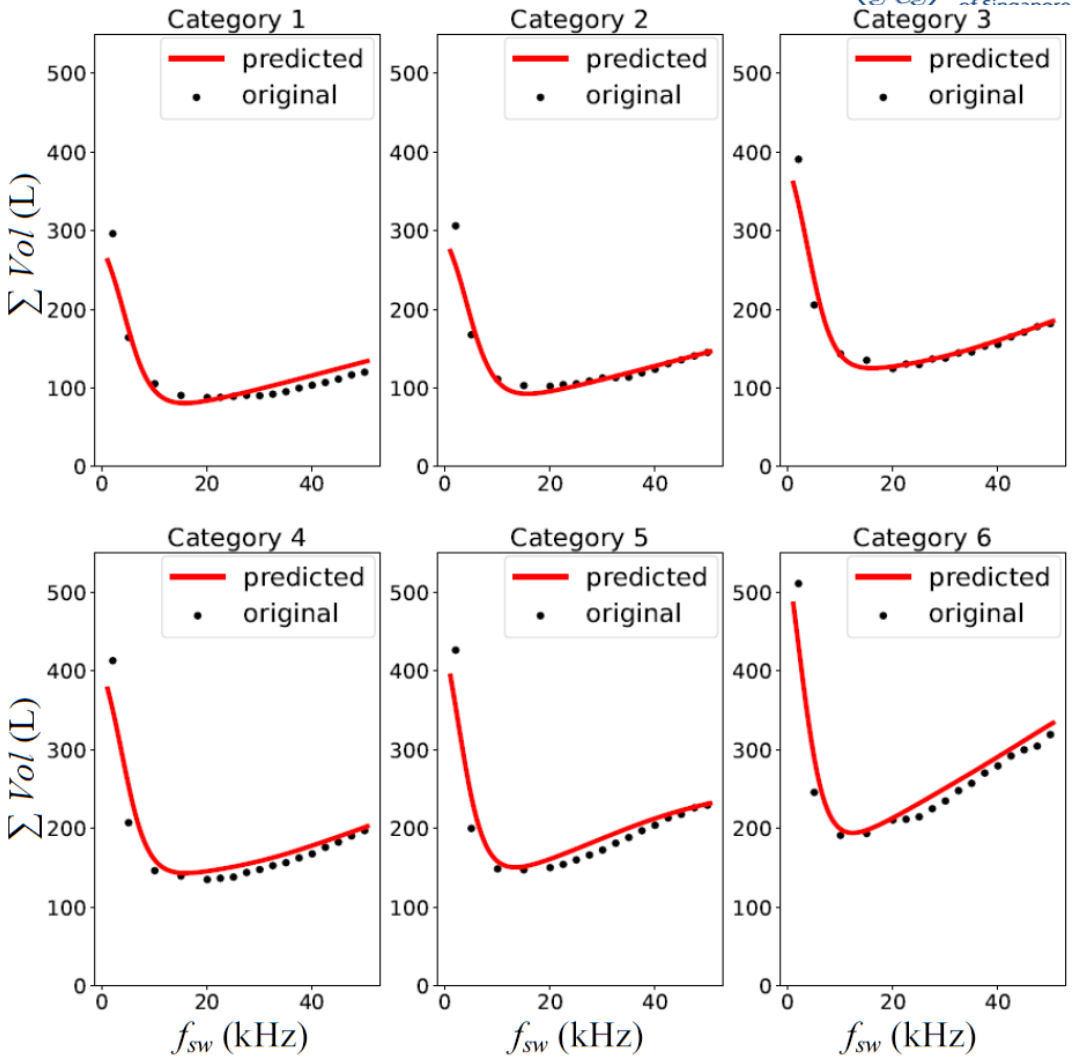

Fig 9. The predicted total volume of optimal SST designs

OPTIMIZATION RESULTS FOR A CMB-DAB SST (CONTD.)

Tab 2. Error Results (MAE and RMSE) for Trained Models using Machine Learning Algorithms

Model	$P_{loss(cond)}$ (W) MAE	RMSE	$P_{loss(Sw)}$ (W) MAE	RMSE	$P_{loss(Cac)}$ (W) MAE	RMSE	$P_{loss(MFT)}$ (W) MAE	RMSE	$P_{loss(Lg)}$ (W) MAE	RMSE	Vol_{HS} (L) MAE	RMSE
Linear Regression												
Least Squares	0.14	0.17	6.53	8.11	1.17	1.4	5.48	7.33	4.11	5.14	0.07	0.08
Lasso	0.21	0.27	6.44	8.06	1.14	1.37	5.46	7.35	3.99	5.01	0.08	0.11
Support Vector												
SVR	0.14	0.17	5.52	8.39	0.71	1.52	5.18	7.19	3.9	4.92	0.08	0.1
Artifical Neural Network												
MLP	0.13	0.18	31.23	37.53	0.57	1.58	3.86	5.3	11.05	15.09	0.24	0.31

Model	Vol_{MFT} (L) MAE	RMSE	Vol_{Cac} (L) MAE	RMSE	Vol_{Lg} (L) MAE	RMSE	C_1=C_2 (μF) MAE	RMSE	$L_{s(MFT)}$ (μH) MAE	RMSE	$Turns_{Lg}$ MAE	RMSE
Linear Regression												
Least Squares	0.32	0.39	0.08	0.09	0.43	0.54	13.07	31.42	5.02	7.73	2.45	3.2
Lasso	0.29	0.37	0.07	0.09	0.42	0.54	13.01	31.3	4.99	7.66	2.32	2.99
Support Vector												
SVR	0.2	0.42	0.06	0.08	0.32	0.68	13.6	58.11	3.36	8.58	1.9	3.62
Artifical Neural Network												
MLP	0.27	0.45	0.11	0.14	0.17	0.37	14.45	26.91	3.92	7.9	1.49	2.94

OPTIMIZATION RESULTS FOR A 1-STAGE MVAC-LVDC SST (CONTD.)

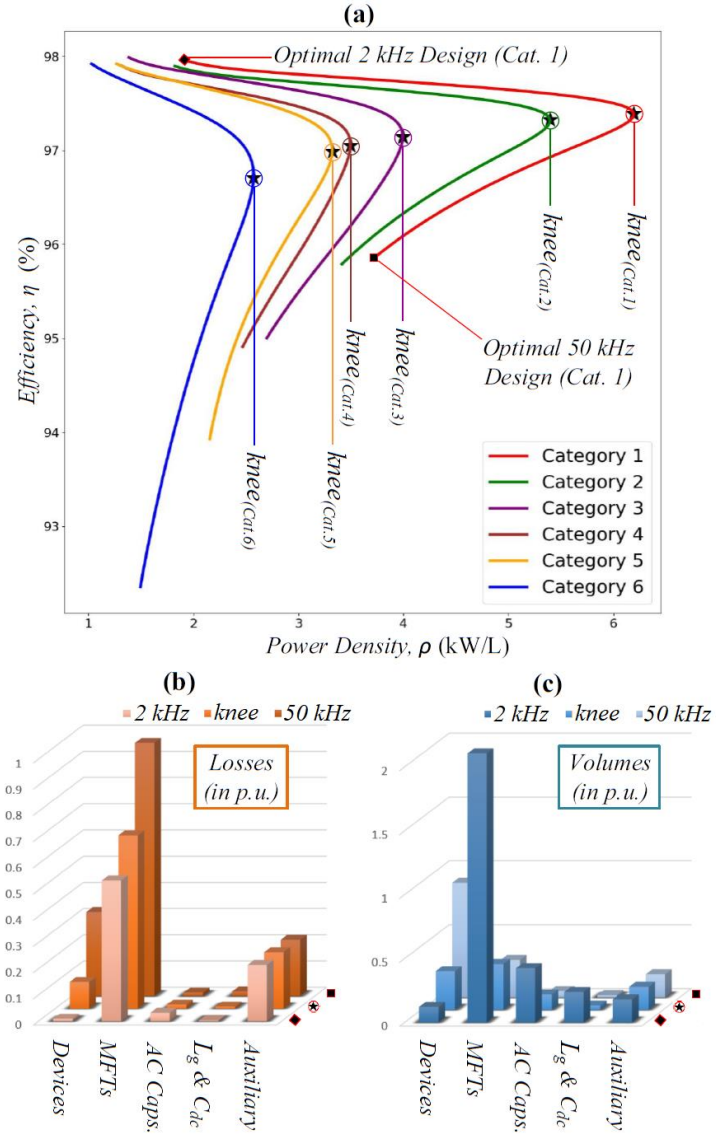

Fig 10. a. The η-ρ design limits obtained in each SST category, presented by η-ρ pareto fronts
b, c. Loss and Volume comparison of SST components for optimal design limits in Category 1 at 2 kHz, knee point and 50 kHz.

Tab 3. MAPE of Total Loss and Volume Evaluations and Knee Point Specifications of ML Model Based 22 kV grid-connected 1 MVA Optimal SST Designs

Label	MAPE		Knee points		
	$\sum P_{loss}$	$\sum Vol$	η (%)	ρ (kW/L)	f_{sw} (kHz)
Category 1	5.02 %	6.09 %	97.3	6.1	16.5
Category 2	5.16 %	5.01 %	97.2	5.3	16.5
Category 3	2.79 %	3.92 %	97.0	3.9	16
Category 4	3.04 %	5.68 %	96.9	3.5	16
Category 5	3.54 %	6.15 %	96.8	3.3	13.5
Category 6	5.06 %	6.05 %	96.6	2.5	13

- Increasing switching frequency need not improve power density indefinitely – realization!!
- Need to find the sweet spot for design based on priorities of efficiency and power density

SCALED-DOWN VALIDATION OF PROPOSED FRAMEWORK

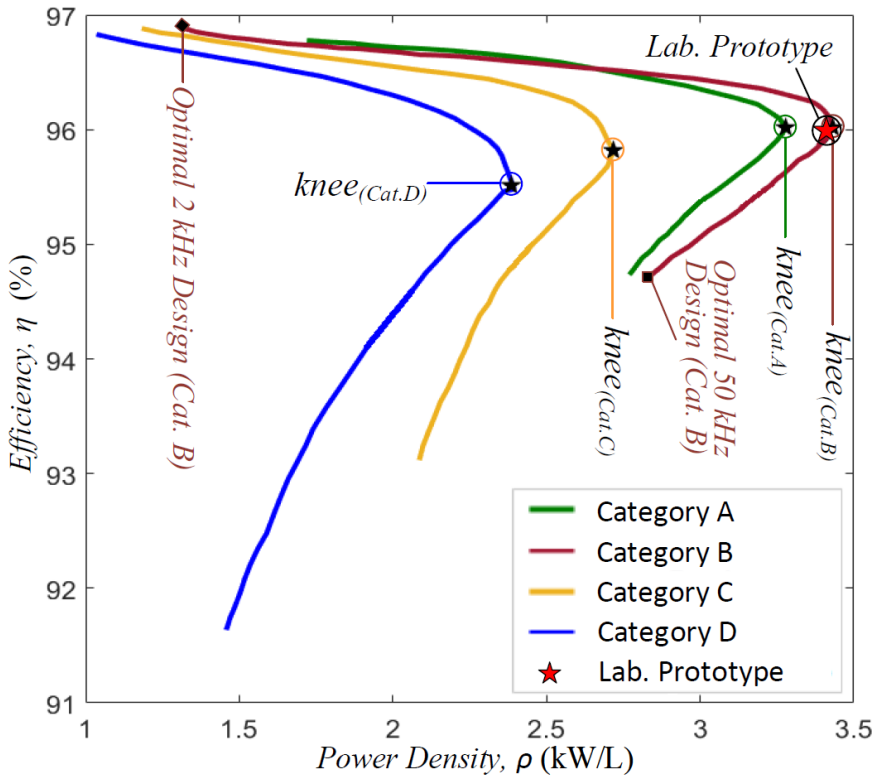

Fig 11. η-ρ pareto fronts for 1.5 kV, 15 kVA CMB-DAB prototype designs

Tab 4. Categories of 1.5 kV, 15 kVA CMB-DAB Prototype Designs According to the FE Voltage Blocking Capability

Cat.	V_{Bpri}	V_{Bsec}	uf_{FE}	$v_{aci(pk)}$	uf_{BE}	V_{dc}	N_{SM}
A	1700V	900V	0.62	1060V	0.5	450V	2
B	1200V	900V	0.59	707V	0.5	450V	3
C	900V	900V	0.59	530.25V	0.5	450V	4
D	650V	900V	0.55	353.5V	0.5	450V	6

Tab 5. MAPE of Total Loss and Volume Evaluations and Knee Point Specifications of ML Based 1.5 kV, 15 kVA Optimal Prototype Designs

Label	MAPE		Knee points/Specification		
	$\sum P_{loss}$	$\sum Vol$	η (%)	ρ (kW/L)	f_{sw} (kHz)
Category A	5.13 %	6.49 %	95.98	3.28	25
Category B	4.78 %	3.82 %	**95.99**	**3.42**	**20.5**
Category C	3.29 %	6.13 %	95.79	2.73	18.5
Category D	3.07 %	5.96 %	95.46	2.4	16
Lab. Proto.	-	-	**95.94**	**3.4**	**20.5**

SCALED-DOWN VALIDATION OF PROPOSED FRAMEWORK (CONTD.)

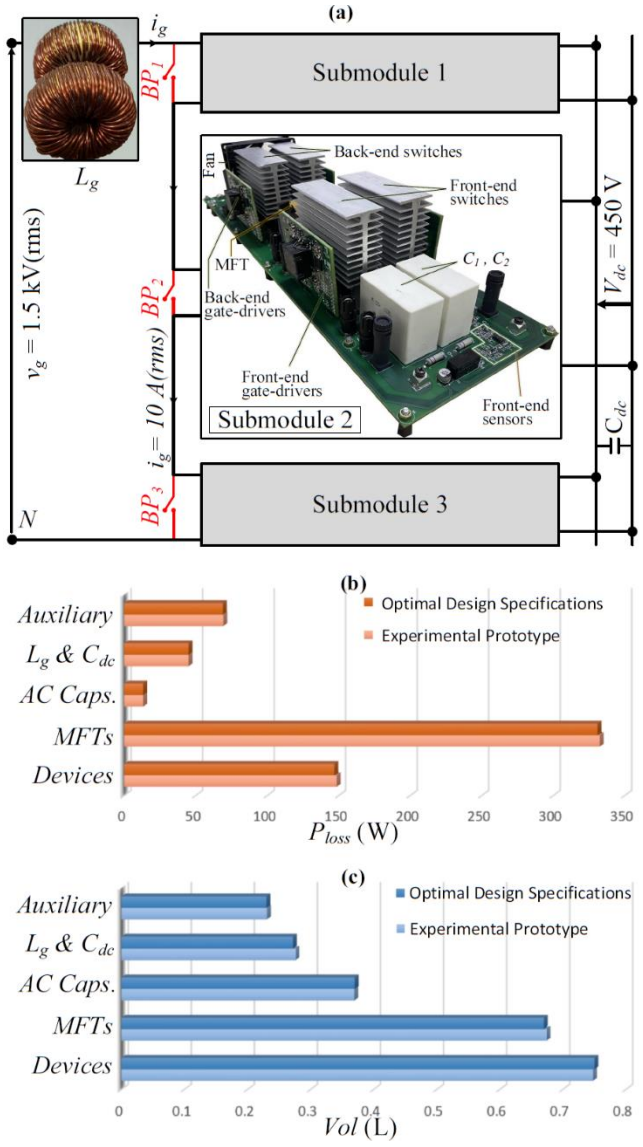

Fig 12. a. Laboratory level prototype schematic for a CMB-DAB
b, c. Loss and volume breakdown of the 15 kVA prototype at f_{sw}=20.5 kHz.

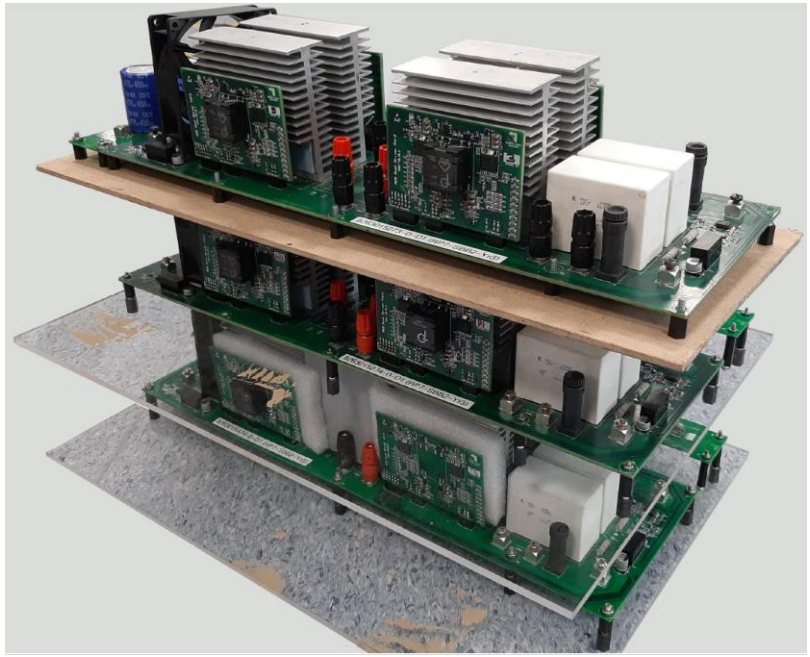

Fig. 13. Fabricated 1.5 kV, 15 kVA CMB-DAB prototype

Tab 6. Components of Laboratory Scale CMB-DAB Prototype

Component	Part number/Specification
FE MOSFET (S_1, S_2)	CREE C3M0032120D, 1200 V/63 A/32 mΩ
BE MOSFET (S_3 - S_6)	2xCREE C3M0065090D, 900 V/36 A/63 mΩ
AC Capacitor (C_1, C_2)	KEMET C4AF3BW5100A3MK, 10 μF
Inductor (L_g)	Micrometals T184-26, Litz wire, 0.5 mH, 15 A
1:1 MF Transformer	E71/33/32-3C94 Ferroxcube, 33 litz wire turns
DC Capacitor (C_{dc})	2x KEMET C4AEHBU5100A11J, 10 μF
MOSFET Driver	SIC1182K SiC MOSFET Gate Driver

COMPARISON WITH OTHER METHODS AND TAKEAWAY POINTS

Tab 7. Comparison of accuracy and computational burden

Parameters	Fully Analytical	Fully Numerical
$n_{ParetoFront}$	768 datasets	768 datasets
n_{FEA}	0	$\simeq 2.6\text{x}10^6$
MAPE ($\sum P_{loss}$,$\sum Vol$)	(12.5,13.1) %	$\simeq$ 2-3 %
time (with i7, 16 GB PC)	$\simeq$ 76 hours	$\simeq$ 2 years
Parameters	**ML-aided Hybrid**	**Standalone Hybrid**
$n_{ParetoFront}$	768 datasets	768 datasets
$n_{MLtraining}$	68 datasets	-
n_{FEA}	$\simeq$ 3400	$\simeq 3.84\text{x}10^4$
MAPE ($\sum P_{loss}$,$\sum Vol$)	(4.7,3.8) %	$\simeq$ 2-3 %
time (with i7, 16 GB PC)	$\simeq$ 137 hours	$\simeq$ 64 days

- Though fully analytical technique requires meagre 76 hours, Mean Absolute % Error > 12%.
- Fully numerical technique is not feasible due to high computational burden.
- Standalone hybrid optimization technique also has considerable computational expense.
- The ML-aided hybrid optimization technique reduces the number of FEA computations; results in feasible computational time and low MAPE (<5%).

RELEVANT PUBLICATIONS

Journals

1. ***Jaydeep Saha*** *and* ***Sanjib Kumar Panda****, "Overview and comparative analysis of bidirectional cascaded modular isolated medium-voltage ac - low-voltage dc (mvac-lvdc) power conversion for renewable energy rich microgrids," Renew. and Sust. Ener. Rev., Mar. 2023.*
2. ***Jaydeep Saha****, Devamanyu Hazarika, Naga Brahmendra Yadav Gorla and* ***Sanjib Kumar Panda****, "Machine-Learning-Aided Optimization Framework for Design of Medium-Voltage Grid-Connected Solid-State Transformers," in IEEE Journ. of Emerg. & Selec. Top. in Power Electronics, vol. 9, no. 6, Dec. 2021.*
3. ***Jaydeep Saha****, Naga Brahmendra Yadav Gorla, Aravinth Subramaniam and* ***Sanjib Kumar Panda****, "Analysis of Modulation and Optimal Design Methodology for Half-Bridge Matrix-Based Dual-Active-Bridge (MB-DAB) AC-DC Converter," in IEEE Journ. of Emerg. & Selec. Top. in Power Electronics, vol. 10, no. 1, pp. 881-894, Feb. 2022.*
4. ***Jaydeep Saha****, Naga Brahmendra Yadav Gorla and* ***Sanjib Kumar Panda****, "Implementation of Power Balance Control Scheme for a Cascaded Matrix-Based Dual-Active-Bridge (CMB-DAB) MVAC-LVDC Converter," in IEEE Transactions on Industry Applications, vol. 58, no. 1, Jan. 2022.*
5. ***Jaydeep Saha****, Naga Brahmendra Yadav Gorla and Sanjib Kumar Panda, "Analytical Expression-Based Modulation for Soft-Switched Matrix-Based Dual-Active-Bridge (S^2MB-DAB) Single-Phase AC-DC Converter," in IEEE Journ. of Emerg. & Selec. Top. in Power Electronics, vol. 10, no. 6, pp. 6511-6522, Dec. 2022.*

Conferences

1. ***Jaydeep Saha****, Naga Brahmendra Yadav Gorla, Aravinth Subramaniam and* ***Sanjib Kumar Panda****, "Computational Feasibility of Multi-objective Optimal Design Techniques for Grid-Connected Multi-cell Solid-State-Transformers," in IECON 2021 [virtual].*
2. ***Jaydeep Saha****, Naga Brahmendra Yadav Gorla and* ***Sanjib Kumar Panda****, "Comparative Overview of Power Balance Control for Two-stage and Single-stage Isolated MVAC-LVDC Cascaded Converters," in IEEE 13th Energy Conversion Congress and Exposition – Asia (ECCE-Asia), 2022.*
3. ***Jaydeep Saha****, Naga Brahmendra Yadav Gorla and* ***Sanjib Kumar Panda****, "Modulation of Direct Matrix-Based Dual-Active- Bridge (MB-DAB) AC-DC Converters," in IEEE 12th Energy Conversion Congress and Exposition – Asia (ECCE-Asia), 2021, pp. 74-79 [virtual]* ***– Best Paper Award.***
4. ***Jaydeep Saha****, Aravinth Subramaniam and Sanjib Kumar Panda, "Design of Integrated Medium Frequency Transformer (iMFT) for Dual-Active-Bridge (DAB) Based Solid-State-Transformers," in IEEE 12th Energy Conversion Congress and Exposition – Asia (ECCE-Asia), 2021, pp. 893-898 [virtual].*
5. ***Jaydeep Saha****, Naga Brahmendra Yadav Gorla and* ***Sanjib Kumar Panda****, "Power Balance Control of Cascaded Matrix-Based Dual-Active-Bridge Converter," in 2020 IEEE International Conference on Power Electronics, Drives and Energy Systems (PEDES), 2020, pp. 1-6 [virtual].*
6. ***Jaydeep Saha****, Naga Brahmendra Yadav Gorla and* ***Sanjib Kumar Panda****, "A Bidirectional Matrix-Based AC-DC Dual-Active Bridge for Modular Solid-State-Transformers," in IECON 2020, Singapore, Singapore, 2020, pp. 1136-1141 [virtual]."*

THANK YOU

Tutorial Topic: Emerging Solid-State-Transformer based Electric-Vehicle Ultra-fast Charging Station

Coordinated Control of Renewable Integrated Ultra-Fast Charging Stations

Tutorial Presentation, IEEE SPEC, 2024, Brisbane

Dr. Jaydeep Saha

Assistant Principal Engineer

ST Engineering Satellite Systems

Ex-Research Fellow

National University of Singapore

IEEE Member

CONTENTS

INTRODUCTION: ULTRA-FAST EV CHARGING STATION

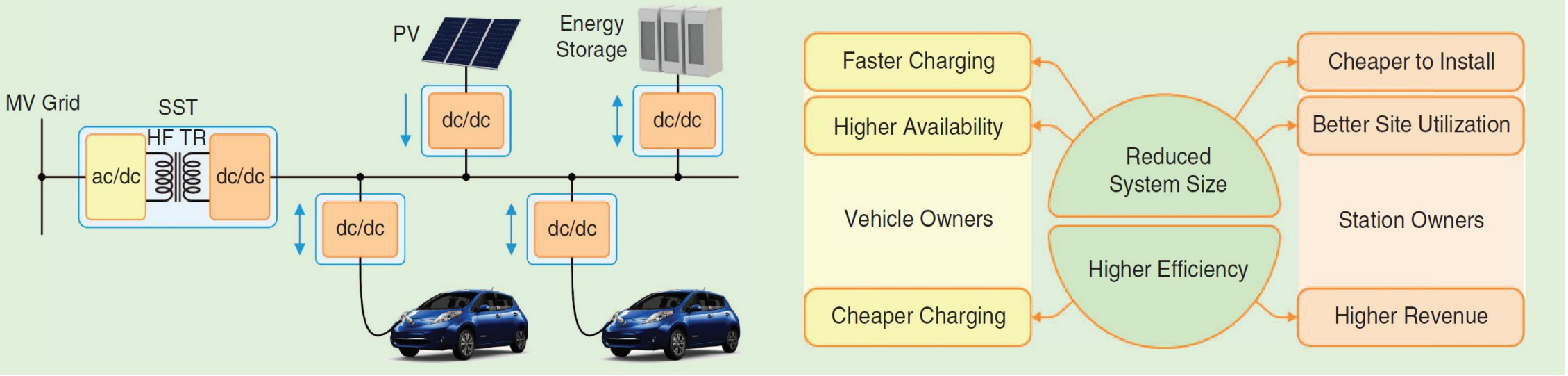

Fig 1. Ultra-fast EV charging station concept based on SST technology [1], [2].

[1] H. Tu, H. Feng, S. Srdic and S. Lukic, "Extreme Fast Charging of Electric Vehicles: A Technology Overview," IEEE Trans. Transport. Electrific., vol. 5, no. 4, pp. 861-878, Dec. 2019.
[2] S. Srdic and S. Lukic, "Toward Extreme Fast Charging: Challenges and Opportunities in Directly Connecting to Medium-Voltage Line," IEEE Electrific. Mag., vol. 7, no. 1, pp. 22-31, Mar. 2019.

ADAPTIVE GRID-SUPPORTIVE CONTROL OF SOLAR-AIDED EV-UFCS

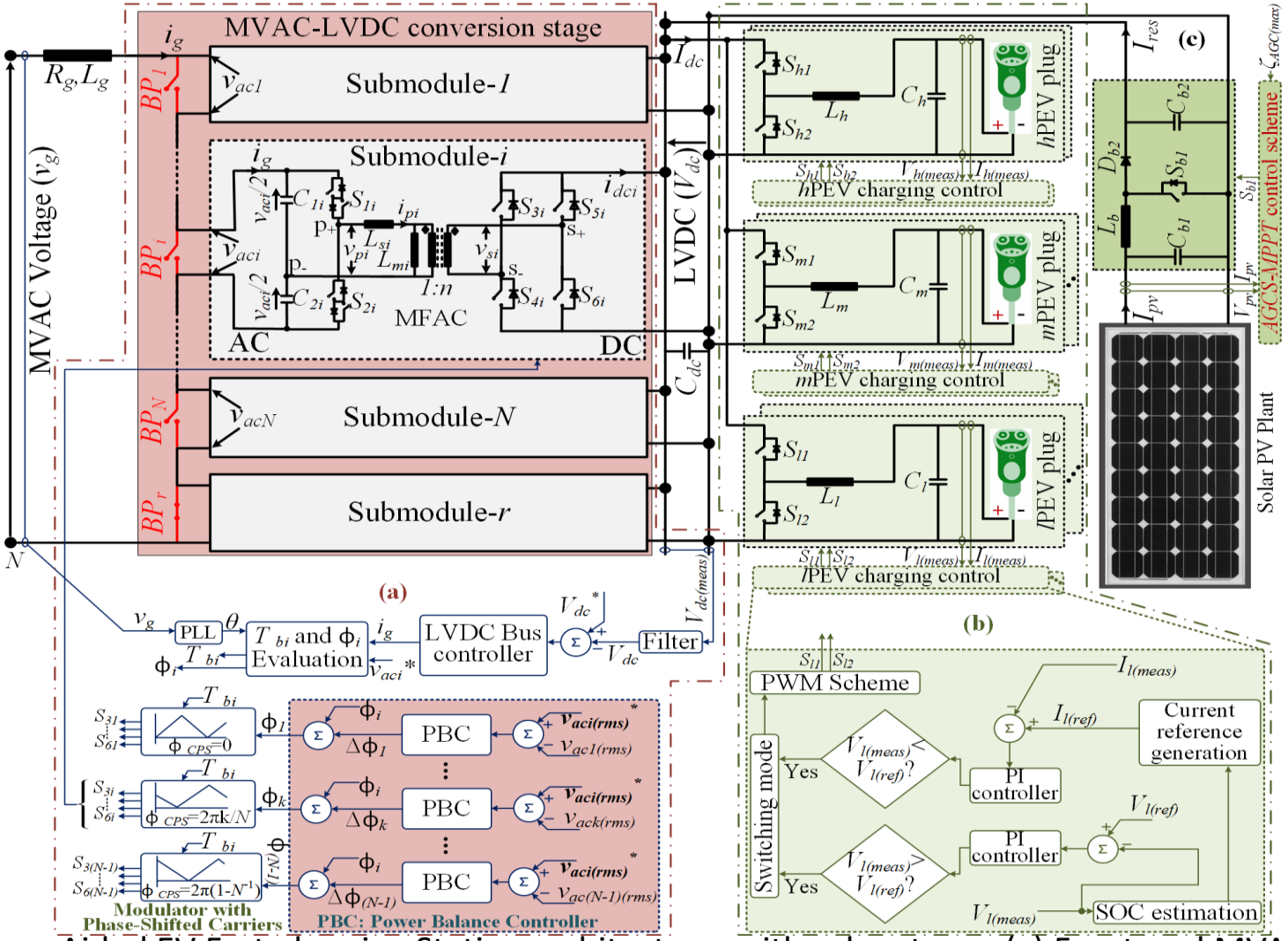

Fig 2. Solar-Power Aided EV Fast-charging Station architecture, with subsystems: (a) Front-end MVAC-LVDC conversion subsystem, (b) Back-end DC-DC conversion subsystem, (c) Solar PV subsystem.

ADAPTIVE GRID-SUPPORTIVE CONTROL OF SOLAR-AIDED EV-UFCS

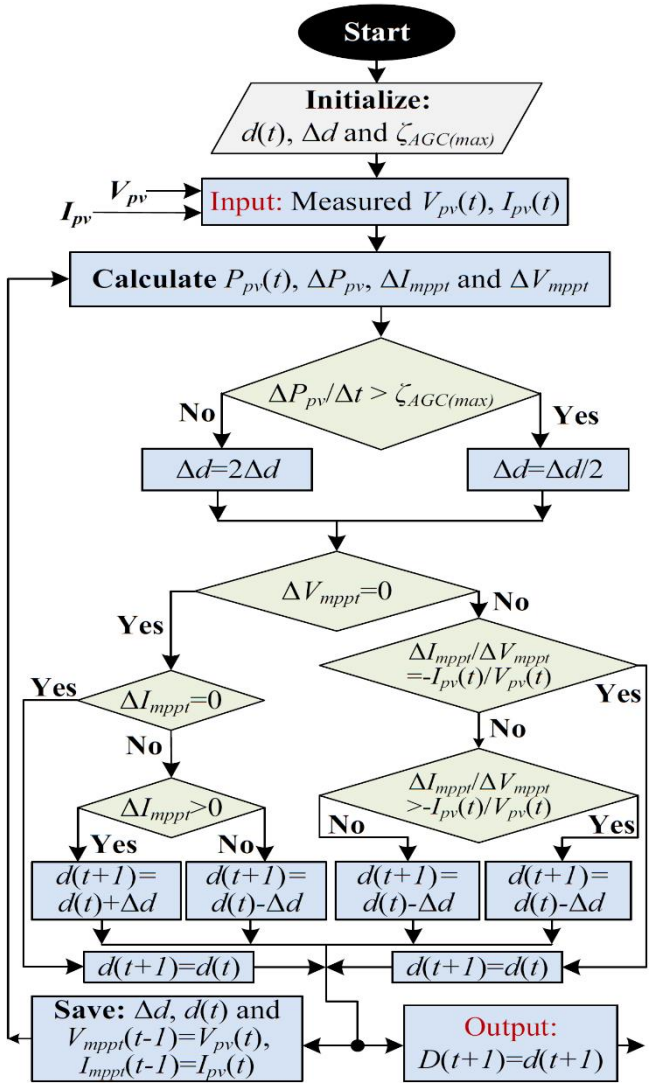

Fig 3. Flow-chart of the proposed AGCS-MPPPT algorithm.

- To restrict the power ramp-rate of solar-energy generation, while following the specified constraint for avoiding utility-side frequency ripples, the following iterative control action is applied:

$$D(t+1) = D(t) \pm 2\Delta d, \text{ when} \frac{\Delta P_{PV}(t)}{\Delta t} < \zeta_{AGC(max)};$$

$$D(t+1) = D(t) \pm \Delta\frac{d}{2}, \text{ when} \frac{\Delta P_{PV}(t)}{\Delta t} > \zeta_{AGC(max)}.$$

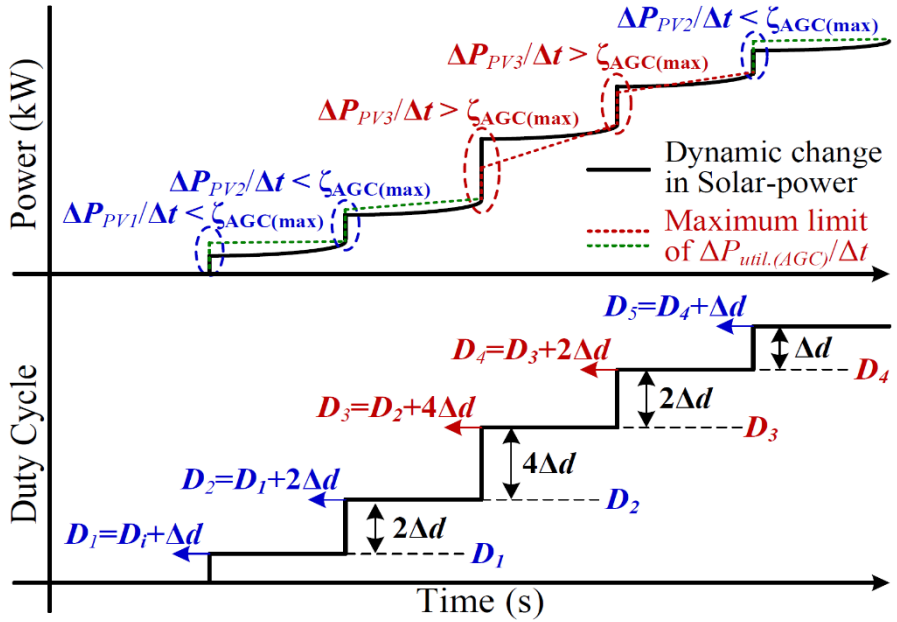

Fig 4. Pictorial representation of the proposed control's action.

ADAPTIVE GRID-SUPPORTIVE CONTROL OF SOLAR-AIDED EV-UFCS

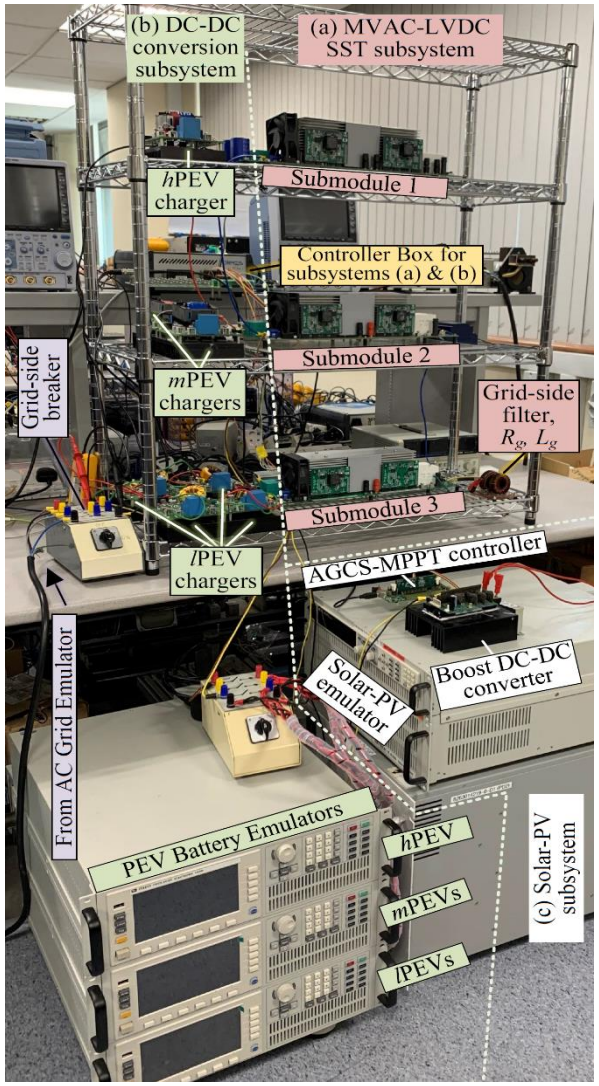

Fig 5. Experimental testbed of Solar-power aided EV-FCS.

Tab 1. Experimental testbed parameters.

Parameter name	Value
Grid voltage, v_g	1 kV
Grid/line frequency, f	50 Hz
Specifications of FE MVAC-LVDC *SST* subsystem (a)	
Nominal power rating, P_{FE}	18 kVA
Number of submodules, N	3
Grid-side voltage reference, v^*_{aci}	472.5 V(pk)
LVDC voltage, V_{dc}	0.5 kV
Switching frequency, f_{sw}	20 kHz
Leakage inductors, $\{L_{s1}, L_{s2}, L_{s3}\}$	20 μH
Phase-shift between carriers, $\phi_{CPS} = 2\pi/N$	$2\pi/3$
Grid-side filter inductor, L_g	0.5 mH
LVDC filter capacitor, C_{dc}	1.41 mF
Half-bridge capacitors, $C_{1i} = C_{2i}$	10 μF
Specifications of BE DC-DC conversion subsystem (b)	
Nominal power ratings, $\{P_h, P_m, P_l\}$	{5.27, 2.63, 0.66} kW
Nominal bat. volt., $\{V_{h(bat)}, V_{m(bat)}, V_{l(bat)}\}$	{400, 200, 100} V
Switching frequency, $f_{s\{h,m,l\}}$	20 kHz
Inductors, $L_{\{h,m,l\}}$	1 mH
Filter capacitors, $C_{\{h,m,l\}}$	1 mF
Specifications of integrated solar PV subsystem (c)	
Rated open-circuit PV voltage, V_{oc}	407 V
Rated short-circuit PV current, I_{sc}	13 A
Voltage at maximum power-point, V_{mpp}	350 V
Current at maximum power-point, I_{mpp}	12.15 A
Power at maximum power-point, P_{mpp}	4.25 kW
Boost converter switching frequency, $f_{s,b}$	10 kHz
Boost converter's inductor, L_b	3.15 mH
Boost converter's capacitors, $\{C_{b1}, C_{b2}\}$	{0.1, 1} mF

ADAPTIVE GRID-SUPPORTIVE CONTROL OF SOLAR-AIDED EV-UFCS

- The steady-state or static MPPT efficiency test sequence of the EN 50530 standard for grid-interfacing systems involves step changes in solar insolation to vary the solar-power, and are defined in two ways: (i) European efficiency (ξ_{Euro}) test, and (ii) California Energy Commission (CEC) efficiency (ξ_{CEC}) test.

- The European and CEC steady-state solar-power extraction efficiencies are defined as follows:

$$\xi_{Euro} = 0.03 \cdot \xi_{5\%} + 0.06 \cdot \xi_{10\%} + 0.13 \cdot \xi_{20\%} + 0.1 \cdot \xi_{30\%} + 0.48 \cdot \xi_{50\%} + 0.2 \cdot \xi_{100\%}$$

$$\xi_{CEC} = 0.04 \cdot \xi_{10\%} + 0.05 \cdot \xi_{20\%} + 0.12 \cdot \xi_{30\%} + 0.21 \cdot \xi_{50\%} + 0.53 \cdot \xi_{75\%} + 0.05 \cdot \xi_{100\%}$$

$P_i = P_{pv(avail)i}/\max(P_{pv(avail)i})$ and $\xi_{Pi\%} = (P_{pvi}/P_{pv(avail)i})\cdot 100\%$, with $P_{pv(avail)i}$ denoting the maximum solar-power that is available at a given solar insolation of G_i and P_{pvi} is the solar-power extracted at steady-state.

- The same ξ_{Euro}-test and ξ_{CEC}-test sequences can be utilized to study the effectiveness of AGCS-MPPT algorithm used for solar-power integration in the PEV-FCS, in comparison with other contemporary techniques

- The utility-grid side maximum $\Delta P_{util.(AGC)}/\Delta t$ (or $\zeta_{AGC(max)}$) received is considered to be 500 W/ 0.1 s (i.e. 500 W per 5 line-frequency cycles) during the test sequence execution time period.

ADAPTIVE GRID-SUPPORTIVE CONTROL OF SOLAR-AIDED EV-UFCS

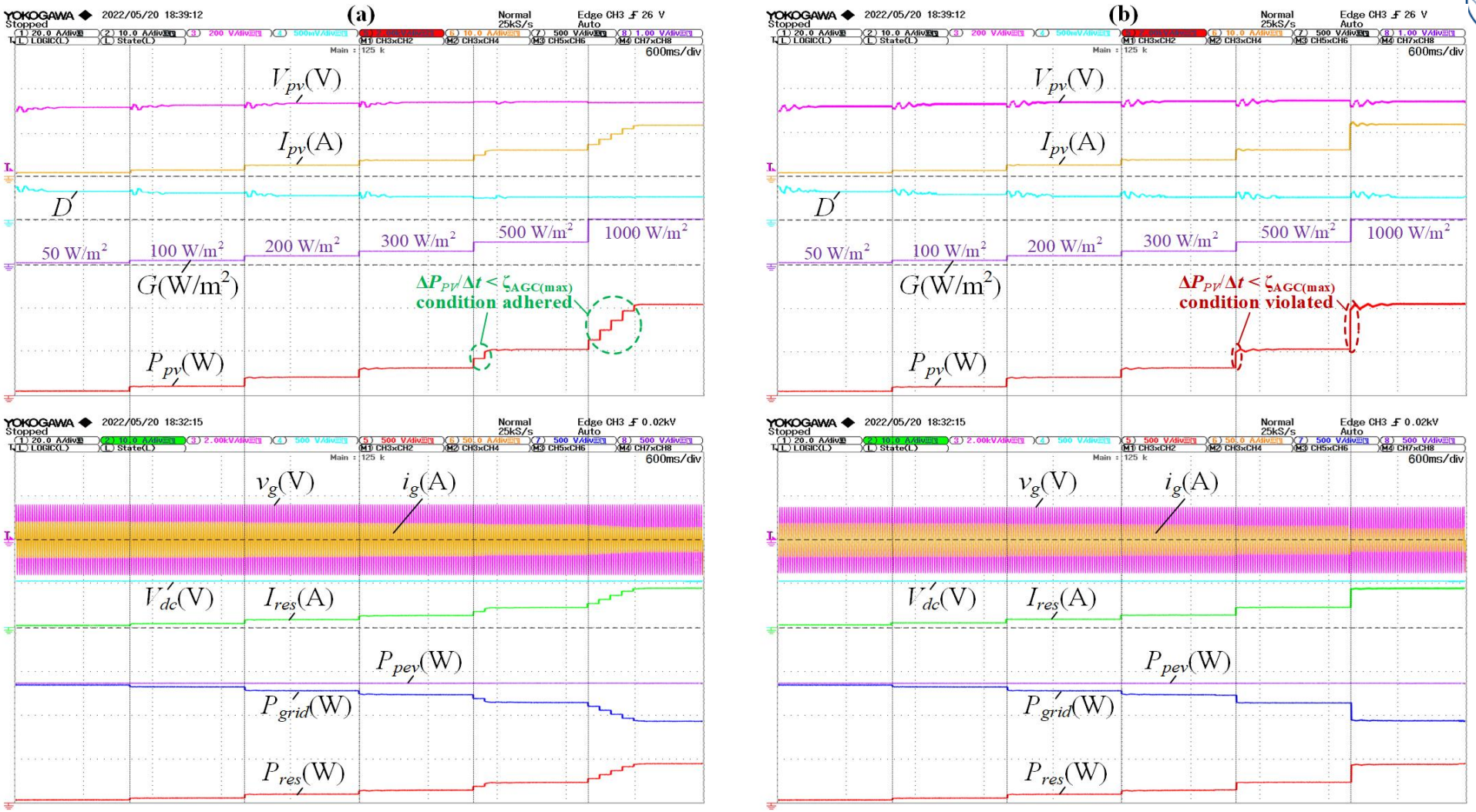

Fig 6. Experimental results for ξ_{Euro}-test as per EN 50530 standard, during implementation of solar-power aided PEV-FCS under G2V functional mode using (a) AGCS-MPPT, (b) SoAT algorithms.

ADAPTIVE GRID-SUPPORTIVE CONTROL OF SOLAR-AIDED EV-UFCS

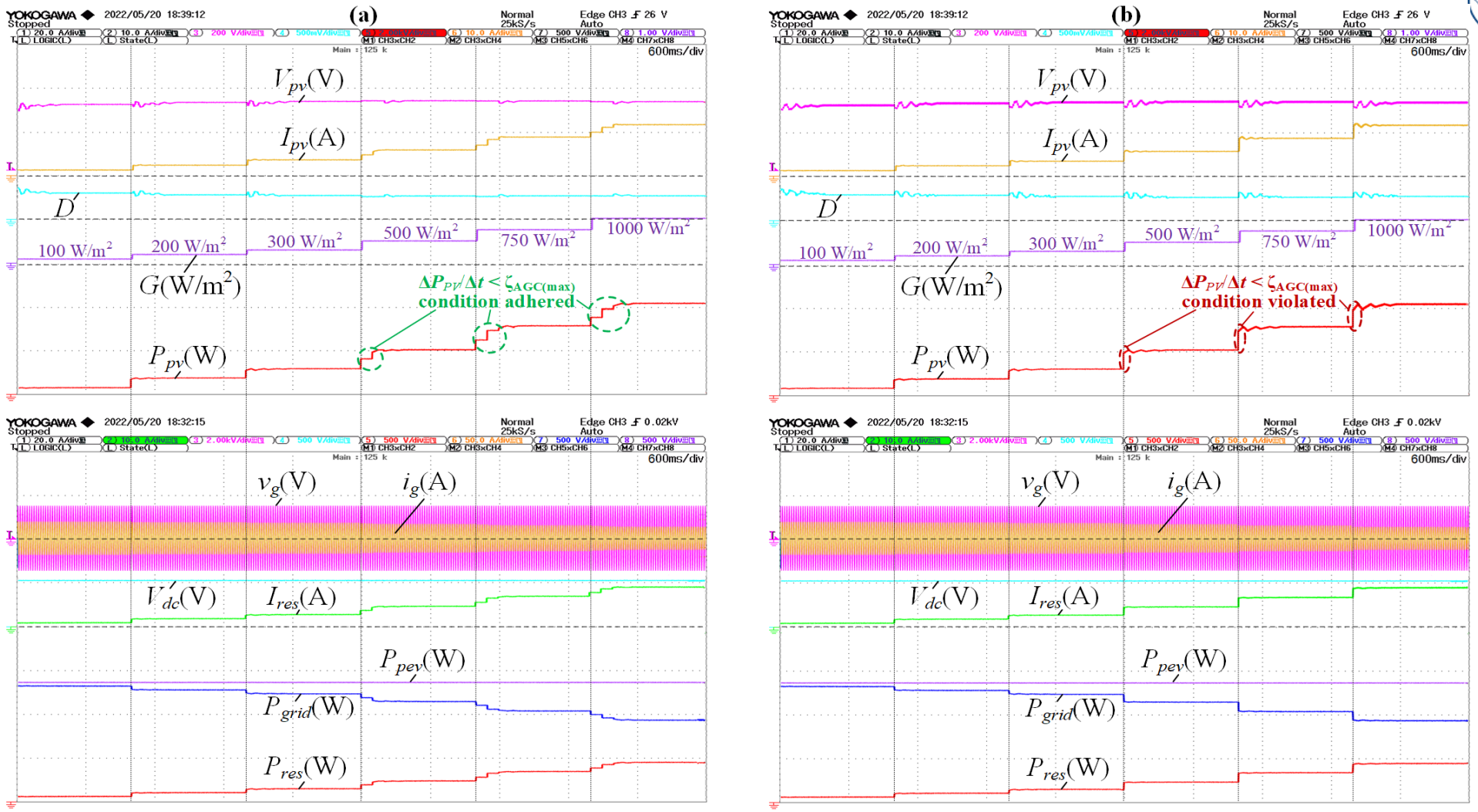

Fig 7. Experimental results for ξ_{CEC}-test as per EN 50530 standard, during implementation of solar-power aided PEV-FCS under G2V functional mode using (a) AGCS-MPPT, (b) SoAT algorithms.

ADAPTIVE GRID-SUPPORTIVE CONTROL OF SOLAR-AIDED EV-UFCS

Tab 2. Comparative evaluation of proposed algorithm

$\xi_{P_i\%}$ or ξ_{Euro}/ξ_{CEC}	AGCS-MPPT	SoAT [45]	P&O [46]
G2V functional mode following ξ_{Euro}-test sequence			
$\xi_{5\%}$	99.01%	98.14%	91.85%
$\xi_{10\%}$	99.23%	98.73%	92.07%
$\xi_{20\%}$	99.29%	99.12%	93.11%
$\xi_{30\%}$	99.48%	99.19%	93.83%
$\xi_{50\%}$	99.58%	99.62%	96.55%
$\xi_{100\%}$	99.65%	99.72%	98.22%
ξ_{Euro}	99.5002%	99.4302%	94.270%
G2V functional mode following ξ_{CEC}-test sequence			
$\xi_{10\%}$	99.21%	98.73%	92.07%
$\xi_{20\%}$	99.28%	99.12%	93.11%
$\xi_{30\%}$	99.50%	99.20%	93.83%
$\xi_{50\%}$	99.57%	99.62%	96.55%
$\xi_{75\%}$	99.59%	99.66%	97.23%
$\xi_{100\%}$	99.65%	99.72%	98.22%
ξ_{CEC}	99.5473%	99.5352%	95.168%
V2G functional mode following ξ_{Euro}-test sequence			
$\xi_{5\%}$	99.01%	98.13%	92.01%
$\xi_{10\%}$	99.22%	98.73%	92.43%
$\xi_{20\%}$	99.27%	99.11%	93.08%
$\xi_{30\%}$	99.48%	99.19%	93.76%
$\xi_{50\%}$	99.57%	99.61%	95.98%
$\xi_{100\%}$	99.61%	99.71%	98.09%
ξ_{Euro}	99.4922%	99.4278%	94.225%
V2G functional mode following ξ_{CEC}-test sequence			
$\xi_{10\%}$	99.20%	99.69%	92.43%
$\xi_{20\%}$	99.29%	99.11%	93.08%
$\xi_{30\%}$	99.49%	99.19%	93.76%
$\xi_{50\%}$	99.58%	99.62%	95.98%
$\xi_{75\%}$	99.59%	99.65%	97.46%
$\xi_{100\%}$	99.61%	99.71%	98.09%
ξ_{CEC}	99.5468%	99.5261%	95.133%

- Various MPPT efficiencies for solar-power integration during G2V and V2G functional modes of grid-connected PEV fast-charging station are shown in the adjacent table, in terms of $\xi_{Pi\%}$ and overall ξ_{Euro}, ξ_{CEC}, for AGCS-MPPT, in comparison with state-of-art technique (SoAT) and improved perturb and observe (P&O) strategy.
- The proposed AGCS-MPPT demonstrates excellent solar-power extraction efficiencies at all studied levels of solar irradiation, which is slightly better compared to the SoAT strategy's extraction efficiencies and significantly better compared to the P&O strategy's corresponding efficiencies.
- Using the proposed algorithm, active-power-curtailment can be minimized while adhering to $(\Delta P_{PV}/\Delta t) < \zeta_{AGC(max)}$.

ADAPTIVE GRID-SUPPORTIVE CONTROL OF SOLAR-AIDED EV-UFCS

Tab 3. Extraction efficiencies of the proposed algorithm during EN 50530 dynamic test sequence.

Rising ramp slope	Falling ramp slope	MPPT Efficiency
Low-to-Medium solar irradiance sequence: 100 W/m^2 to 500 W/m^2		
+40 W/m^2/s	-40 W/m^2/s	99.009%
+100 W/m^2/s	-100 W/m^2/s	99.237%
+150 W/m^2/s	-150 W/m^2/s	99.264%
+200 W/m^2/s	-200 W/m^2/s	99.303%
Medium-to-High solar irradiance sequence: 300 W/m^2 to 1000 W/m^2		
+40 W/m^2/s	-40 W/m^2/s	99.011%
+100 W/m^2/s	-100 W/m^2/s	99.256%
+150 W/m^2/s	-150 W/m^2/s	99.271%
+200 W/m^2/s	-200 W/m^2/s	99.312%

- The dynamic efficiency for a certain insolation band is calculated as follows, where the solar-power extraction efficiency over each section *u* of rising and falling insolation ramps is averaged over *λ* total number of sections in that solar insolation band:

$$\xi_{Dyn} = \frac{1}{\lambda}\sum_{u=1}^{\lambda}\left(\int_u P_{pvu} \Big/ \int_u P_{pv(avail)u}\right)$$

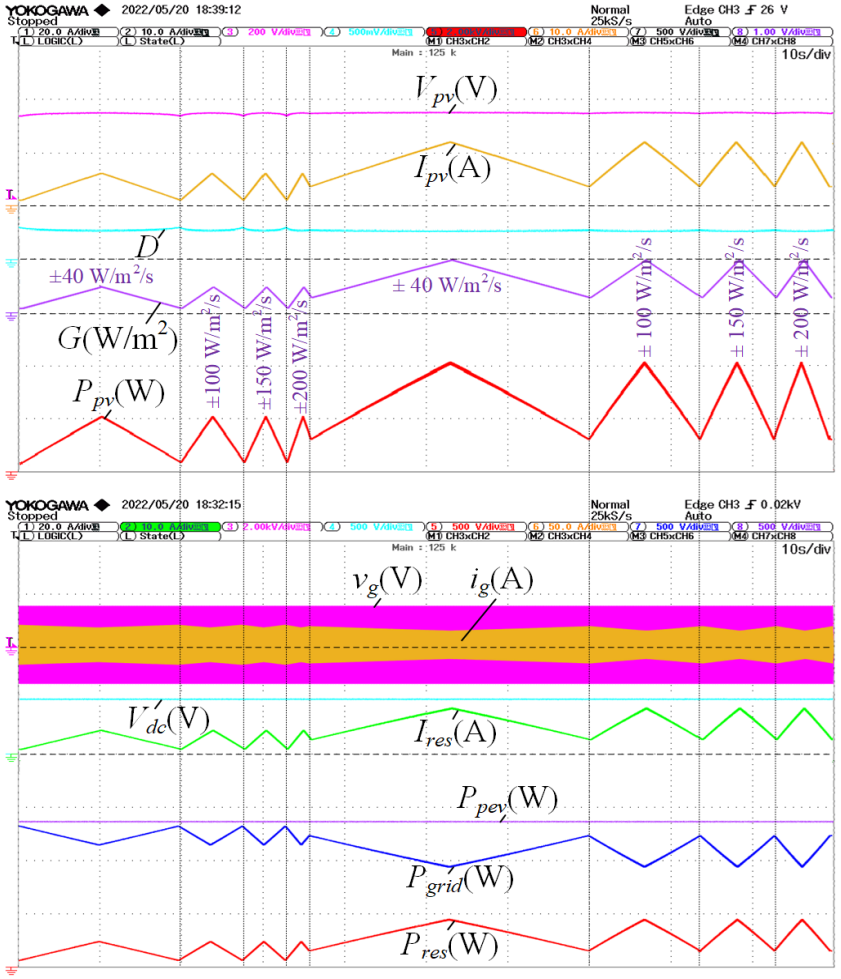

Fig 8. Experimental results for dynamic test sequences in Low-to-Medium and Medium-to-High solar insolation bands.

COORDINATED CONTROL TECHNIQUE FOR SOLAR-AIDED EV-UFCS

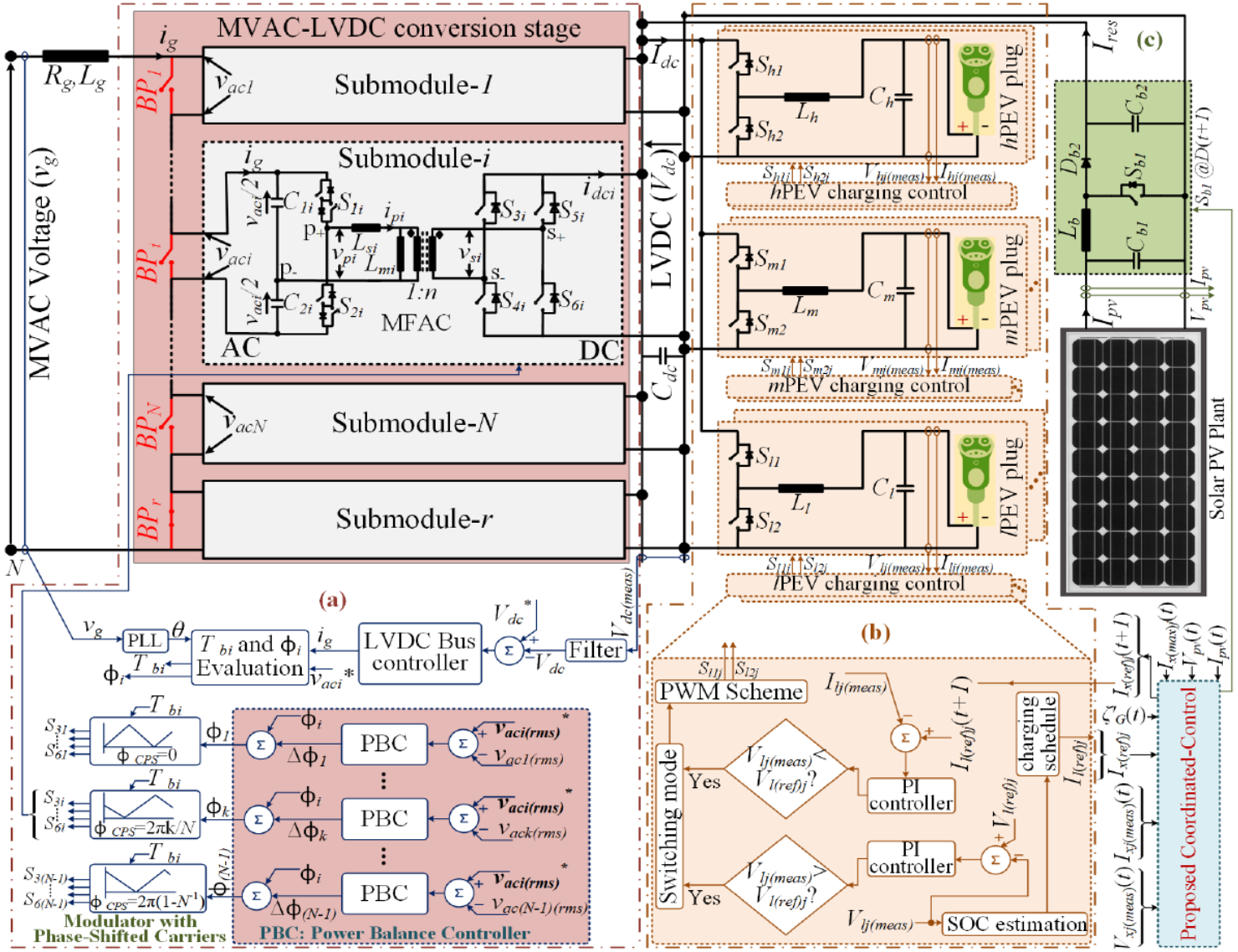

Fig 9. SST-based EV-UFCS architecture: (a) FE MVAC-LVDC SST subsystem, (b) BE DC-DC charger subsystem, (c) Solar-PV subsystem.

COORDINATED CONTROL TECHNIQUE FOR SOLAR-AIDED EV-UFCS

Tab 4. Comparative advantages of the proposed method with other control methods for solar-aided EV-UFCS

Control Method	Grid power-ramp constraint	Solar MPPT	Charging Energy	Computational Complexity
Method 1	Not adhered	Yes	E_{PEV-CS}*	$O(n_{pv}, n^0_{port})$
Method 2	Might violate	No	E_{PEV-CS}*	$O(n_{pv}, n^0_{port})$
Method 3	Might violate	Yes	$<E_{PEV-CS}$*	$O(n_{pv}, n_{port})$
Proposed	**Adhered**	**Yes**	$\sim \mathbf{E_{PEV-CS}}$*	$\mathbf{O(n_{pv}, n_{port})}$

*E_{PEV-CS} represents the total PEV charging energy demand in the EV-UFCS, while following each PEV's specified charging schedule

- Method 1 (base case): grid-side power-ramp-rate constraint is ignored and maximum solar-power is extracted, as well as maximum energy is delivered to the PEVs as per respective charging schedules.
- Method 2: power-ramp-rate-control (PRRC) is implemented only for solar-plant leading to solar active-power-curtailment (APC), whereas, PEVs are supplied as per the charging schedules.
- Method 3: current-ramp-rate-constrained (CRRC) control is implemented for PEV, whereas unconstrained solar MPPT is implemented

Tab 5. Summary of other PV-EV coordinated control methods with different control objectives

Method	Main objective(s)	Research gap/demerits
[25]	Grid's frequency fluctuation reduction through coordinated control of PV/EV/ESS	ESS required, EV battery constraints and energy delivery not considered
[26]	Residential peak-load reduction through coordinated-control of PV/EV/BESS	ESS required, minimal EV and no grid power-ramp constraints considered
[27]	Coordinated-control for freq. regul., opt. sizing of PV/BESS and min. BESS degradation	ESS required, EV SoC approx., no grid ramp constraints considered
[28]	Coordinated EV charging to reduce solar-PV penetration induced voltage fluctuations	Rudimentary EV models, no grid power-ramp or EV constraints considered
[29]	Adaptive control to achieve regulated charging under param. uncertain. and non-ideal grid	Rudimentary EV models, no grid power-ramp or EV constraints considered
[30]	Coordinated-control for volt. regul. and congestion manag.	No grid power-ramp or EV constraints considered
[31]	Coordinated-control for increas. resilience during islanding event	Rudimentary EV models, no EV constraints considered
[32], [33]	Hierarchical optimization for optimal EV charging scheduling	No grid power-ramp-rate, min. EV constraints considered
[34], [44]	Coordinated-control for off-grid PV/EV systems	Rudimentary EV models, no EV constraints considered

COORDINATED CONTROL TECHNIQUE FOR SOLAR-AIDED EV-UFCS

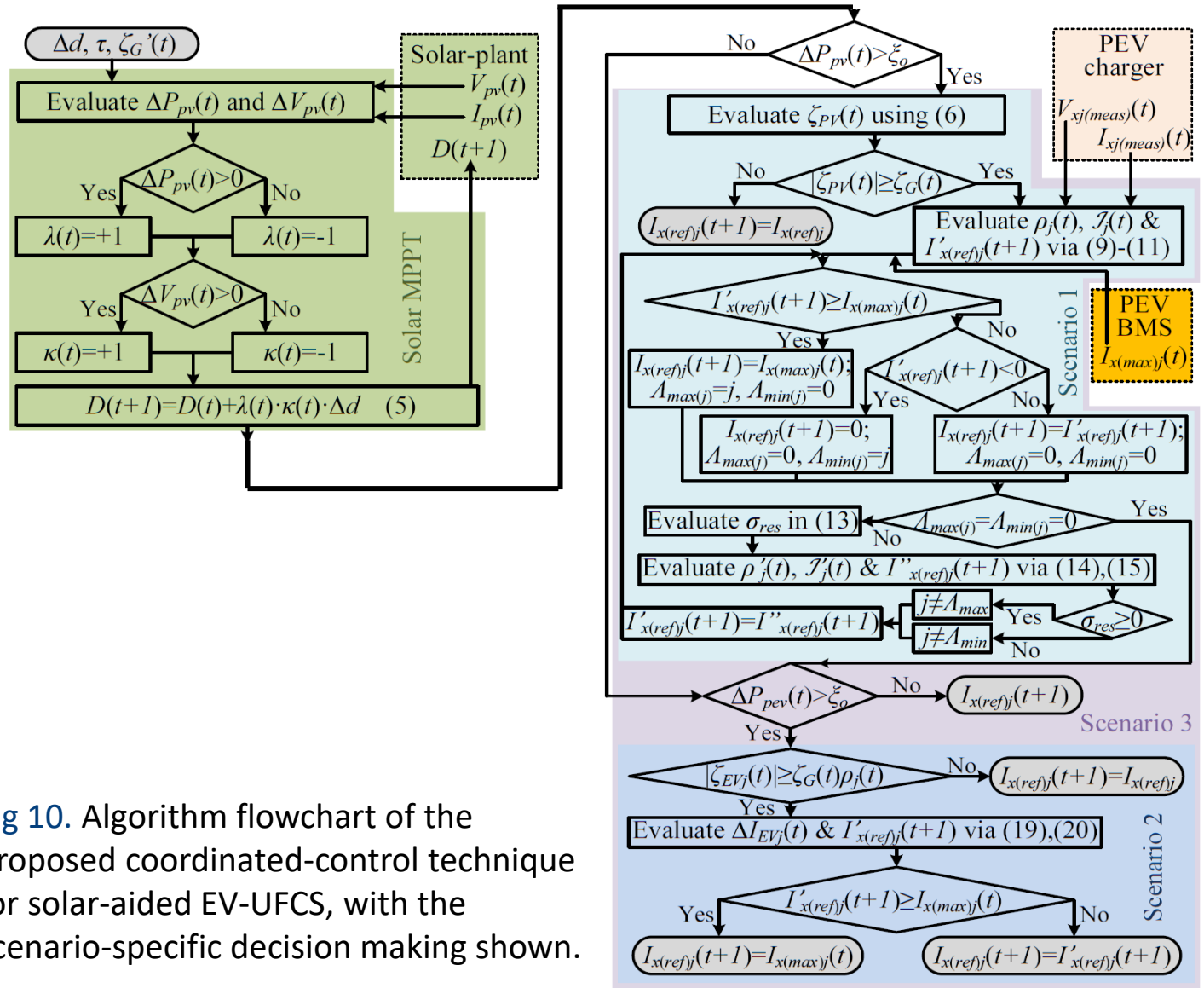

Fig 10. Algorithm flowchart of the proposed coordinated-control technique for solar-aided EV-UFCS, with the scenario-specific decision making shown.

- Scenario 1: Sudden-change in solar-plant power with near-constant PEV fast-charging load
- Scenario 2: Sudden-change in PEV fast-charging load with near-constant solar-plant power
- Scenario 3: Simultaneous sudden-changes in solar-plant power and PEV fast-charging load

COORDINATED CONTROL TECHNIQUE FOR SOLAR-AIDED EV-UFCS

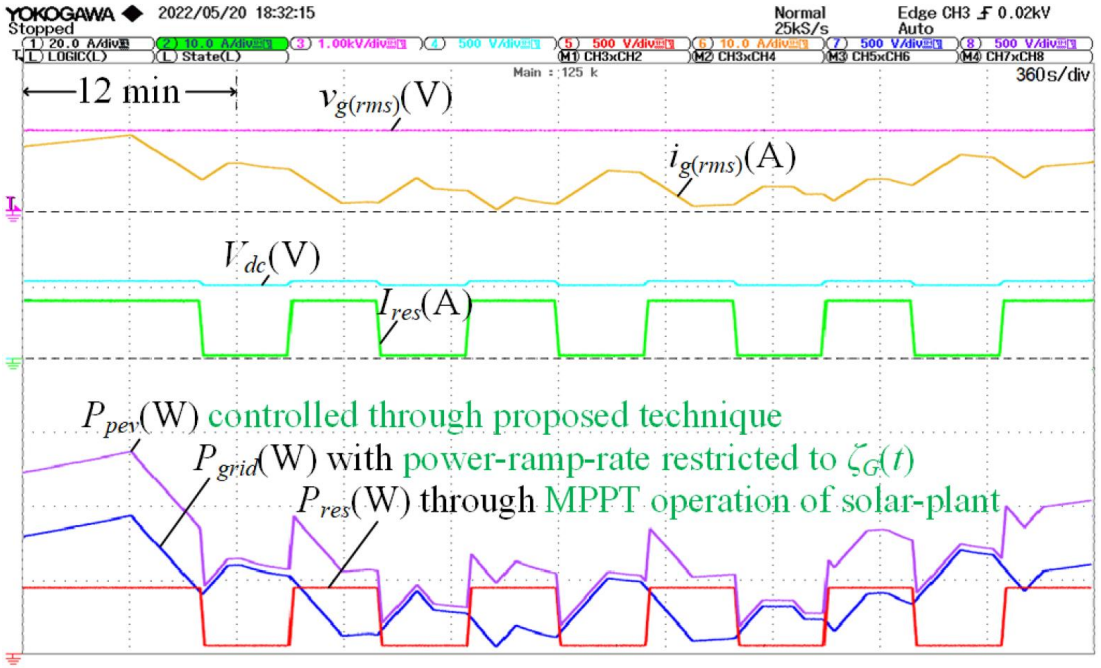

Fig 11. 1 hour experimental results of relevant grid-side and LVDC bus-side quantities: $v_{g(rms)}$ [1 kV/div], $i_{g(rms)}$ [10 A/div], V_{dc} [500 V/div], I_{res} [10 A/div], P_{grid} [5 kW/div], P_{pev} [5 kW/div] and P_{res} [5 kW/div].

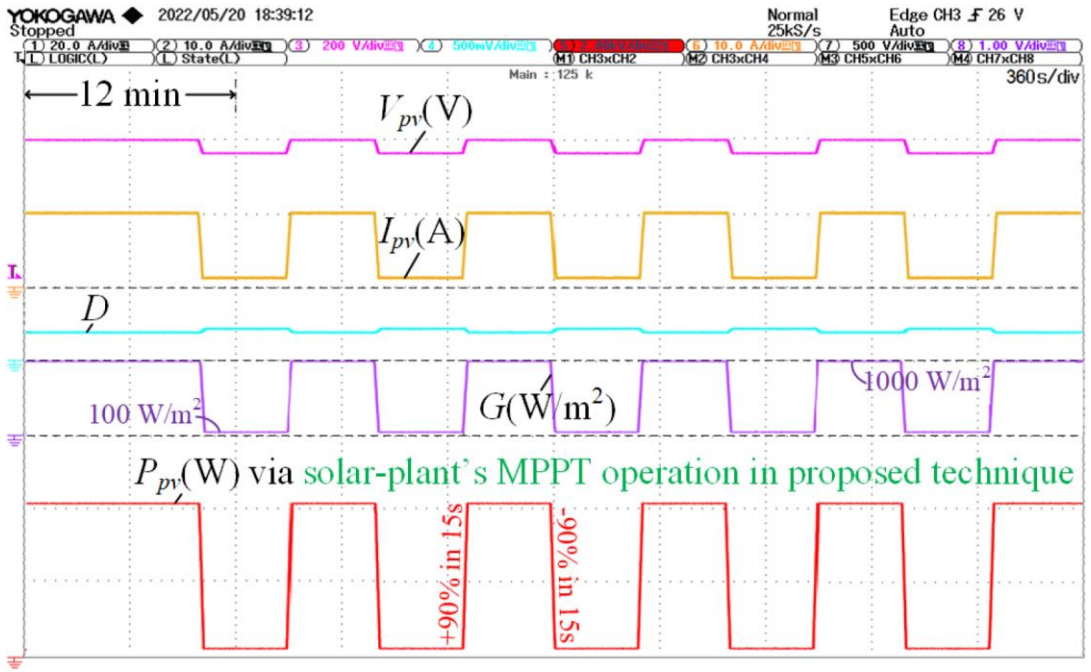

Fig 12. An hour-long experimental measurements of relevant quantities for solar-PV subsystem operating at MPPT: V_{pv} [200 V/div], I_{pv} [10 A/div], D [0.5/div], G [1000 W/m2/div], P_{pv} [2 kVA].

COORDINATED CONTROL TECHNIQUE FOR SOLAR-AIDED EV-UFCS

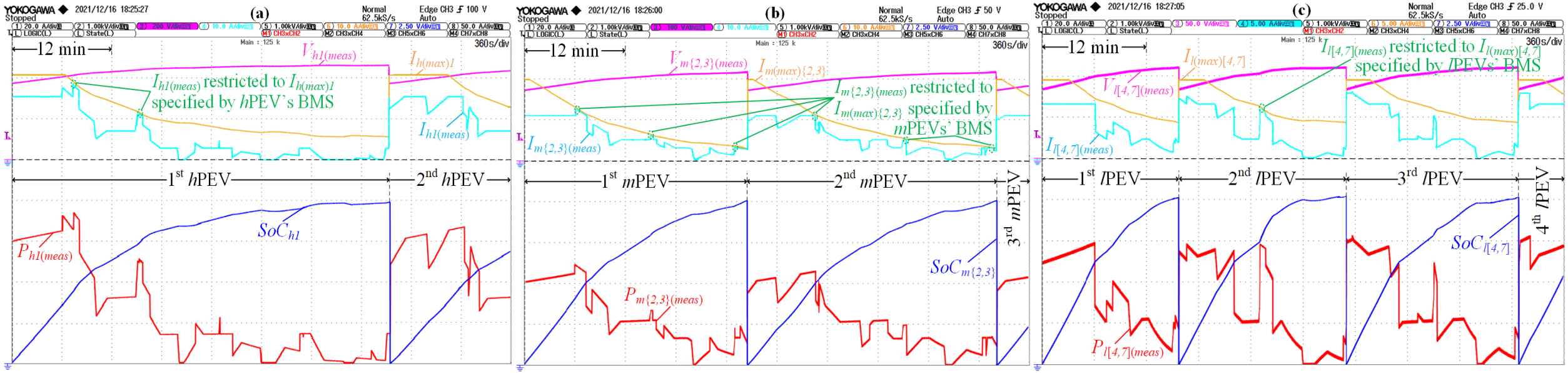

Fig 13. Hour-long experimental measurements for 3 types of PEV ultra-fast charging-ports: (a) *h*PEV charging-port with $V_{h1(meas)}$ [200 V/div], $I_{h1(meas)}$ [10 A/div], $I_{h(max)1}$ [10 A/div], $P_{h1(meas)}$ [1.5 kW/div] and SoC_{h1} [25%/div]; (b) 2 *m*PEV charging-ports connected to identical *m*PEVs with $V_{m\{2,3\}(meas)}$ [100 V/div], $I_{m\{2,3\}(meas)}$ [10 A/div], $I_{m(max)\{2,3\}}$ [10 A/div], $P_{m\{2,3\}(meas)}$ [1 kW/div] and $SoC_{m\{2,3\}}$ [25%/div]; and (c) 4 *l*PEV charging-ports connected to identical *l*PEVs with $V_{l[4,7](meas)}$ [50 V/div], $I_{l[4,7](meas)}$ [5 A/div], $I_{l(max)[4,7]}$ [5 A/div], $P_{l[4,7](meas)}$ [0.25 kW/div] and $SoC_{h[4,7]}$ [25%/div].

COORDINATED CONTROL TECHNIQUE FOR SOLAR-AIDED EV-UFCS

Tab 6. Quantification of charging energy delivered by various PEV ports during hour-long experimentation

Charging pattern	*h*PEV port's charging energy	2 *m*PEV ports' charging energy	4 *l*PEV ports' charging energy
Schedule in Tab. V	3.26 kWh (E_{h-CS}*)	1.35x2 kWh (E_{m-CS}*)	0.48x4 kWh (E_{l-CS}*)
Proposed Technique	3.25 kWh ($0.99 \cdot E_{h-CS}$*)	1.36x2 kWh ($1.01 \cdot E_{m-CS}$*)	0.48x4 kWh ($\approx E_{l-CS}$*)

*CS represents the multi-step CC-CV charging schedule as per Tab. V

The experimental results validate that the proposed technique's implementation in the EV-UFCS, which ensure:

- Adherence to the instantaneous grid power-ramp-rate constraint,
- Solar MPPT,
- Near maximum PEV charging energy delivery,
- Adherence to instantaneous PEV-BMS constraint.

Tab 7. Experimental comparison of the proposed coordinated control with other solar-aided EV-UFCS control strategies

Control Method	Grid-side power-ramp-rate	Solar MPPT	PEV Charging-ports' Energy	PEV-BMS constraint
[15], [20]	Violates $\zeta_G(t)$ substantially	Yes, >99%	E_{l-CS}, E_{m-CS} and E_{h-CS}	Have not considered
[21]–[23]	Violates $\zeta_G(t)$ occasionally	No	E_{l-CS}, E_{m-CS} and E_{h-CS}	Have not considered
[24]	Violates $\zeta_G(t)$ occasionally	Yes, >99%	$0.9E_{l-CS}$, $0.9E_{m-CS}$ and $0.83E_{h-CS}$	Adhered mostly
[30]	Violates $\zeta_G(t)$ occasionally	Mostly, <99%	E_{l-CS}, E_{m-CS} and E_{h-CS}	Adhered mostly
[31]	Violates $\zeta_G(t)$ occasionally	Yes, >99%	E_{l-CS}, E_{m-CS} and E_{h-CS}	Have not considered
Proposed	**Adheres to $\zeta_G(t)$ always**	**Yes, >99%**	$\mathbf{E_{l-CS}}$, $1.01\mathbf{E_{m-CS}}$ and $0.99\mathbf{E_{h-CS}}$	**Adhered always**

*CS represents the multi-step CC-CV charging schedule as per Tab. V

The proposed control technique facilitates in meeting all the operational requirements of a MV grid-connected solar-aided EV-UFCS without requirement of any energy-storage

COORDINATED CONTROL OF RENEWABLE INTEGRATED EV-UFCS

- An adaptive grid-supportive AGCS-MPPT control algorithm is proposed for PV integration in a PEV-FCS.

- The SST-based PEV-FCS testbed implementation is discussed, along with the experimental test-sequences following EN 50530 standard to validate the adaptive grid-supportive AGCS-MPPT control .

- The experimental results for AGCS-MPPT control-based solar-power integration in the PEV-FCS testbed exhibit:

(i) maximum steady-state solar-power extraction efficiencies (ξ_{Euro}, ξ_{CEC}) during respective G2V and V2G functional modes of the PEV-FCS;

(ii) superior performance and MPPT efficiency during dynamic test sequences;

(iii) strong adherence to the utility-grid side power ramp-rate limit condition $(\Delta P_{PV}/\Delta t) < \zeta_{AGC(max)}$.

- A novel coordinated-control technique for a battery-less solar-aided EV-UFCS is presented to ensure maximum solar extraction and PEV fast-charging energy delivery, while adhering to the instantaneous grid-side and PEV-BMS's constraints.

- The presented comprehensive experimental results sufficiently validate all the objectives and constraints (both at grid-side and PEV-side) of the proposed coordinated-control technique implemented in a solar-aided SST-based EV-UFCS testbed

RELEVANT PUBLICATIONS

Journals

1. ***Jaydeep Saha**, Nishant Kumar and **Sanjib Kumar Panda**, "A Futuristic Silicon-Carbide (SiC) Based Electric-Vehicle Fast Charging/Discharging (FC/dC) Station," in IEEE Journ. of Emerg. & Selec. Top. in Power Electronics, 2022.*
2. ***Jaydeep Saha**, Nishant Kumar and **Sanjib Kumar Panda**, "Adaptive Grid-Supportive Control for Solar-Power Integrated Electric-Vehicle Fast Charging Station," in IEEE Transactions on Energy Conversion, 2023.*
3. ***Jaydeep Saha** and **Sanjib Kumar Panda**, "Overview and comparative analysis of bidirectional cascaded modular isolated medium-voltage ac - low-voltage dc (mvac-lvdc) power conversion for renewable energy rich microgrids," Renew. and Sust. Ener. Rev., Mar. 2023.*
4. ***Jaydeep Saha**, Nishant Kumar and **Sanjib Kumar Panda**, "A Multi-constraint-adhered Coordinated-Control Algorithm for Solar-Plant Integrated Futuristic Electric-Vehicle Ultra-Fast Charging-Station," in IEEE Transactions on Consumer Electronics, 2025.*

Conferences

1. ***Jaydeep Saha**, Nishant Kumar and **Sanjib Kumar Panda**, "A Grid-Supportive Current Ramp-Rate Constrained (GS-CR2C) Control Strategy for a SST-Based Bidirectional Multi-Port Fast-Charging Station," 2022 IEEE International Conference on Power Electronics, Drives and Energy Systems (PEDES), Jaipur, India, 2022, pp. 1-6.*
2. ***Jaydeep Saha**, Naga Brahmendra Yadav Gorla, Aravinth Subramaniam and **Sanjib Kumar Panda**, "Computational Feasibility of Multi-objective Optimal Design Techniques for Grid-Connected Multi-cell Solid-State-Transformers," in IECON 2021 [virtual].*
3. ***Jaydeep Saha**, Naga Brahmendra Yadav Gorla and **Sanjib Kumar Panda**, "Comparative Overview of Power Balance Control for Two-stage and Single-stage Isolated MVAC-LVDC Cascaded Converters," in IEEE 13th Energy Conversion Congress and Exposition – Asia (ECCE-Asia), 2022.*
4. ***Jaydeep Saha**, Naga Brahmendra Yadav Gorla and **Sanjib Kumar Panda**, "Modulation of Direct Matrix-Based Dual-Active- Bridge (MB-DAB) AC-DC Converters," in IEEE 12th Energy Conversion Congress and Exposition – Asia (ECCE-Asia), 2021, pp. 74-79 [virtual] **– Best Paper Award.***
5. ***Jaydeep Saha**, Aravinth Subramaniam and Sanjib Kumar Panda, "Design of Integrated Medium Frequency Transformer (iMFT) for Dual-Active-Bridge (DAB) Based Solid-State-Transformers," in IEEE 12th Energy Conversion Congress and Exposition – Asia (ECCE-Asia), 2021, pp. 893-898 [virtual].*
6. ***Jaydeep Saha**, Naga Brahmendra Yadav Gorla and **Sanjib Kumar Panda**, "Power Balance Control of Cascaded Matrix-Based Dual-Active-Bridge Converter," in 2020 IEEE International Conference on Power Electronics, Drives and Energy Systems (PEDES), 2020, pp. 1-6 [virtual].*
7. ***Jaydeep Saha**, Naga Brahmendra Yadav Gorla and **Sanjib Kumar Panda**, "A Bidirectional Matrix-Based AC-DC Dual-Active Bridge for Modular Solid-State-Transformers," in IECON 2020, Singapore, Singapore, 2020, pp. 1136-1141 [virtual]."*

THANK YOU

Tutorial Topic: Emerging Solid-State-Transformer based Electric-Vehicle Ultra-fast Charging Station

Concluding Remarks

Tutorial Presentation, IEEE SPEC, 2024, Brisbane

Prof. Sanjib Kumar Panda
Director of Power & Energy group
Department of Electrical and Computer Engineering
National University of Singapore
IEEE Fellow

SUMMARY OF VARIOUS SEGMENTS

NUS National University of Singapore | College of Design and Engineering

- **Introduction and Comprehensive Review**

✓ Having a LVDC interface makes SST technology economically competitive compared to LFT based solutions.

✓ Various MW-scale SST-grid-interface based ultra-fast EV charging concepts (predominantly cascaded modular type) has been implemented with some of them getting commercialized.

- **Universal EV Ultra-fast Charging Concept**

✓ Futuristic MV grid-connected bidirectional FC/dC station architecture is proposed for facilitating bidirectional (G2V and V2G) functionality for all three PEV categories, with peak efficiency of 96.4% and power-density >3 kVA/L.

✓ Proposed multi-objective analytical balance control is capable of not only ensuring complete ZVS for all MOSFETs for wide load range, but also restricts the grid-side current harmonics within the grid-code limits.

- **ML-aided Design Optimization of Grid-interface**

✓ The developed ML-aided optimization framework, based on hybrid (analytical + numerical) models, helps power electronics design engineers to find optimal SST design in reasonable time while using common PCs.

✓ This technique reduces the number of FEA computations; results in feasible computational time and low MAPE.

- **Coordinated-control of Renewable Integrated Ultra-fast Charging Stations**

✓ An adaptive grid-supportive AGCS-MPPT control algorithm and coordinated-control technique for a battery-less solar-aided EV-UFCS are presented.

✓ The coordinated-control technique ensure maximum solar extraction and PEV fast-charging energy delivery, while adhering to the instantaneous grid-side and PEV-BMS's constraints.

MAJOR CHALLENGES FACED BY SST TECHNOLOGY

- **Efficiency Improvement:**

✓ Though MVAC-LVAC SSTs have much more functionalities than an LFT, in terms of efficiency it can't match a LFT due to extra losses in the semiconductor device (still a bottleneck!).

✓ Having a LVDC integration requirement leads to necessity of power electronics even for LFT based solutions – in such cases SSTs are comparable in terms of efficiency even while considering today's WBG devices.

- **Reliability Improvement:**

✓ Opposed to LFTs, which are fundamentally a combination of resistances and inductances (majorly), SSTs are isolated power converters and thus exhibit higher failure rate.

✓ For cascaded SSTs, redundant submodules are used for enhancing reliability, but having increased number of redundant submodules reduces power density (unavoidable trade-off!).

- **Financial burden:**

✓ A MVAC-LVAC SST is 3-5 times more expensive compared to a conventional LFT.

✓ A SST with MVAC-LVDC stage however has similar cost compared to (LFT + back-to-back converter).

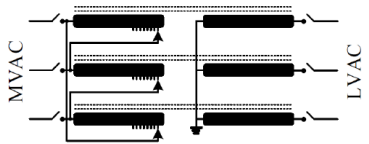

Fig. 1. Low-frequency transformer (LFT)

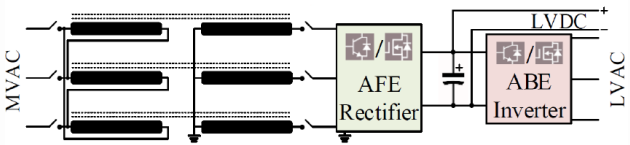

Fig. 2. LFT reinforced with AFE rectifier + ABE inverter

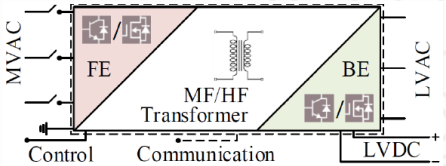

Fig. 3. Solid-state transformer (SST)

[1] J. E. Huber and J. W. Kolar, "Applicability of Solid-State Transformers in Today's and Future Distribution Grids," in IEEE Trans. Smart Grid, vol. 10, no. 1, pp. 317-326, Jan. 2019.

[2] J. E. Huber and J. W. Kolar, "Volume/weight/cost comparison of a 1MVA 10 kV/400 V solid-state against a conventional low-frequency distribution transformer," 2014 IEEE Energy Conversion Congress and Exposition (ECCE), 2014, pp. 4545-4552.

MAJOR CHALLENGES FACED BY SST TECHNOLOGY

- **Incompatibility Issues:**

✓ It is standard for LFTs to supply 25 times of the rated current for at least 2 seconds during faults (in line with the power system protection scheme), but SSTs can't withstand this current as the thermal time constant of semiconductor devices is only 10s of milliseconds.

✓ SSTs have the ability to limit the short circuit current, but it requires advanced protection concepts such as communication between SSTs, circuit breakers, etc., which will incur more cost; protection of SSTs against over-voltages due to lightning strikes or faulty switching are still quite challenging.

- **Competition from Alternative Solutions:**

✓ Automatic on-load tap-changing transformers (also known as voltage regulation distribution transformer), in combination with active series voltage regulators and static VAr compensators can also fulfill most of the functionalities of SSTs with only partial power electronics-based power processing (but at lower power density).

✓ Various Hybrid transformers and other series/parallel hybridization of LFT and power electronics can fulfill most of the SST functionalities with partial power electronics-based power processing.

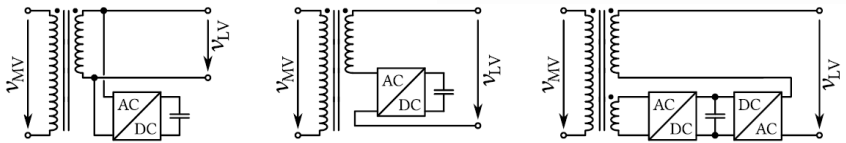

Fig. 4. Various configurations of hybrid transformers

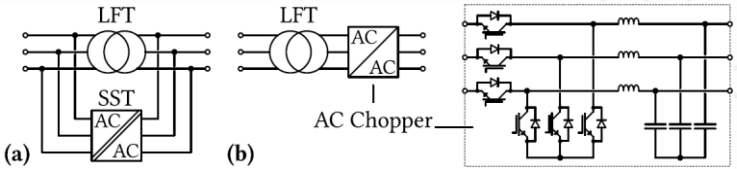

Fig. 5. (a) LFT-SST parallel combination; (b) Series combination of LFT+AC-chopper

[1] J. E. Huber and J. W. Kolar, "Applicability of Solid-State Transformers in Today's and Future Distribution Grids," in IEEE Trans. Smart Grid, vol. 10, no. 1, pp. 317-326, Jan. 2019.

[2] J. E. Huber and J. W. Kolar, "Volume/weight/cost comparison of a 1MVA 10 kV/400 V solid-state against a conventional low-frequency distribution transformer," 2014 IEEE Energy Conversion Congress and Exposition (ECCE), 2014, pp. 4545-4552.

POTENTIAL AREAS OF SST APPLICATION

- **AC-DC applications**

✓ Applications with need to interface the MVAC grid with a LVDC grid, such as integration of DES and DERs, integration of DC microgrids, supply for EV fast charging stations, supplying DC data-centres from MV grid.

✓ For such applications, LFT technology alone is not sufficient and has to be reinforced with AC-DC bidirectional converters.

✓ For solely AC-DC applications, SST is a superior choice compared to LFT in terms of efficiency, power density and cost.

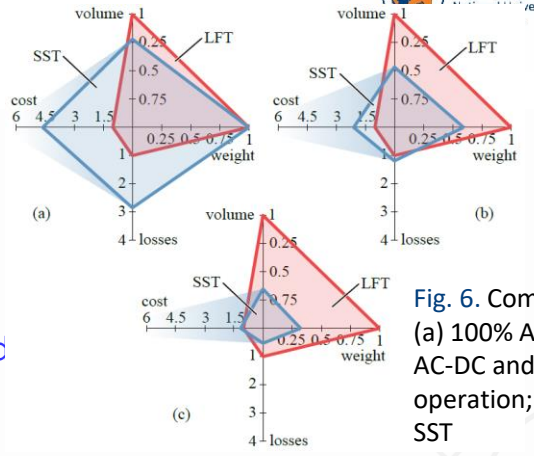

Fig. 6. Comparisons with LFT: (a) 100% AC-AC SST; (b) 50% AC-DC and 50% AC-AC SST operation; (c) 100% AC-DC SST

- **Weight/area constrained applications**

✓ SST technology has high power density, which beats the LFT technology even for MVAC-LVAC application

✓ Favourable solution for weight/area constrained domains like traction applications, railways auxiliary MVAC-LVDC power lines (for air-conditioning, etc.), flying wind turbines and so on.

✓ Grid-connected power systems application where space is a major constraint like subsea applications such as oil drilling, underground transmission/distribution networks, urban centres, etc.

- **DC-DC applications**

✓ Emerging MVDC transmission/distribution network, e.g offshore substations for offshore wind-power farms

EMERGING APPLICATION OF MEDIUM-VOLTAGE INTERFACE

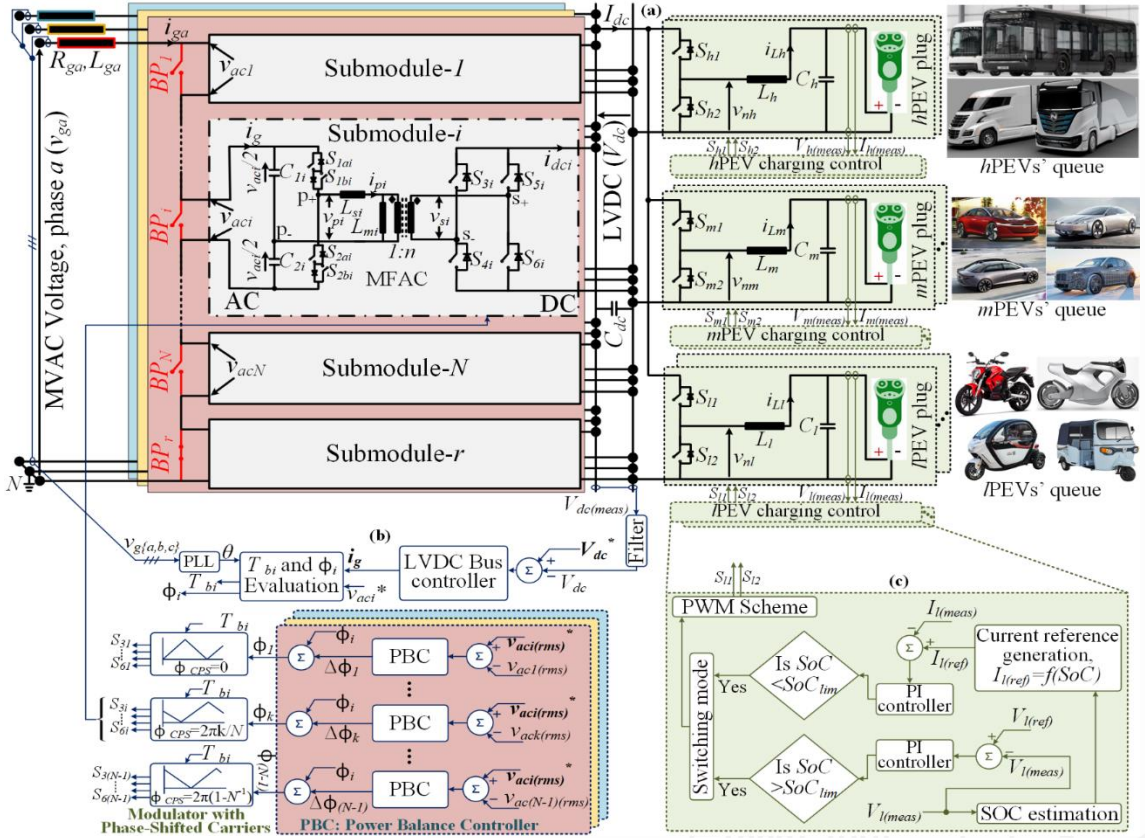

Fig. 6. Schematic of a proposed MV grid-connected bidirectional fast-charging station

- Ultra-fast-charging stations of the future are expected to mimic the conventional refueling stations today.
- Should be capable of charging all three types of vehicles (heavy, medium, light).
- The infrastructure should be bidirectional in nature to facilitate V2G and G2V.
- MV grid-connected SST based ultra-fast-charging station capable of providing better efficiency (>96%) and power density (>3 kW/L).

Thank you

EMERGING APPLICATIONS OF MEDIUM-VOLTAGE CONVERSION

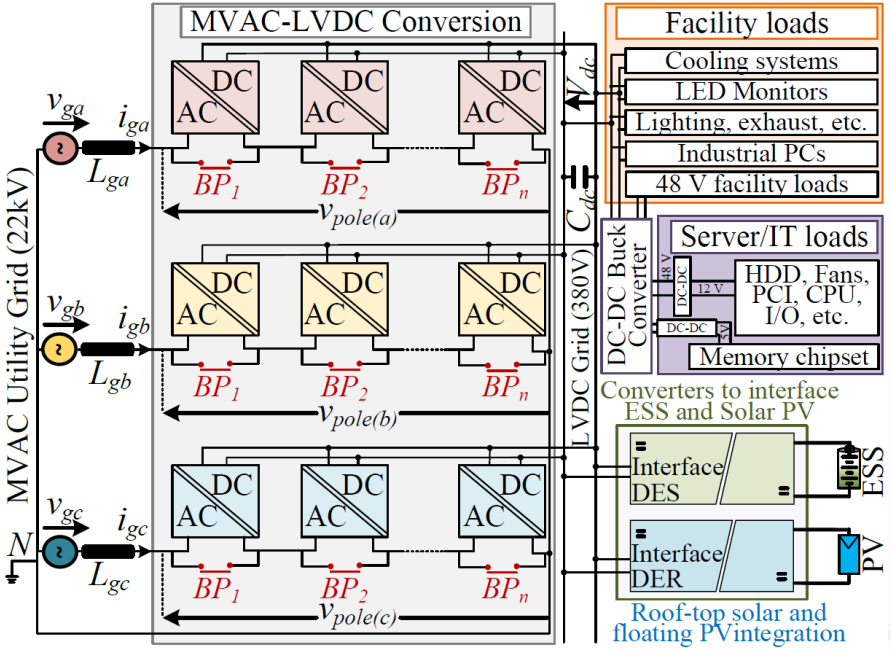

Fig. 7. Schematic of a proposed MVAC-LVDC conversion stage for MV grid-interfacing of DC based data-centre distribution grid.

- There is a push to make data-centers more sustainable by reducing their power usage effectiveness (PUE) index.
- MVAC-LVDC SST is a potential competitor for the grid-interface service – this solution provides better efficiency than low voltage grid-connected alternative.
- Easier to connect the solar PV, energy storage and predominantly DC loads by interfacing with the LVDC distribution architecture.
- Expected peak efficiency of >95%
  Expected power density of ~ 3 kW/L